Pukekawa aquifer: groundwater flow modelling

Waikato

REGIONAL COUNCIL

Te Kaunihera ā Rohe o Waikato

Prepared by:
Blair Thornburrow
Pattle Delamore Partners Ltd

For:
Waikato Regional Council
Private Bag 3038
Waikato Mail Centre
HAMILTON 3240

24 March 2017

Peer reviewed by:
Edmund Brown   Date   May 2017

Approved for release by:
Dominique Noiton   Date   November 2017

Disclaimer

This technical report has been prepared for the use of Waikato Regional Council as a reference document and as such does not constitute Council's policy.

Council requests that if excerpts or inferences are drawn from this document for further use by individuals or organisations, due care should be taken to ensure that the appropriate context has been preserved, and is accurately reflected and referenced in any subsequent spoken or written communication.

While Waikato Regional Council has exercised all reasonable skill and care in controlling the contents of this report, Council accepts no liability in contract, tort or otherwise, for any loss, damage, injury or expense (whether direct, indirect or consequential) arising out of the provision of this information or its use by you or any other party.

Pukekawa Aquifer: Groundwater Flow Modelling

• Prepared for

Waikato Regional Council

• March 2017

Quality Control Sheet

TITLE	Pukekawa Aquifer: Groundwater Flow Modelling
CLIENT	Waikato Regional Council
VERSION	Draft
ISSUE DATE	24 March 2017
JOB REFERENCE	T01580500
SOURCE FILE(S)	T01580500R001_Pukekawa GW Modelling Report_Final Draft.docx

DOCUMENT CONTRIBUTORS

Prepared by

SIGNATURE

Blair Thornburrow

Reviewed and Approved by

SIGNATURE

Alan Pattle

Limitations:

This report has been prepared by Pattle Delamore Partners Limited (PDP) on the basis of information provided by Waikato Regional Council. PDP has not independently verified the provided information and has relied upon it being accurate and sufficient for use by PDP in preparing the report. PDP accepts no responsibility for errors or omissions in, or the currency or sufficiency of, the provided information.

This report has been prepared by PDP on the specific instructions of Waikato Regional Council for the limited purposes described in the report. PDP accepts no liability if the report is used for a different purpose or if it is used or relied on by any other person. Any such use or reliance will be solely at their own risk.

Executive Summary

Waikato Regional Council (WRC) commissioned Pattle Delamore Partners (PDP) to develop a groundwater flow model for the Pukekawa Basalt aquifer in the Lower Waikato catchment. The primary objective of the work was to guide WRC in water allocation decisions. Central to this objective was characterisation the influence of groundwater abstraction on surface water low flows in the catchment.

A three dimensional geological model was constructed from available geological data and a groundwater flow model was developed using FEFLOW. A catchment water balance model was calibrated to produce rainfall recharge data for the groundwater model. Calibration of the groundwater flow model was focussed on simulating groundwater discharge dynamics influencing surface water low flows.

Predictive simulations were developed to evaluate the impacts of varying levels of groundwater allocation on groundwater levels and surface water low flows. Scenarios included continuation of current abstraction rates based on flow metering data; full usage of current consented allocation; and allocation to 35% of rainfall recharge to the basalt aquifer.

Results of these scenarios helped to establish the relationship between allocation limits and low flow impacts (i.e. reductions to the 5 year low flows in streams). Results indicated that impacts to low flows will increase with increasing allocation but at a diminishing rate relative to the increase in allocation.

The simulations were also useful in characterising the spatial and temporal aspects of stream depletion. For instance, the degree to which stream depletion effects are attenuated in time compared to seasonally variable abstraction for irrigation. Results indicated that peak low flow impacts are considerably less than peak abstraction stresses.

From a groundwater management perspective, the results were useful for guiding the allocation approach for this aquifer. With a relationship between allocation limits and low flow impacts established, this enables WRC to set a limit based on a low flow impact which is deemed acceptable in consideration of environmental and stakeholder objectives. The modelling supports the combined management of the Pukekawa basalt aquifer and underlying sand aquifer as a single allocation unit, with individual consideration of localised stream depletion effects for groundwater take resource consent applications.

The value in applying periodic water take restrictions to groundwater users is considered to be limited based on the results of the modelling largely owing to the degree attenuation occurring between groundwater abstraction and stream depletion effects and the offset timing of peak stream depletion effects and low flows. Furthermore, it is not recommended that surface water flow gauging be adopted as a basis for setting resource consent conditions.

Table of Contents

Table of Tables

Appendices

1.0 Introduction

Waikato Regional Council (WRC) engaged Pattle Delamore Partners Ltd (PDP) to develop a groundwater flow model of the Pukekawa aquifer in the Lower Waikato catchment. This report documents the objectives, methodology and findings of the modelling exercise.

1.1 Background

The Pukekawa aquifer, as defined in Table 3-6 in the Waikato Regional Plan, covers an approximate 10 km by 20 km in the Lower Waikato catchment. The aquifer is delineated in Aquifer Map 5 of the Waikato Regional Plan[1] and includes both the Pukekawa and Onewhero Basalt cones.

The focus area of this study comprises 126 km^2 within the eastern half of the management area, as shown in Figure 1. This area includes the productive Pukekawa Basalt aquifer and an underlying sand aquifer. This part of the management area has been assessed separately from the Onewhero Basalt aquifer to the west. The two adjacent basalt aquifers are considered to be in poor hydraulic connection.

---

[1] http://www.waikatoregion.govt.nz/Council/Policy-and-plans/Rules-and-regulation/Regional-Plan/Waikato-Regional-Plan/3-Water-Module/33-Water-Takes/Water-allocation-maps/
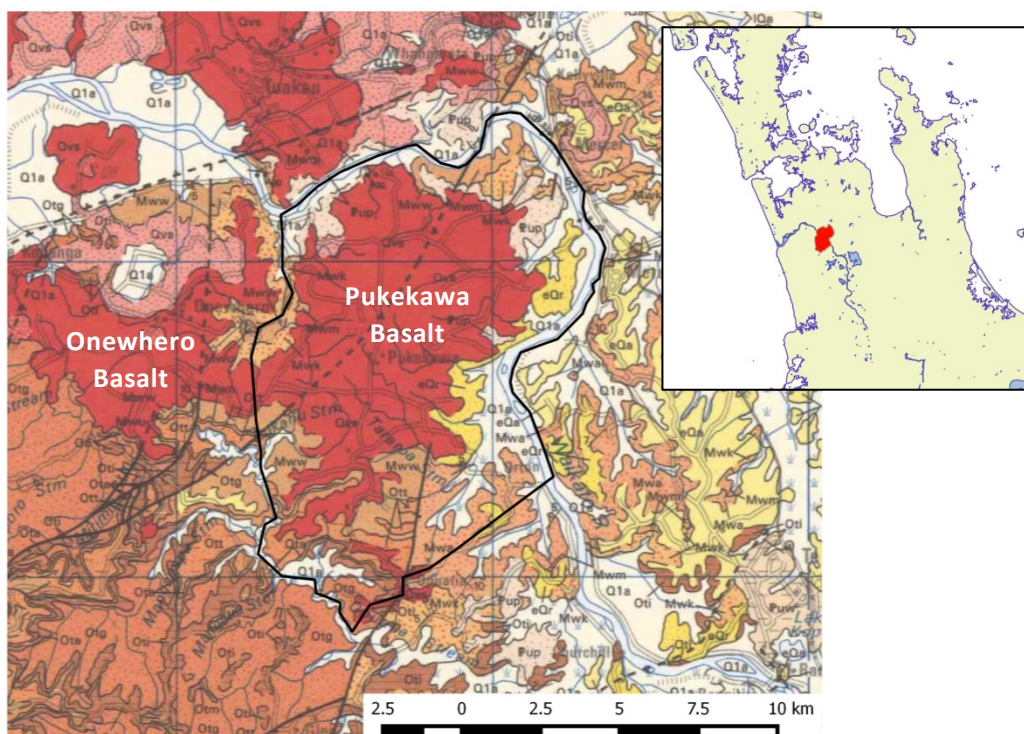
Figure 1: Study Area and Surface Geology

According to the Plan, once water allocation in an aquifer has reached its management level, further work is required to define a more robust sustainable yield. The Pukekawa Aquifer has reached management level hence a sustainable yield is to be determined. This study is focussed on the Pukekawa Basalt aquifer, rather than the Onewhero Basalt aquifer, because it represents the larger resource and higher demand centre.

1.2   Objectives

The primary objective of the work documented in this report was to guide WRC in water allocation (limit setting) decisions. Key to this was characterising the influence of groundwater abstraction on surface water flows ultimately discharging to the Lower Waikato River. Impacts on low flows were of particular concern, both at a local tributary scale and to the Lower Waikato River downstream of the study area.

The specific objectives of this study were to:

- Undertake a detailed assessment of the groundwater resource including an overall water balance;

- Quantify the effects of groundwater abstraction on the groundwater resource and discharges to surface water;

- Examine the spatial distribution of groundwater demand compared with the spatial distribution of surface water impacts; and,

- Examine the seasonal variability of groundwater demand compared with the timing of surface water impacts and low flow events.

1.3   Previous Studies

The work presented in this report follows previous phases of work which developed the conceptual hydrogeology of the study area and set up a numerical flow modelling framework.

Bell et al. (1991) presented hydrological and geological information and a conceptual model of the area.

Golder Associates (2013) documented development of a preliminary steady-state groundwater flow model for the Pukekawa area. The work documented in this report is a continuation of this initial work, with development of a more detailed flow model.

2.0   Conceptual Hydrogeology

Conceptual hydrogeology of the Pukekawa area has been previously investigated in depth by others (Bell et al., 1991; Golder Associates, 2013). The work

documented in this report largely relies on the existing conceptual models. A basic summary of the conceptual hydrogeology is presented in this report with a focus on aspects relevant to the objectives of the numerical modelling.

2.1   Climate and Rainfall

Daily rainfall and potential evapotranspiration (PET) data were obtained from the NIWA virtual climate station network (VCSN) for the period 1972 to 2015. Data were obtained from VCS agent number 28640, located within the study area. Mean annual precipitation was 1,280 mm and average annual PET was 803 mm. Annual rainfall totals varied between 948 mm in 1993 to a maximum 1,649 mm in 2011.

Mean monthly rainfall and PET depths are presented in Figure 2. Seasonally, rainfall is generally in excess of PET for 8 of 12 months (March – October), with PET exceeding rainfall for the remaining four months (November – February).
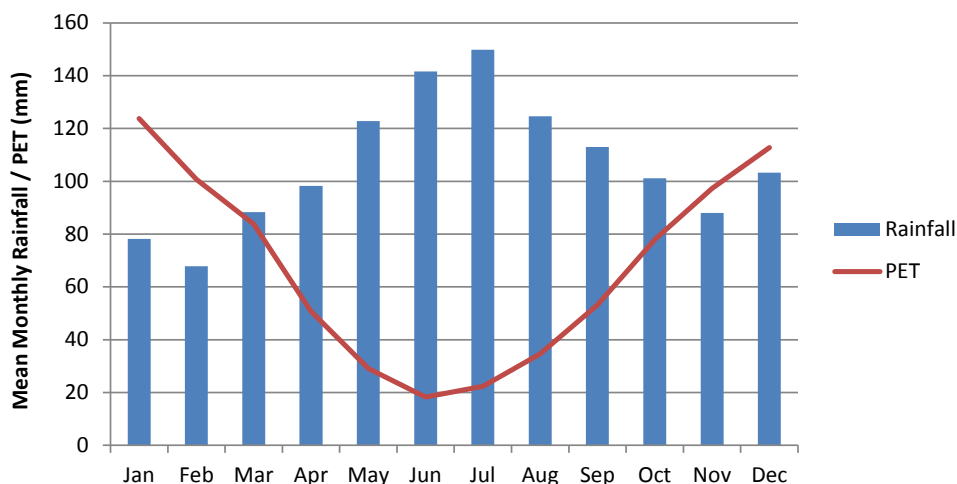
Figure 2: Mean monthly precipitation and PET (1972 – 2014)

2.2   Geology

Geology of the Pukekawa area is described in Golder Associates (2013) and key geological units relevant to this assessment can be summarised as follows:

- Te Kuiti Group siltstone, sandstone and coal measures;

- Waitemata Group sandstones and siltstones;

- Tauranga Group alluvial deposits including Puketoka Formation silts and sands, Waeranga Gravels, Karapiro Formation sands silts and clays, and Piako Subgroup swamp and alluvial deposits; and,

- South Auckland Volcanics including basalt lavas and airfall deposits.

As part of the work by PDP, a three-dimensional geological model of the study area was developed using the Leapfrog Geo software based on mapped surface geology and available geological logs for boreholes in the area. The geological model was divided into five key hydrostratigraphic units (HSUs), according to the anticipated influence of these units on groundwater flow processes and the detail available in geological logs. The HSUs were defined as follows:

- Te Kuiti and Waitemata Group Rocks: This unit underlies the entire model domain and forms the basement unit of the geological model. There are few bores drilled into these formations and these rocks are typically not targeted for water supply, indicating poor groundwater yield potential.

- Tauranga Group (sand/gravel dominant): The sand and gravel HSU of the Tauranga Group overlies the Te Kuiti and Waitemata Group rocks and extends over much of the study area including beneath the basalt. This forms an aquifer targeted by several bores drilled within the basalt extent.

- Tauranga Group (silt/clay dominant): The upper HSU of the Tauranga Group sediments, this has a similar extent to the sand/gravel HSU.

- Unweathered basalt: Overlies Tauranga Group Sediments in most locations but directly overlies Te Kuiti / Waitemata rocks in thicker sections. This unit is up to approximately 150 m thick in its centre and thins out towards its margins. Includes fractured and fresh basalt, scoria and ash/tuff units associated with multiple flow sequences.

- Weathered basalt (clay): A zone of weathered clays typically makes up the top 10 – 20 m of the basalt. In thinner areas near the basalt extent, most of the basalt thickness may be weathered.

Figure 3: Snapshot of the Pukekawa geological model

2.3 Groundwater Levels

2.3.1 Groundwater Level Data

Thirty-nine (39) groundwater level monitoring records were available within the study area at varying locations and durations from the early 1980s through to the present. The available groundwater level data are shown in Figure 4. The vertical accuracy of most records is unknown and a proxy ground level datum is often assigned via interpolation from the digital elevation model (DEM).

Most of the available records span a period from the mid-1980s to the mid-1990s. Only eight of the thirty nine records contain data from the last ten years and four of these contain data from both periods.

Figure 4: Available groundwater level monitoring data in the study area

Only two bores have groundwater level records available between the mid-1990s and mid-2000s. Groundwater level data for these sites are shown in Figure 5.
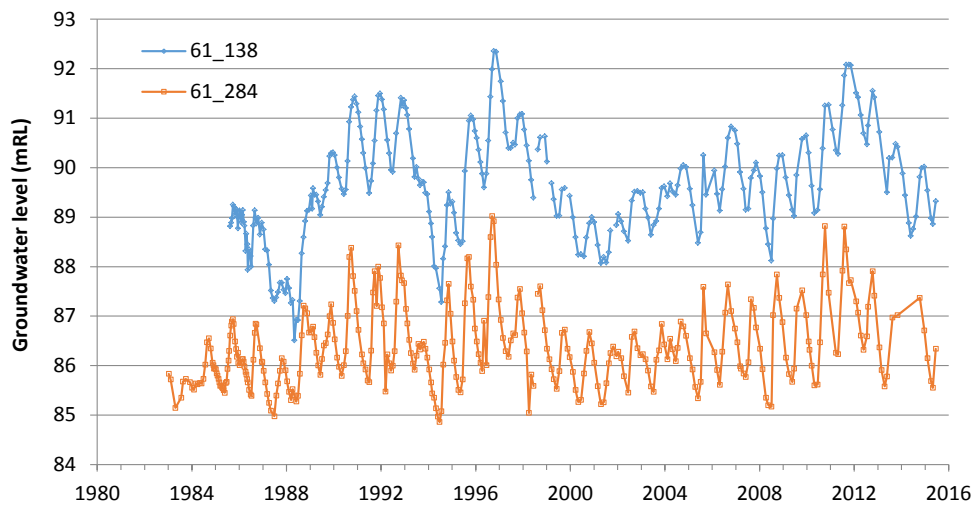
Figure 5: Long duration groundwater level records at Pukekawa

2.3.2   Temporal Groundwater Level Behaviour

Seasonal and inter-annual trends are evident in the long term groundwater level records. Seasonally, water levels respond to winter recharge in a roughly sinusoidal manner, with a tendency for more gradual recessions. It is difficult to determine the degree of influence on groundwater levels during this period from abstraction, as records of water use were not kept over the duration of monitoring. However, the influence of periods of lower rainfall (e.g. 1997 to

2002) can be seen by declines in groundwater levels of up to 4 m, experienced over several years (Figure 6).
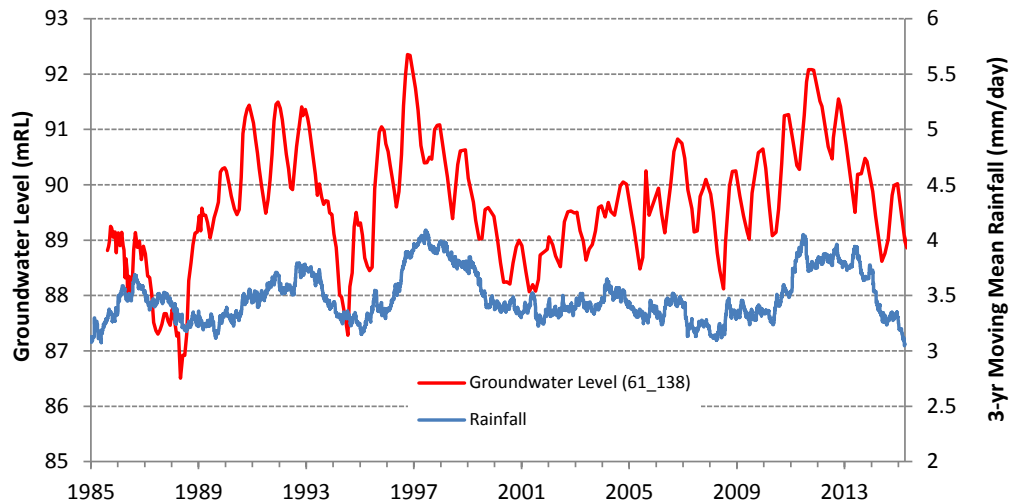
Figure 6: Groundwater levels and preceding 3-yr moving mean rainfall at Pukekawa

2.3.3   Vertical Head Distribution

The Pukekawa Basalt Aquifer is characterised by strong downwards vertical groundwater head gradients, with a clear relationship evident between average head and drilled depth. This relationship is evident in Figure 7, which shows sample elevation (the mean elevation of the screened or open cased borehole section) on the horizontal axis, and average groundwater level on the vertical axis.

This observation is consistent with the conceptual model of the basalt aquifer put forward by Bell et al. (1991), which describes a groundwater flow system dominated by inter-layered basalt flows. This describes layers of more permeable material (fractured basalt and scoria) interbedded with lower permeability ash, tuff and clay. As such, flow is thought to preferentially flow horizontally along higher permeability zones and is impeded from vertical movement. Thus the bulk vertical hydraulic conductivity of the basalt is expected to be significantly lower than its horizontal hydraulic conductivity. Bell et al. (1991) also noted anecdotal evidence of groundwater "cascading" between basalt flows within uncased boreholes through the basalt.

Figure 7: Mean groundwater level vs. sample elevation in Pukekawa bores

2.3.4   Horizontal Head Distribution

Groundwater levels are typically highest in the centre of the Pukekawa basalt aquifer and fall radially towards the basalt flow margins and adjacent lower lying ground. However, it is difficult to visualise the horizontal distribution of groundwater levels given the large vertical head gradients represented in monitoring data.
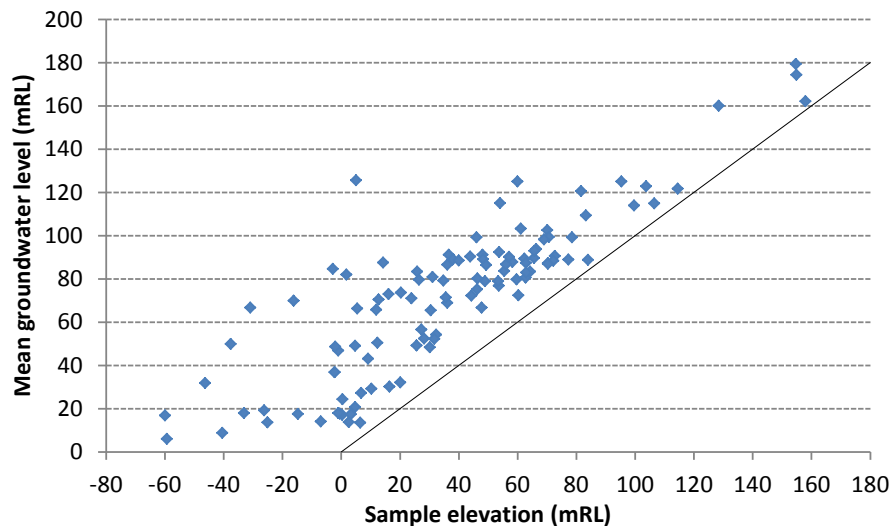
2.4   Recharge and Discharge

The regime of aquifer recharge and discharge in the study area is governed largely by the topographic and geological structures. Topographic highs associated with basalt cones and flows are surrounded by lower ground at the lateral extents of the basalt. The low lying areas all eventually drain towards the lower Waikato River.

Hence, recharge is solely from infiltration of rainfall at the ground surface, plus any minor infiltration of irrigated water. Groundwater flows radially from the centre of the basalt to ultimately discharge to surface water entering the Waikato River. The geological structure and distribution of groundwater levels does not suggest any significant regional outflow of groundwater (e.g. towards the west coast).

The primary mechanism of groundwater discharge is via springs at the lower flanks of the basalt formation, near its interface with surrounding Tauranga Group Sediments or Waitemata/Te Kuiti formation rocks. These springs support baseflows in a number of streams that drain radially from the basalt formation. Minor groundwater exchanges between the basalt and underlying or adjacent Tauranga Group Sediments is also likely, although its relative quantum spring

discharges is unknown. Recharge to the Tauranga Group Sediments will ultimately support discharges to surface water draining to the lower Waikato River.

2.4.1   Recharge Estimation

Rainfall recharge in the study area was estimated using a simple catchment water balance spreadsheet model. Results derived from the spreadsheet model were used as a key input for the subsequent groundwater flow modelling.

Inputs to the model included daily rainfall and evaporation depths, and model outputs included time series of catchment runoff, infiltration, stream baseflow and evaporation losses. The model was calibrated using available stream flow gauging data including two continuous flow records and several spot gauging records. Details of the recharge estimation methodology are provided in Appendix B.

Modelled recharge time series were developed for two zones within the basalt and for the modelled areas of weathered basalt and beyond the extent of basalt. A map showing the extents of these zones is included in Appendix B. On average, rainfall recharge to the basalt aquifer was estimated at between 280 and 350 mm/year, or 22% to 28% of mean annual rainfall. These estimates of rainfall recharge are similar to those used in preliminary modelling by Golder Associates (2013) – their baseline calibrated model assumed a rainfall recharge rate of 300 mm/year to the basalt.

For the areas of weathered basalt and other surface geological units (e.g. Tauranga Group), modelled recharge with an average 50 mm/y, or 4% of mean annual rainfall was assigned.

2.5   Aquifer Hydraulic Properties

Hydraulic properties of the three main hydrogeological units are described by Bell et al (1991). Of primary interest to this study were the properties of the South Auckland Basalts, as the majority of abstraction is from bores screened in this formation. The basalts comprise a variety of formations with a range of hydraulic properties. The structure of these formations influences groundwater flow and levels in the broader aquifer. Bell et al (1991) reports thick, fractured basalt flows near eruptive centres and thinner, fractured basalt flow layers interbedded with ash, tuff and scoria elsewhere. Ash, tuff and weathered basalt act as local aquitard layers between the more productive fractured basalt and scoria layers. As a bulk hydrogeological unit, the South Auckland Basalts can be conceptualised as anisotropic with horizontal hydraulic conductivity in excess of vertical hydraulic conductivity. The aquifer is considered to have progressively increasing hydraulic confinement with depth.

A collation of historic aquifer test information is presented in Golder Associates (2013). A large range of aquifer transmissivity values (0.2 – 30,000 m^2/d) were obtained from various pumping tests performed on bores screened within the South Auckland Basalts, resulting from the variable distribution of formations as described above. Pumping tests were reported as frequently showing evidence of boundary effects, suggesting that local zones of elevated permeability are discontinuous in extent and bounded by less permeable formations.

Limited hydraulic testing information was available to characterise hydraulic properties of the Tauranga Group Sediments and Waitemata/Te Kuiti Formation rocks. However, these have been assumed to have generally lower permeability than the Basalts. Some productive strata were noted for the Tauranga Group Sediments, with Golder Associates (2013) reporting a mean transmissivity of 11 m/d. The Waitemata and Te Kuiti Formation rocks are understood to have consistently lower permeability, with hydraulic conductivity values ranging from 0.01 to 0.08 m/d reported by Golder Associates (2013).

2.6   Groundwater Abstraction and Use

As at the date of model development (January 2016), there were 28 currently active consents for groundwater abstraction in the study area. Of these, 21 were listed as takes from the basalt aquifer and 5 were listed as taking from the underlying Tauranga Group Sediments. Two of the consents were related to mining operations.

Most groundwater take consents in the area are defined seasonally, with maximum daily abstraction rates assigned for each calendar month. Annual take limits are also defined which in most cases assume that pumping would not occur continuously over the entire irrigation season. Based on annual consent limits, the total allocation volume for bores within the study area at the date of model development was 2.5 million m^3/year. This excludes one consented take of up to 12.2 million m^3/year for quarry dewatering; however, this quarry is located at the northern limit of the basalt extent and is considered to largely comprise seepage derived from the Waikato River. It is also unknown how much of the allocation limit is actually used. Water extracted for dewatering is also returned to the Waikato River. This take was not included in subsequent modelling.

Of the 2.5 million m^3/year of consented groundwater abstraction for consumptive purposes, 95% of this is for irrigation, and 92% of this is for horticulture/market garden irrigation.

The distribution of groundwater takes is shown in Figure 8. The majority of abstraction is centred in the north and east of the study area, within the basalt extent.
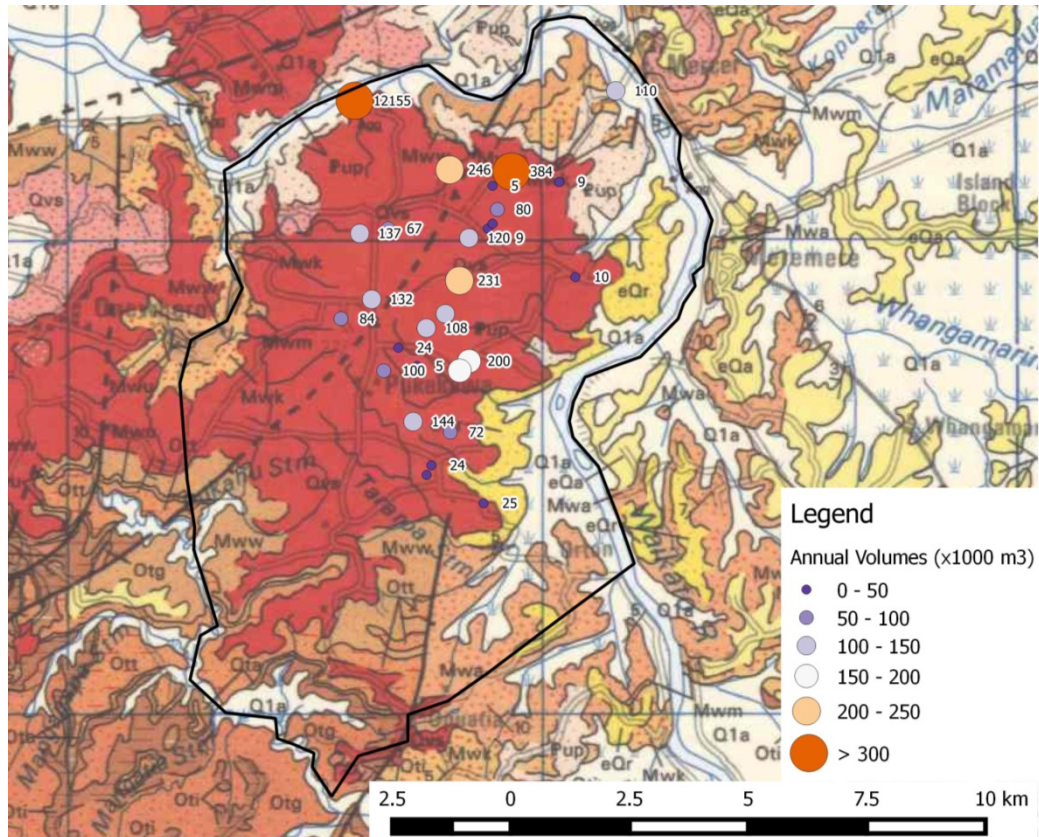
Figure 8: Distribution of consented groundwater takes in the study area

Actual rates of abstraction are metered for the majority of the consented takes in the study area. Groundwater users with water meters currently account for at least 86% of the consented annual volume (excluding the quarry).

Cumulative metered abstraction for the 24 records within the study area is presented in Figure 9. According to the metering data, total abstraction from the study area appears to vary significantly from year to year. This large variability appears to be driven by preceding rainfall in the months leading up to the irrigation season. For example, very low abstraction during the 2011-2012 irrigation season was preceded by five consecutive months of higher than average rainfall and rainfall during the irrigation season was generally above average. In the following three irrigation seasons, abstraction was greater as conditions were generally average to dry. However, some of the increase in metered abstraction over the period shown in Figure 9 may be attributable to an increasing number of bores being metered.
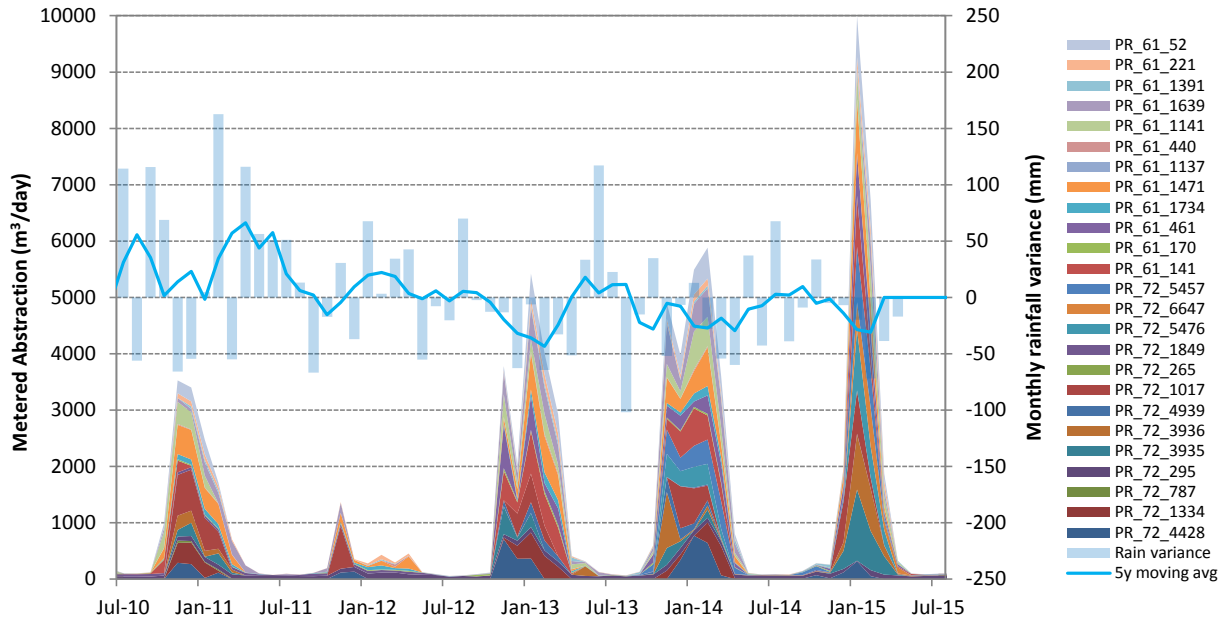
Figure 9: Recorded abstraction for metered groundwater users in the study area

2.7   Expected Outcomes

Based on the existing understanding of hydrogeology in the Pukekawa area, it is expected that the modelling will help to confirm the following:

- The majority of rainfall recharge to the basalt is likely to be discharged to springs/streams at the basalt margins;

- Groundwater abstraction from bores in the study area will be offset by reductions in discharge to the springs/streams;

- The surface water flow depletion effects of the seasonally variable abstraction from groundwater will be temporally attenuated to a degree such that surface water impacts will be less than peak abstraction;

- The spatial extent of surface water flow depletion effects caused by abstraction will vary depending on the proximity and depth of abstraction bore; and,

- How the overall distribution of demand translates to a distribution of impacts, and whether division of the management areas is warranted.

3.0   Model Design and Construction

This section provides a brief description of numerical model design and construction, with details provided in Appendix C.

3.1   Model Domain

A finite element 3D numerical groundwater flow model was developed using the FEFLOW (version 6.2) software package by MIKE-DHI. The model domain was assigned based on natural flow boundaries beyond the extent of basalt and on perceived no flow boundaries. The groundwater model domain boundary is shown in Figure 1. The northern and eastern boundaries of the model were terminated at the Waikato River. The western model boundary was terminated along surface water flow lines outside the basalt extent, and along a catchment divide between the Pukekawa and Onewhero Basalts. The southern model boundary was terminated at a catchment divide sufficiently distant from the Pukekawa Basalt aquifer boundary.

3.2   Mesh and Layer Structure

The two dimensional finite element mesh was discretised with refinement around formation boundaries, surface water features and bores. The mesh comprised 19,348 nodes and 38,273 triangular elements.

Five model layers were defined to represent the various lithologies and to provide adequate representation of vertical head gradients. Table 1 provides a summary of the geological units defined within each layer. Variable layer interfaces were assigned based on outputs from the 3D geological model developed in Leapfrog Geo. Layer thicknesses varied from 1 m to 179 m and the vertical extent of the model was between -110 m RL and 274 m RL.

Table 1: Model Layer Structure		
Layer	Primary units represented	Secondary units[1]
1 & 2	Pukekawa Basalt	Tauranga Group Sediments, Waitemata/Te Kuiti Formation
3	Tauranga Group Sediments (Silt/Clay)	Tauranga Group Sediments (Sand/Gravel), Waitemata/Te Kuiti Formation
4	Tauranga Group Sediments (Sand/Gravel)	Waitemata/Te Kuiti Formation
5	Waitemata / Te Kuiti Formation	n/a
Notes: 1. Assigned where layer extent is beyond the primary unit extent and a nominal layer thickness is defined.		

3.3   Stresses and Boundary Conditions

Time varying recharge was applied at the top surface of the model (i.e. ground level). Three recharge zones, each with a unique recharge time series, were defined across the model domain. Recharge was defined at a monthly time step.

Groundwater abstraction was simulated using Well boundaries set at the appropriate model layer with time varying abstraction records, defined monthly.

Discharge of groundwater to surface water springs and streams was simulated using seepage face boundaries set at the top model surface (ground level), with specified heads set to ground level. These boundary conditions operate on the basis of maintaining a maximum head equal to its elevation. Discharge occurs to maintain the maximum head. Heads are allowed to fall below the specified head and no recharge may occur via these boundaries.

3.4   Time Stepping

The model was run in transient mode using automatic, variable time steps. At a minimum, time steps were created at each change in stress (recharge or abstraction) as defined in their input data sets. This corresponded to new time steps for the first day of each calendar month. Further interim time steps were automatically inserted as necessary by FEFLOW such that residual error criteria were met. Typically, one interim time step was defined for each monthly period.

3.5   Representation of Confined / Unconfined Conditions

FEFLOW offers several approaches for simulation of confined / unconfined aquifer conditions. The simplest and most numerically stable option is simulation of fully confined conditions. The 3D mesh structure is constant and head is computed for all model nodes, including those with negative pore pressures (i.e. where unconfined conditions may occur). Although not an ideal representation of unconfined conditions, this simulation mode can be used for representing systems with an unconfined water table, with adjustment of the specific storage terms in upper model layers to account for unconfined storage.

This mode was selected for use in this modelling study following trialling of the alternative approaches, which were deemed less favourable. This approach was considered appropriate given the anisotropy of the layered basalt aquifer and progressive confinement with depth. Hence, the system is more appropriately described by confined than unconfined aquifer behaviour.

The alternative modes include "phreatic" and "free/movable" methods for simulating unconfined conditions. Phreatic mode maintains the model structure but scales layer conductivity based on the calculated portion of layer saturation. This operation mode was unfavourable because of large numerical instabilities in response to stresses such as recharge and abstraction. Free/movable mode deforms the model layer structure to conform to the saturated zone. When run

in this mode, the model was not able to adequately reflect observed vertical head gradients and also caused undesirable numerical instability.

4.0   Calibration and Sensitivity Analysis

This section provides a brief overview of the model calibration and sensitivity analysis. Further detail is provided in Appendix D.

4.1   Approach to Model Calibration

There are a number of approaches that can be taken when configuring and parameterising a groundwater flow model during the process of model calibration. In most circumstances, this would involve the adjustment of hydraulic parameters and other settings to achieve a satisfactory agreement between simulated and observed groundwater head data.

Ideally, the approach to model calibration should consider the intended purpose of the model and the variables of interest analysed when assessing simulation results. In many situations, groundwater flow models are used for making predictions of water level drawdown as a result of abstraction. Therefore, a focus on groundwater levels during calibration is usually considered appropriate.

In the case of this study, the primary variable of interest was the discharge of groundwater to springs / streams. Hence the calibration was focussed more on achieving a satisfactory representation of groundwater discharges, with representation of groundwater levels treated as a secondary calibration target.

An iterative trial and error approach was taken to model calibration whereby model parameters were varied between subsequent model runs and calibration results evaluated. This approach provides the modeller with a progressive understanding of model sensitivity to key parameters and enables both a quantitative and qualitative assessment of model performance.

4.2   Calibration to Flow Data

Continuous surface water flow records were available for two gauged catchments within the study area. Groundwater discharge to boundary conditions representing surface drainage in these catchments was analysed for comparison to gauged data. The gauged flow data represents a combination of groundwater derived base flow and surface runoff from the catchment. Model results representing the base flow portion of the catchment hydrographs were compared semi-quantitatively to gauged flows, ignoring the surface runoff component of flows and focussing on low flows.

During calibration, both the average quantum of flow and seasonal variability in base flow discharge was considered. Parameters adjusted during this process included horizontal and vertical hydraulic conductivities of the aquifer and storage parameters. Some adjustments were made to the calibration of the

rainfall recharge model to improve the model's representation of base flow variability.

Figure 10 presents surface water flow data for catchment 83_1, situated within the basalt boundary on the eastern side of the Pukekawa, as shown in Appendix B. Simulated groundwater discharge for the same catchment, according to the FEFLOW model, is shown in red. This demonstrates that both the overall quantity of base flow, seasonal variability in base flow and annual flow minima are represented accurately by the groundwater flow model. While its catchment area is only 2.9 km^2, calibration to data for this gauged catchment was prioritised as it represents discharge solely from the basalt aquifer, and is in an area coinciding with higher levels of aquifer use.
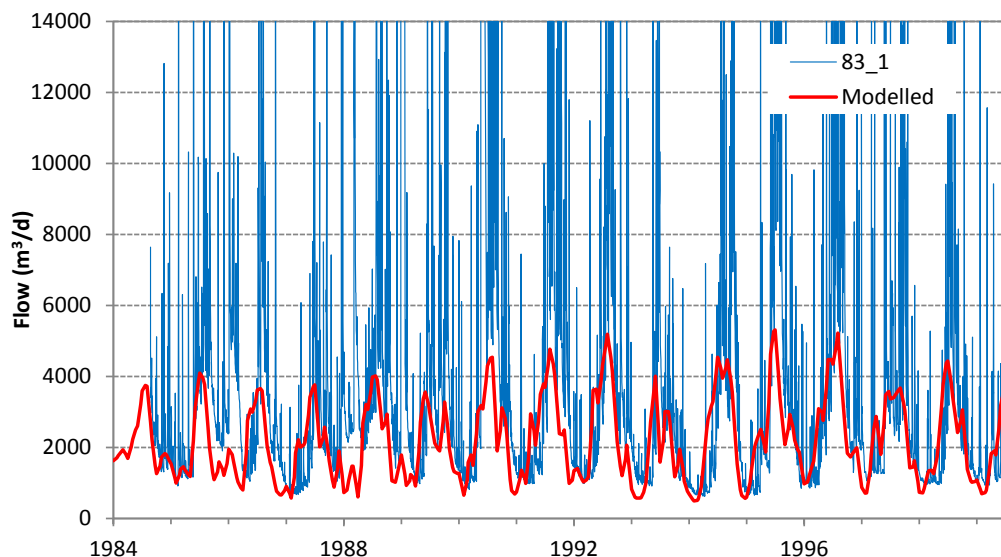
Figure 10: Measured flow in surface water gauge "83_1" and modelled groundwater discharge

Measured catchment flow and modelled groundwater discharge for the catchment "960_1" are shown in Figure 11. While the model does not represent base flow in this catchment as accurately as in "83_1", a reasonable match is achieved. The overall quantum of base flow and representation of summer low flows appear to be reasonable, however higher base flows during winter are less accurately represented. A lower priority was placed on calibrating the model to this gauge as it covers areas outside the aquifer extent, and is away from the area of greatest aquifer use.
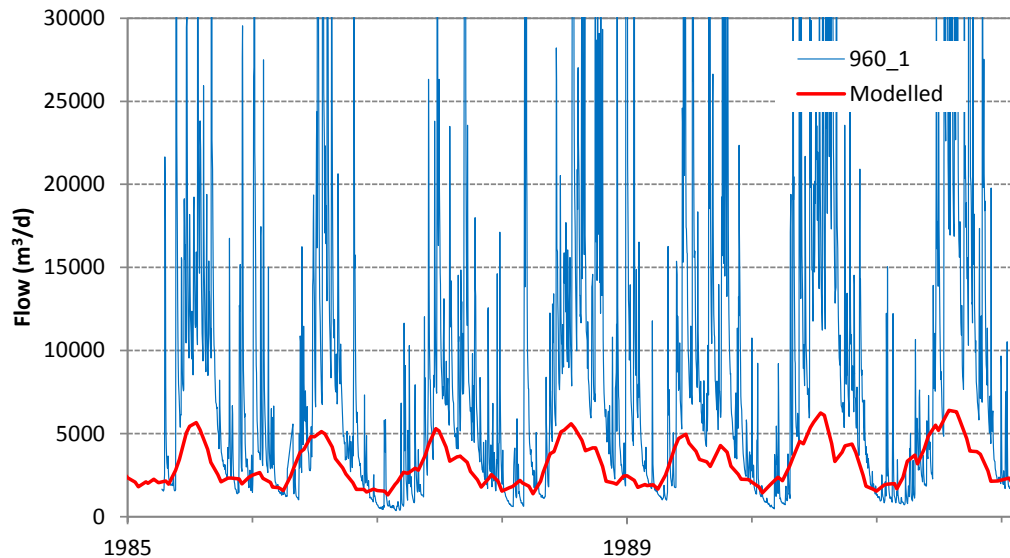
Figure 11: Measured flow in surface water gauge "960_1" and modelled groundwater discharge.

A number of spot gauging datasets were also available for various streams around the Pukekawa basalt aquifer. These were also compared to modelled baseflow discharges to provide an additional check of calibration performance.

4.3   Calibration to Groundwater Levels

As discussed above, the calibration of this model considered groundwater levels as a secondary calibration dataset, in recognition of the intended use of the model as a predictor of discharge impacts. In other words, greater priority was given to improving the model's ability to represent groundwater discharges, at the expense to representation of recorded groundwater levels.

Furthermore, the elevation datum of most of the monitoring bores was unknown and interpolated from the digital elevation model. Hence, derived groundwater heads relative to sea level in these bores was only considered accurate to within approximately 20 m. The calibration hydrographs presented in this section (Figure 12 - Figure 14) are for those which have a more accurate datum (i.e. to within 0.1 m accuracy).
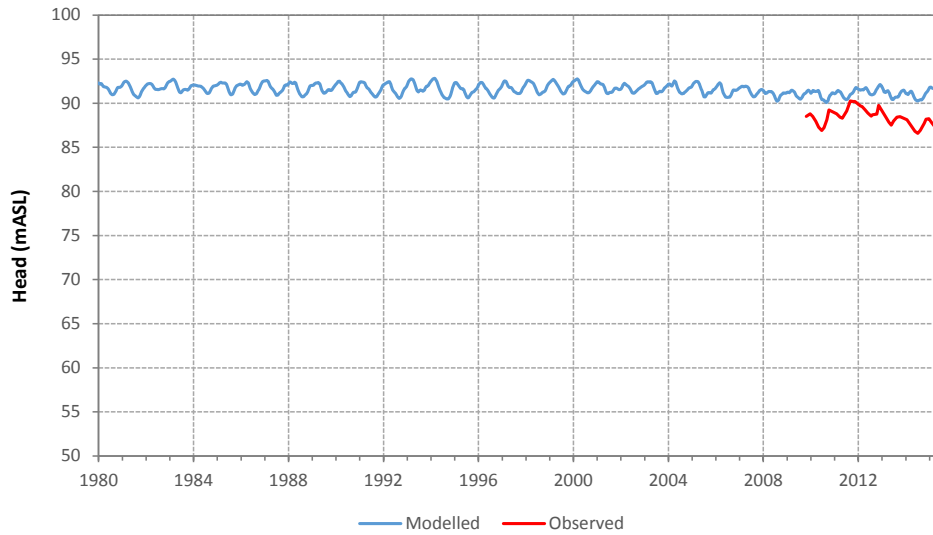
Figure 12: Modelled and observed groundwater heads in monitoring bore 61_1639, located in the north-west of the Pukekawa Basalt.
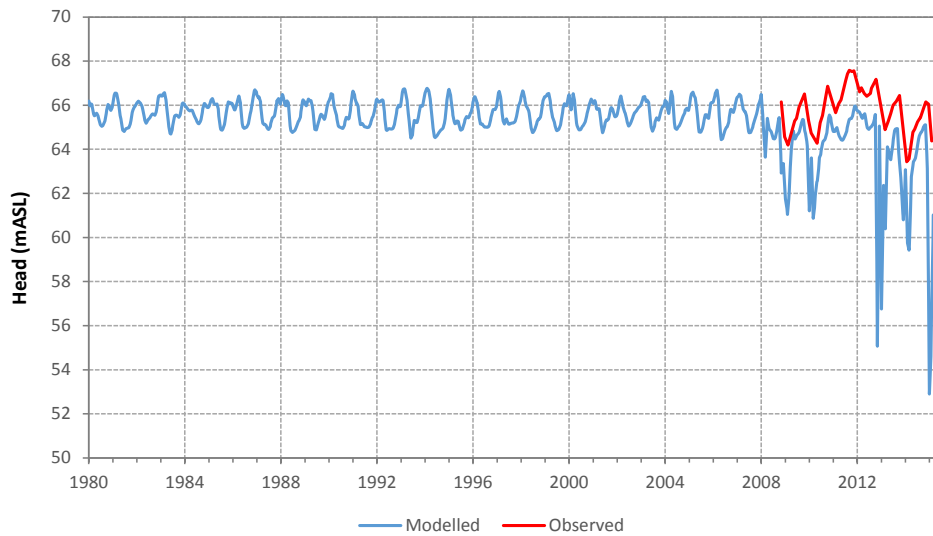

Figure 13: Modelled and observed groundwater heads in monitoring bore 61_461, located in the north-east of the Pukekawa Basalt.
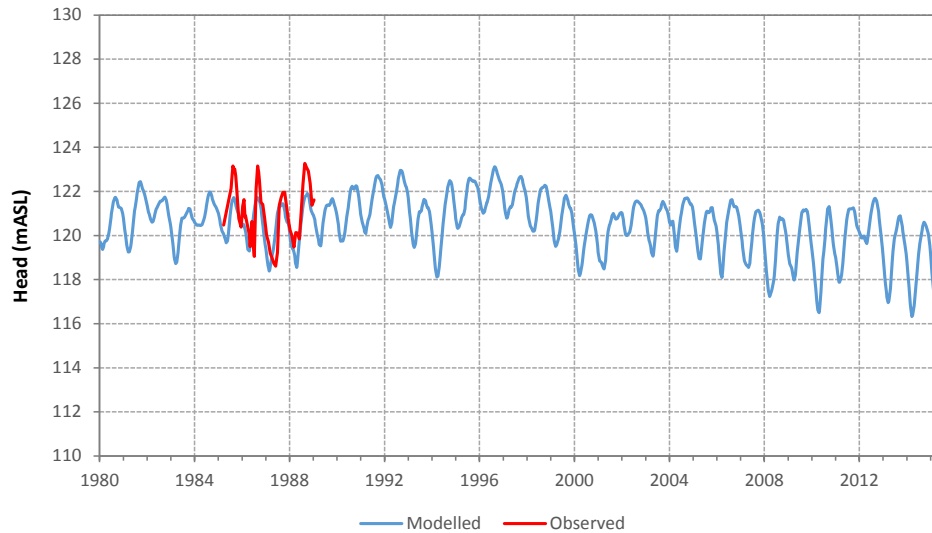
Figure 14: Modelled and observed groundwater heads in monitoring bore 61_26, located in the south-west of the Pukekawa Basalt.

Figure 15 shows a scatter plot of all time series of measured head data compared to the corresponding modelled values. This shows a reasonable agreement overall, despite the uncertainty in most of the data. The normalised RMS error based on groundwater levels is 7.9%, based on calibration to 3,663 observed data points.

Figure 16 shows the same comparison of modelled and measured heads, but over the range of 60 – 100 m RL, in which most of the recorded data reside.
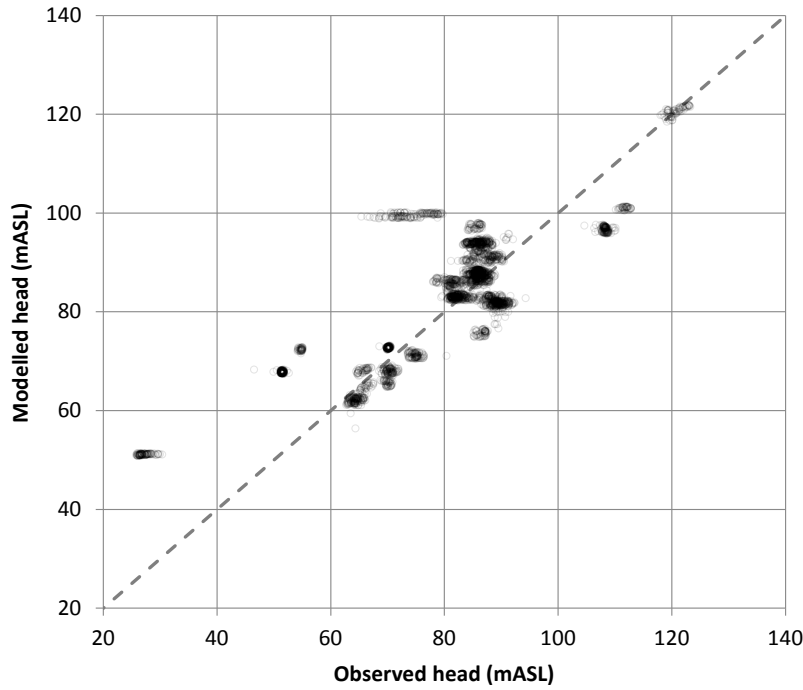
Figure 15: Scatter plot of observed and modelled groundwater levels
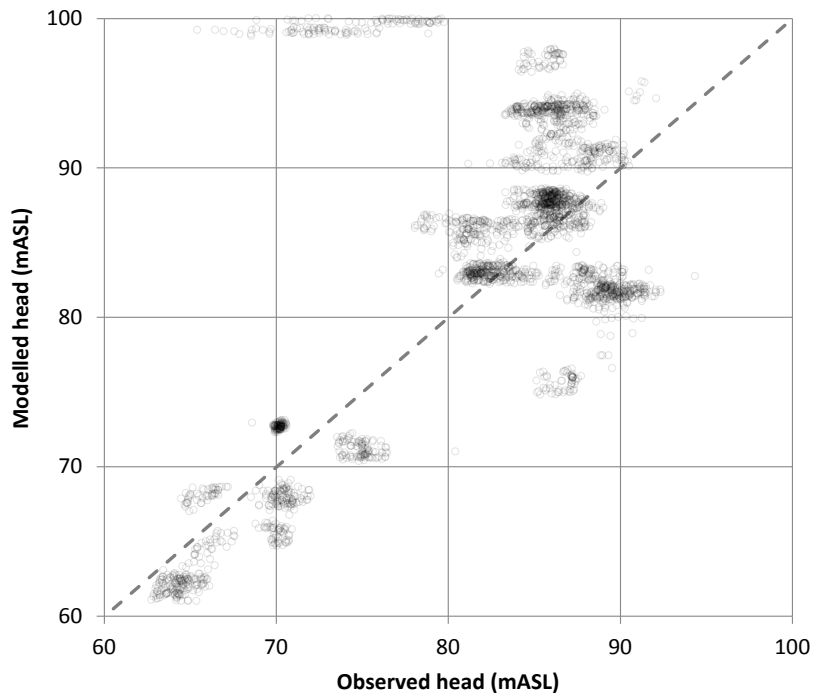
Figure 16: Scatter plot of observed and modelled groundwater levels (60 – 100 m)

4.4   Calibrated Model Parameters

Model parameters selected during calibration are shown in Table 2.

Table 2: Calibrated groundwater model parameters			
Hydrostratigraphic Unit (HSU)	Horizontal hydraulic conductivity K_h (m/d)	Vertical hydraulic conductivity K_v (m/d)	Specific storage[2] S_s (m^{-1})
Basalt[1]	2 – 3	0.001	5×10^{-6} – 5×10^{-4}
Weathered basalt	0.1	0.001	5×10^{-4}
Tauranga Group silt/clay	0.05	0.01	5×10^{-6}
Tauranga Group sand/gravel	0.5	0.05	5×10^{-6}
Waitemata/Te Kuiti Formation	0.001	0.0001	5×10^{-6}

Notes:
1.   The basalt HSU was subdivided into two hydraulic conductivity zones.
2.   Units in the top model layer were assigned a higher specific storage of 5×10^{-4} m^{-1} to represent unconfined behaviour while the model was being run in confined mode. Confined specific storage values of 5×10^{-6} m^{-1} were assigned for layers 2 – 5.

Calibrated model parameters represent bulk hydrogeological characteristics of the hydrostratigraphic units. As such, calibrated horizontal and vertical hydraulic conductivity values differ from results of some of the hydraulic tests, which suggest high aquifer conductivity in the basalt aquifer. The tendency for calibrated bulk conductivity parameters to be low relative to hydraulic tests supports the conceptual model that permeable fracture zones are localised and do not extend across the basalt domain. It is likely that the network of fractures and permeability zones is quite complex. However, it is considered appropriate for the purposes of this study to simulate the general behaviour of the aquifer using bulk parameters.

4.5   Calibrated Model Results

4.5.1   Head Distribution

The simulated distribution of heads is illustrated in Figure 17, showing contours of equal groundwater head for the top model surface (at ground level) and base of the first model layer. Layer 1 is typically 50 – 100 m thick in the centre of the basalt and 10 – 50 m thick at its margins. This demonstrates the horizontal and

vertical distribution of modelled heads. With the model operating in confined mode, groundwater heads are computed at all model nodes, including those at the ground surface above saturated aquifer conditions. Hence, some contours may represent unsaturated aquifer conditions.

This illustrates a radial distribution of heads in keeping with the conceptual model, which describes recharge across the extent of the basalt and outward groundwater flow towards points of discharge around the margins of the basalt. Horizontal head gradients are relatively flat across the basalt aquifer, as a result of its relatively high conductivity. Steeper gradients are modelled around the margins of the basalt, where it becomes thin, more weathered and ceases giving way to Tauranga Group or Waitemata/Te Kuiti Formations. The steeper head gradients also coincide with steeper topography at the margins of the basalt flows.

The zone of elevated groundwater levels at the western extent of the model domain coincides with the boundary between the Pukekawa basalt and Onewhero basalt to the west. This area is topographically elevated and considered to be an east-west flow divide. The basalt in this area is relatively thin and more weathered compared to the bulk of the basalt formation. Groundwater levels reported by the model in this area follow the conceptual model and are not considered indicative of model boundary issues.
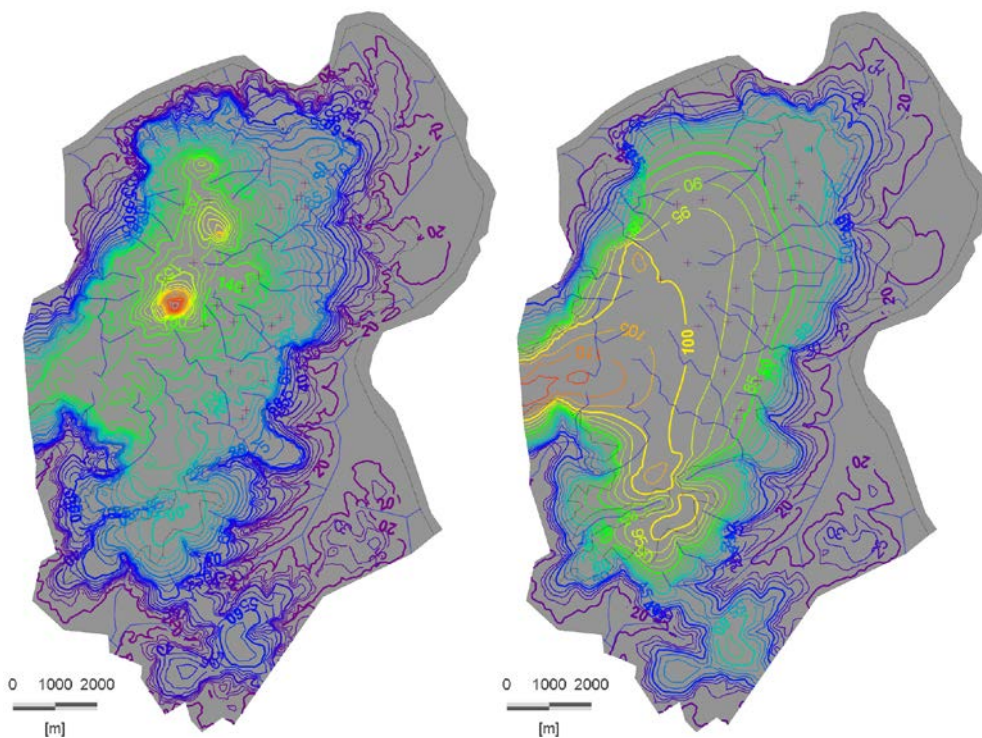
Figure 17: Calibrated model heads at ground surface elevation (left) and the base of Layer 1 (right).

Figure 18 shows a west-east cross section through the model and the modelled head distribution, shown as equipotential contours. This highlights the very strong vertical head gradient through the basalt aquifer and radial groundwater flow towards the basalt margins. The solid blue line represents the calculated phreatic surface, based on interpolation of a zero pressure head surface. However, it is acknowledged that groundwater occurs higher in the profile, and may reside in perched aquifer layers in some locations.
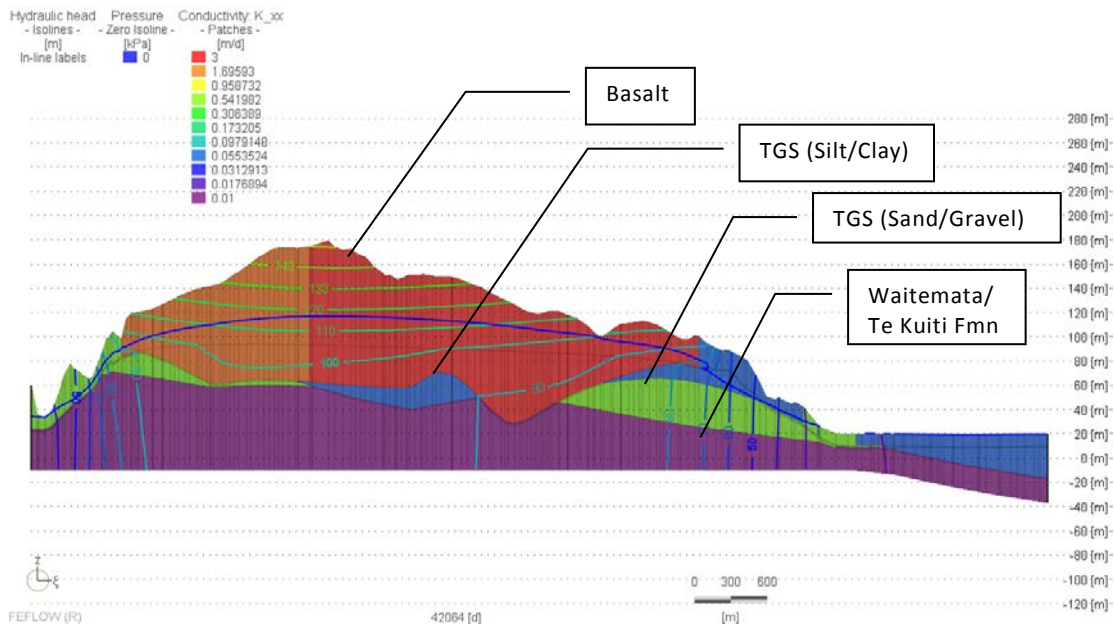
Figure 18: Cross section showing modelled head and unit distribution

4.5.2   Groundwater Flow Budget

The simulated groundwater flow budget for the model calbiration period is summarised below. Figure 19 illustrates that in the absence of abstraction (prior to records being available from around 2005), recharge and surface water discharge are essentially in balance. Captures and releases from storage are primarily seasonal, in the form of groundwater level rises during winter and recessions during summer.
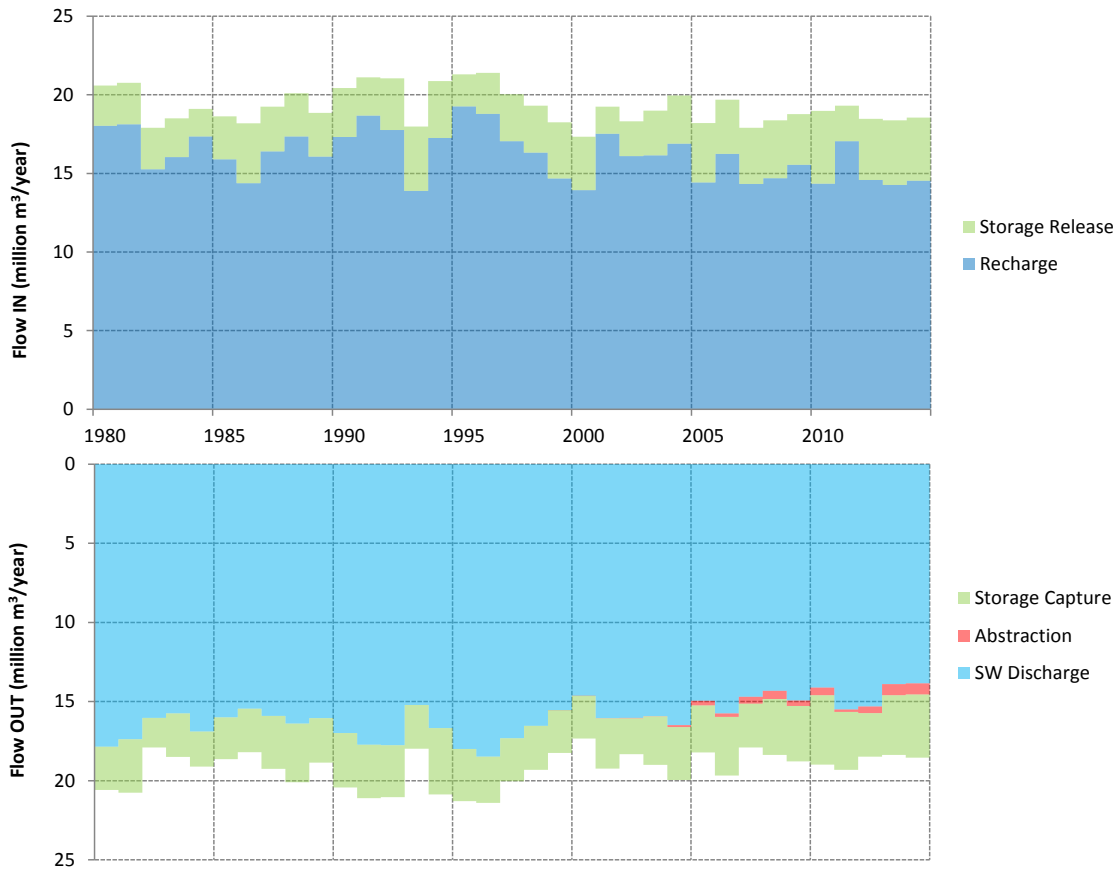
Figure 19: Annual groundwater flow budget for the calibrated model

The month by month flow budget over the final five years of the calibration period is shown in Figure 20. This illustrates how the aquifer responds seasonally to variations in recharge and to a lesser extent, pumping. The results suggest that the system as a whole is relatively efficient at storing high winter recharge and discharging to surface water at a relatively steady rate throughout the year. This is supported by surface water gauging data in the area.

While groundwater abstraction is occurring for summer irrigation, the response is a combination of enhanced releases from aquifer storage and reduced discharges to surface water. It should be noted that storage capture and release will always balance in the long terms, such that the volume of water abstracted will be balanced by the same volume lost from surface discharges. Aquifer storage does however provide an effective buffer to attenuate and dampen the impacts of variable abstraction on surface water flows over time.
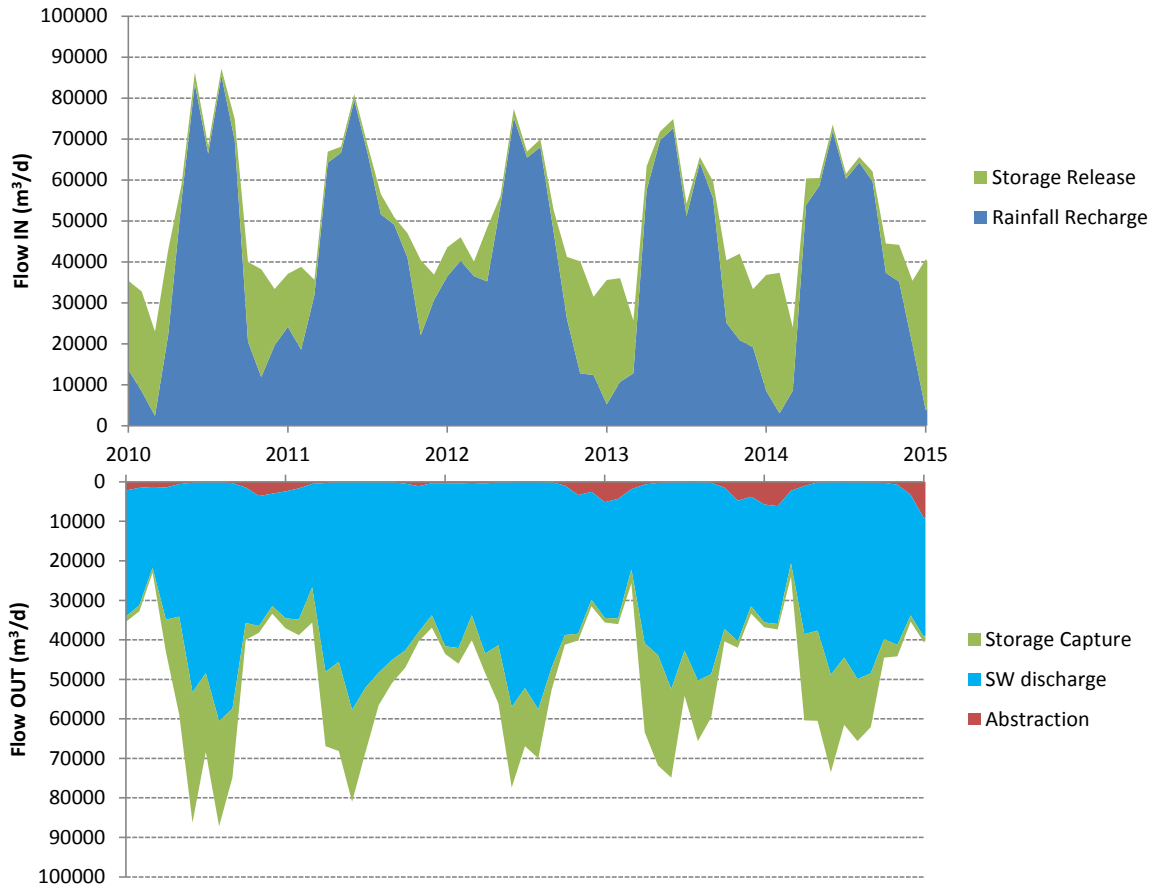
Figure 20: Monthly groundwater flow budget (2010 – 2015) for the calibrated model

Table 3 presents the average model flow budget for the model calibration period (1980 – 2015). This shows that over this period, 99% of recharge was discharged to surface water. The remaining 1% was taken up by abstraction, however this is likely to be an underestimate of pumping over this period due to a lack of metering and unconsented abstraction.

Table 3: Calibrated model flow budget				
Flow component	**Flow IN (m3/d)**	**Flow OUT (m3/d)**	**Net Flux (m3/d)**	**Budget Proportion**
Recharge	44,132	-	44,132	100% (IN)
Net Storage Release/Capture	-	-61	-61	0.1% (OUT)
Surface Discharge	-	-43,708	-43,708	99.0% (OUT)
Abstraction	-	-363	-363	0.8% (OUT)
TOTAL	**44,132**	**-44,132**	**0**	**-**
Notes:				
Inflow terms are positive while outflow terms are negative. A total net flux of zero indicates that the model flow balance is closed.				

Table 4 shows the flow budget for the basalt formation during the calibration period. The imbalance in total flows for this area indicates the net export of groundwater from the basalt to other areas of the model. Overall, the flow budget for the basalt zone suggests that of the 34,716 m^3/d of average inflow, 58% either discharges to streams or is abstracted by bores within the basalt domain and the remaining 42% either discharges to surface water bodies or is abstracted from bores outside the basalt domain.

Table 4: Calibrated model flow budget (basalt subdomain)				
Flow component	**Flow IN (m³/d)**	**Flow OUT (m³/d)**	**Net Flux (m³/d)**	**Budget Proportion**
Recharge	34,490	-	34,490	99.3% (IN)
Net Storage Release/Capture	226	-	226	0.7% (IN)
Surface Discharge	-	-19,945	-19,945	57.5% (OUT)
Abstraction (within Basalt)	-	-202	-202	0.6% (OUT)
TOTAL	**34,716**	**-20,147**	**-14,569**	**42.2% (OUT)**
Notes:				
Inflow terms are positive while outflow terms are negative. A total net flux of -14,569 m³/d indicates the average flow from the basalt subdomain to other parts of the model domain.				

The modelled distribution of groundwater discharges to the surface (i.e. to springs and streams) is shown in Figure 21. Given the sensitivity of discharge to ground elevation and modelled groundwater levels, the exact distribution of discharge, particularly at higher elevations, is considered relatively uncertain. It is considered likely that discharges to the surface would occur at higher

elevations on the basalt than reported by the model, due to local scale heterogeneity associated with the alternating sequences of aquifers and aquitards. At lower reaches of the surface water catchments, these uncertainties are reduced as more flow is accumulated over a broader area. Consequently, model predictions regarding flows at a broad scale are considered more appropriate for assessment than local scale impacts.

The modelled distribution of surface water discharges suggests that most discharge is associated with changes in slope or geological interfaces. The highest discharges tend to occur near the edges of the basalt and in some valleys where Tauranga Group Sediments outcrop.
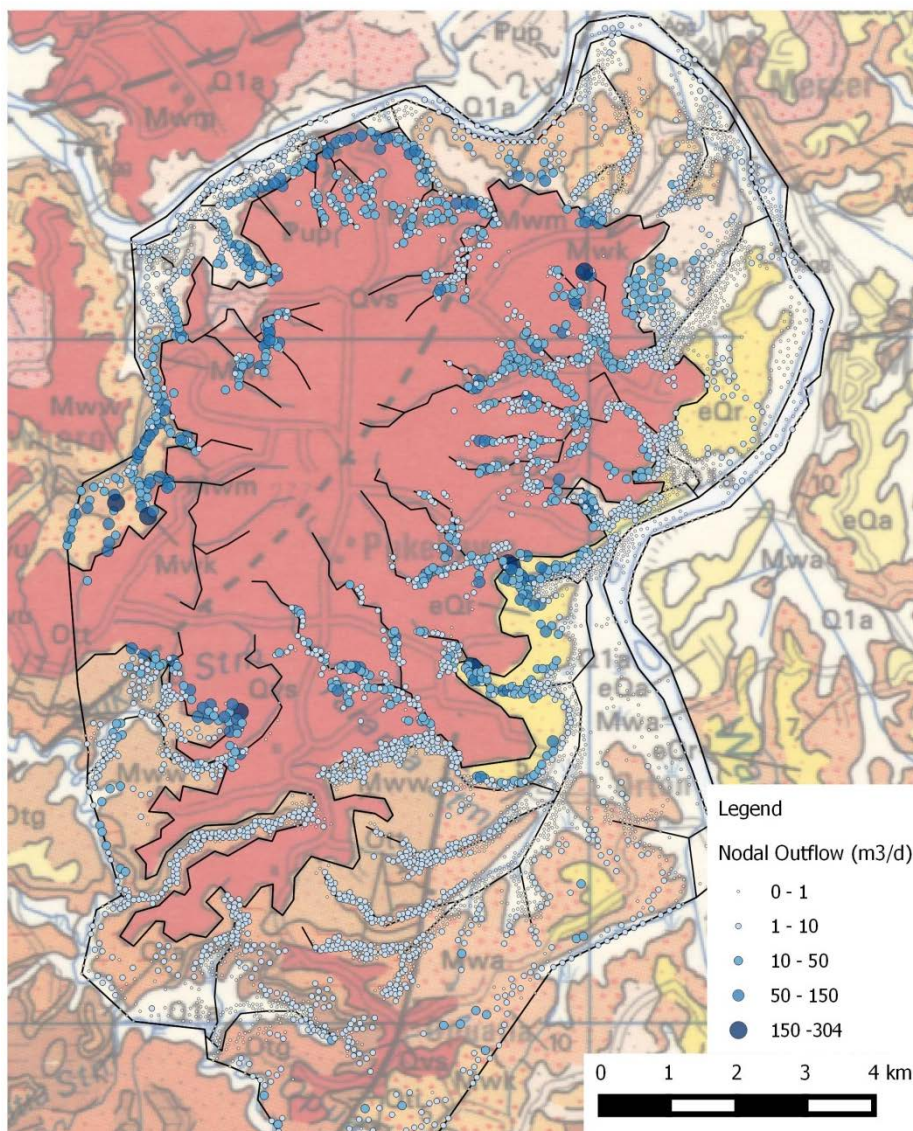
Figure 21: Modelled distribution of surface discharge

4.6   Sensitivity Analysis

The sensitivity of the model calibration performance to various parameters was established primarily during the trial and error calibration process. The following general comments can be made regarding parameter sensitivity:

- The model's ability to reproduce strong observed vertical head gradients was highly sensitive to the definition of vertical hydraulic conductivity in the basalt, and the ratio of horizontal to vertical hydraulic conductivity.

- The quantity of groundwater discharge to surface water was highly sensitive to vertical hydraulic head in the basalt aquifer. Low K_v values were required to support simulated discharge within the gauged catchments. When K_v was set too high, insufficient discharge was simulated within the gauged catchments as it occurred at lower elevations.

- The variability in groundwater discharge and groundwater levels was sensitive to the storage properties set for the top model layer and horizontal and vertical hydraulic conductivity. These were adjusted until a reasonable level of head variation and flow variation was simulated. Discharge variability was also sensitive to recharge variability.

A specific sensitivity assessment was also performed on the calibrated model. The aim of this assessment was to vary selected parameters to find "alternative calibrated models" which could also be considered acceptable but would result in different predictions. These alternative calibrated models form the basis of the predictive uncertainty assessment discussed later in Section 5.4. Results of the sensitivity analysis are discussed below for each of the parameter types analysed. Further details of the sensitivity analysis are provided in Appendix D.

4.6.1   Hydraulic Conductivity

During the calibration process, calibration performance was sensitive to horizontal and vertical hydraulic conductivity, primarily within the basalt geology. Sensitivity to K was observed in average groundwater heads, vertical head gradients, seasonal head fluctuations, average surface water discharges and the variability of discharges.

Calibrated K_h and K_v parameters in the basalt zones were varied iteratively using a multiplier and the various aspects of the calibration performance were evaluated. Parameters were varied (higher and lower) until it was determined that the model outputs (heads and flows) could no longer be considered acceptable in terms of their match to observations. This was judged based on both quantitative measures of calibration performance (i.e. the nRMS error for heads) and semi-quantitative comparison (i.e. visual comparison of low flow and head variability).

Following the approach described above, it was deemed that the model calibration could still be deemed acceptable with K multipliers of 0.5 and 2. Using multipliers of 2 and greater, the variability in discharges to surface water and groundwater levels was too low compared to observations. Reductions in K had a less pronounced influence on the calibration performance. However, with continued reduction in K (e.g. using a factor less than 0.5), modelled discharges to surface water depart from observations and are in general either too variable or overstated. Furthermore, with these reductions to K, model parameters become too far departed from those derived from hydraulic testing and can be justified to a lesser degree. Hence, for the purposes of evaluating model uncertainty, a low K multiplier of 0.5 was selected, resulting in K_h in the basalt ranging from 1 to 1.5 m/d.

4.6.2   Specific Storage

Following a similar approach to that adopted for K, specific storage in layer 1 of the model was varied according to a multiplier. Based on a calibrated S_s of 5×10^{-4} m^{-1}, it was found that the calibration could still be deemed acceptable with multipliers of 0.2 and 2.

5.0   Predictive Simulations

5.1   Scenarios

The calibrated model was used to evaluate two key water abstraction scenarios:

- Abstraction at "current levels" based on recent metering data (1.1 million m^3/year and 8.5% of recharge to the basalt aquifer);

- Abstraction at "consented levels" (2.4 million m^3/year and 19.3% of recharge to the basalt aquifer) assuming all groundwater consents are fully exercised within annual and seasonal limits; and,

- Abstraction at 35% of recharge to the basalt aquifer, or 4.3 million m^3/year. This scenario was created by scaling up the abstraction of existing consented takes by a factor of 1.75, thereby maintaining the same seasonal variation in demand.

A "base case" scenario with no groundwater abstraction was also developed for the purposes of evaluating the absolute groundwater impacts and enabling comparison between scenarios.

All scenarios were run for a period of 35 years with climate data from 1980 to 2015 (the same period as the calibration model) to evaluate impacts under a range of climate conditions.

5.2   Simulated Drawdown

Drawdown was assessed for two simulation times representing winter and summer conditions at the end of each model run – i.e. following 35 years of abstraction at the assumed volumes. Drawdown was calculated as the absolute head difference between the scenario in question, and the "base case" scenario representing no abstraction. Therefore the drawdown results indicate an absolute drawdown impact rather than an expected change to current water levels. Results were analysed in this way so that the absolute magnitude of impacts for different scenarios could be compared and to eliminate the effects of natural, climate driven variability.

Figure 22 shows drawdown contours for the "current abstraction" scenario, shown for the base of model layer 1. This layer was selected as it represents an equivalent elevation to the majority of abstraction, and corresponds to the highest level of drawdown in the vertical profile. Drawdown is typically less for higher and lower model layers.
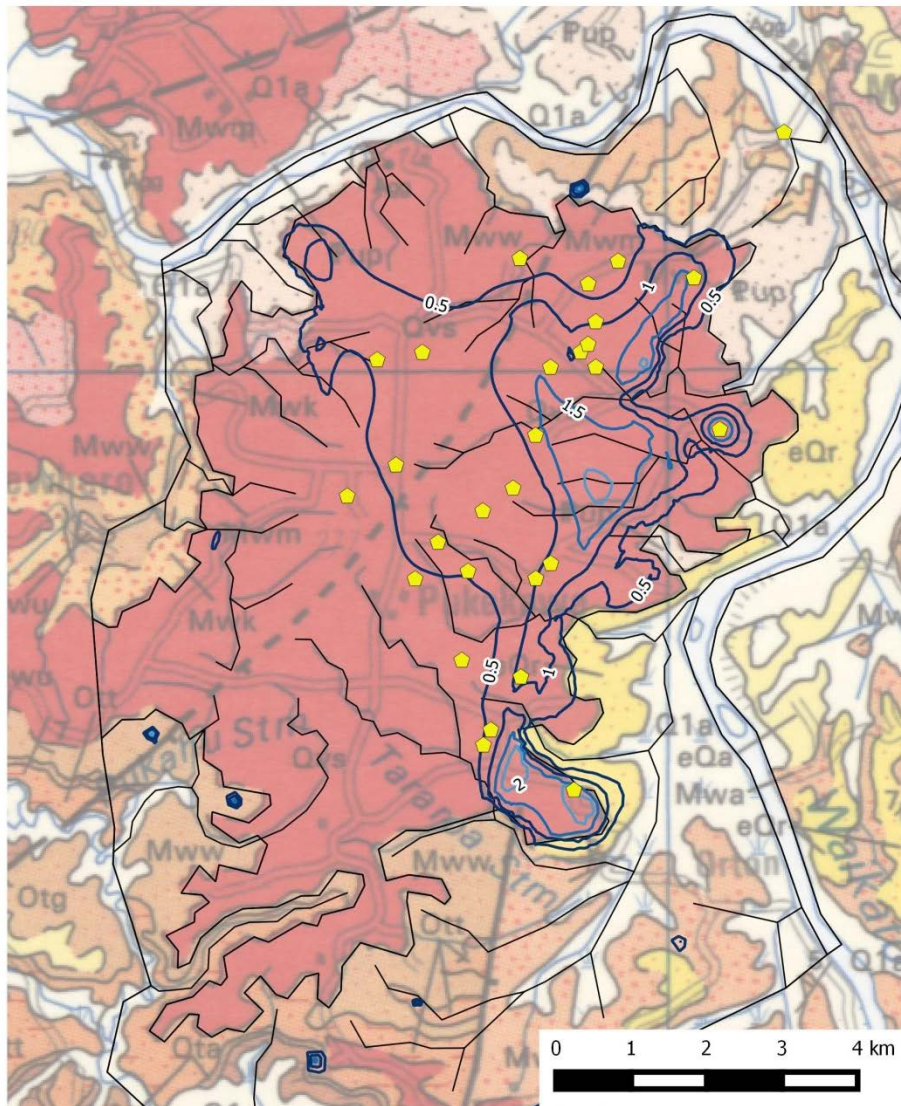
Figure 22: Simulated winter drawdown for current levels of groundwater abstraction at base of model layer 1

The drawdown result for the winter period, where groundwater abstraction is at a minimum, indicates the long term, cumulative aquifer drawdown. Despite the majority of abstraction occurring in the north and east of the model domain, the maximum drawdown occurs in the centre of the basalt, corresponding to the higher existing groundwater pressures. This is indicative of a broad and spread-out drawdown across the bulk of basalt aquifer extent. Drawdown is contained almost entirely within the basalt, suggesting that it behaves in relative isolation from the surrounding units.

Figure 23 shows drawdown for the same layer and time period for the consented abstraction scenario.
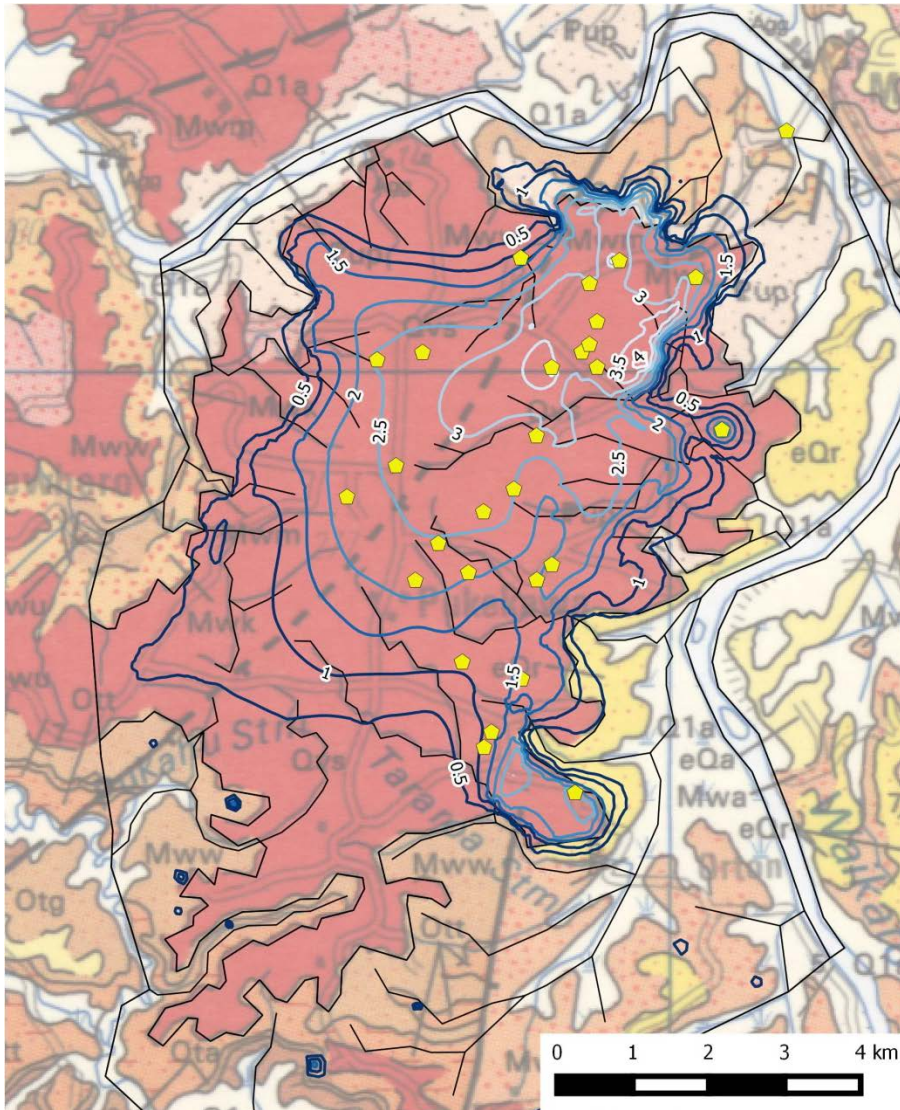
Figure 23: Simulated winter drawdown for consented levels of groundwater abstraction at base of model layer 1

The distribution of drawdown is similar to the current abstraction scenario, however, the magnitude of drawdown is increased corresponding to the increase in abstraction volumes. The cumulative drawdown magnitude in most areas is more than twice that of the current abstraction scenario.
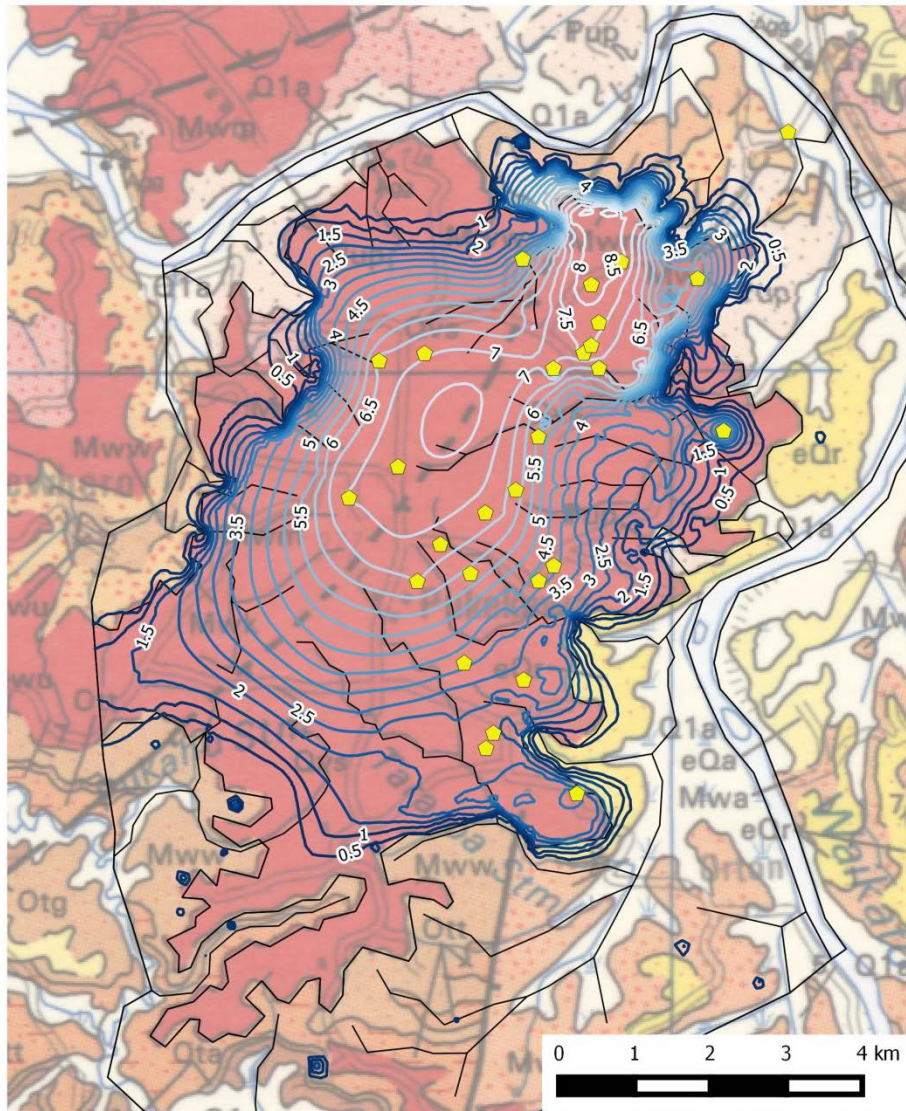
Figure 24: Simulated winter drawdown for groundwater abstraction equivalent to 35% of rainfall recharge at base of model layer 1

Drawdown during the peak irrigation season in summer is subject to local scale drawdown around abstraction bores. Figure 23 shows the simulated drawdown contours corresponding to a January time step at the end of the simulation period, during which pumping is at a seasonal maximum. The drawdown cones around individual takes can be seen.
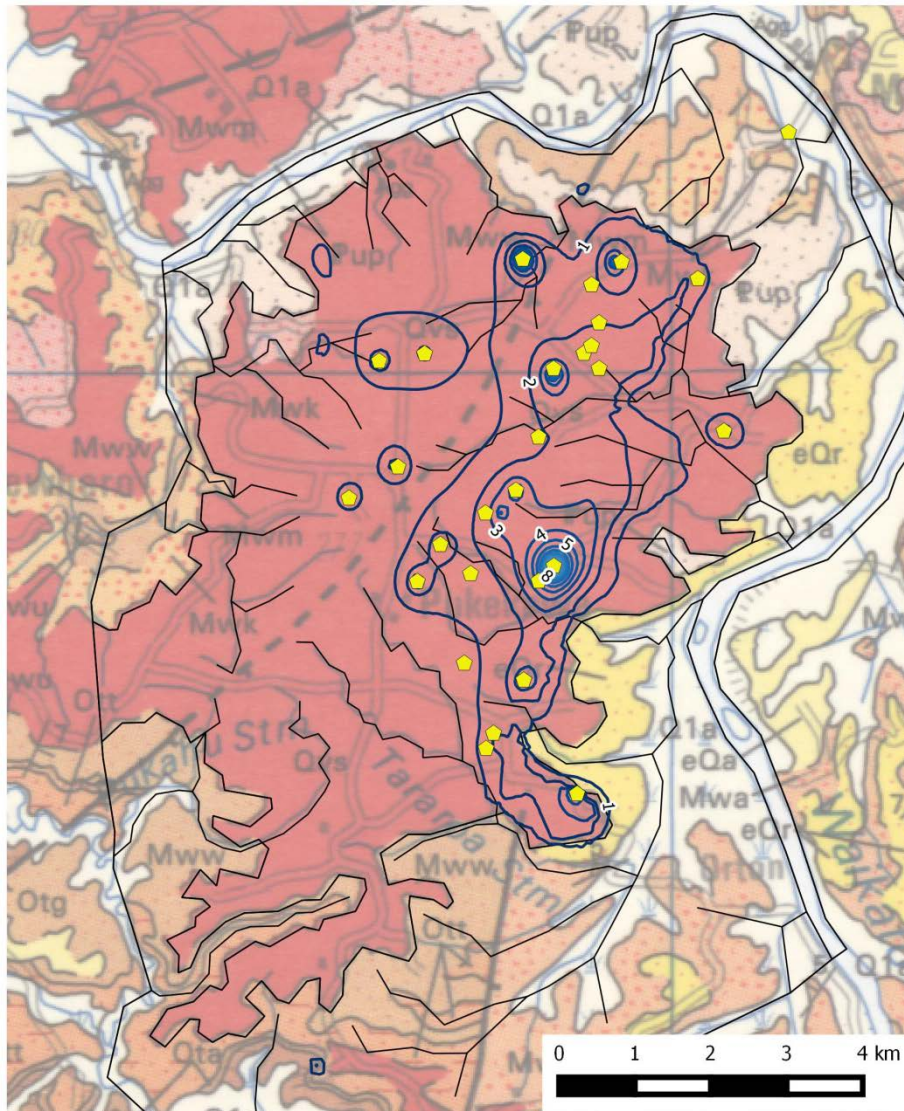
Figure 25: Simulated summer drawdown for consented levels of groundwater abstraction at base of model layer 1

Model results indicating local scale drawdown have a greater degree of uncertainty due to the role of local scale aquifer properties.

5.3   Impacts on Surface Water Discharges

5.3.1   Average Surface Water Impacts

The average groundwater flow budgets for each of the model simulations are shown in Figure 26. This illustrates the relative magnitude of abstraction in each of the scenarios and the corresponding reductions in surface water discharge. Over the 35 year simulation period, net changes in aquifer storage in response to

abstraction are negligible and abstraction is balanced in equal volume by reductions to surface water discharge.
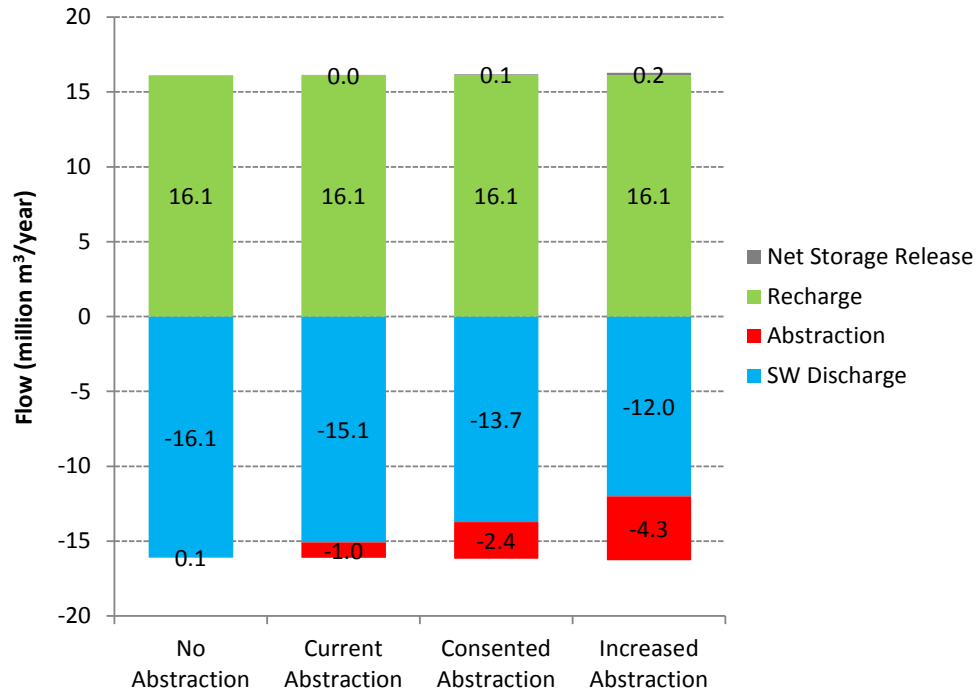
Figure 26: Model flow budgets for the predictive scenarios

Abstraction represents 6.4% and 15.1% of total rainfall recharge to the model domain in the current and consented abstraction scenarios, respectively. Expressed as a portion of recharge to the basalt aquifer (12.6 million m³/year), these become 8.2% and 19.3% of basalt recharge.

5.3.2   Spatial Distribution of Impacts

Figure 27 shows the spatial distribution of reductions in groundwater discharge to surface water for the consented abstraction scenario. This suggests that the majority of impacts are contained within the extent of the basalt, with relatively few impacts to surface water discharge occurring beyond the basalt extent. This is the case despite almost half of the recharge to the basalt discharging to surface water beyond the basalt aquifer extent. This can be explained by the distribution of predicted drawdown effects (see Figure 22 and Figure 23). Discharges to surface water are dependent on groundwater heads in relation to the ground surface elevation at discharge locations. Most of the flow impacts are confined to within the basalt extent because most of the drawdown is within the same area.
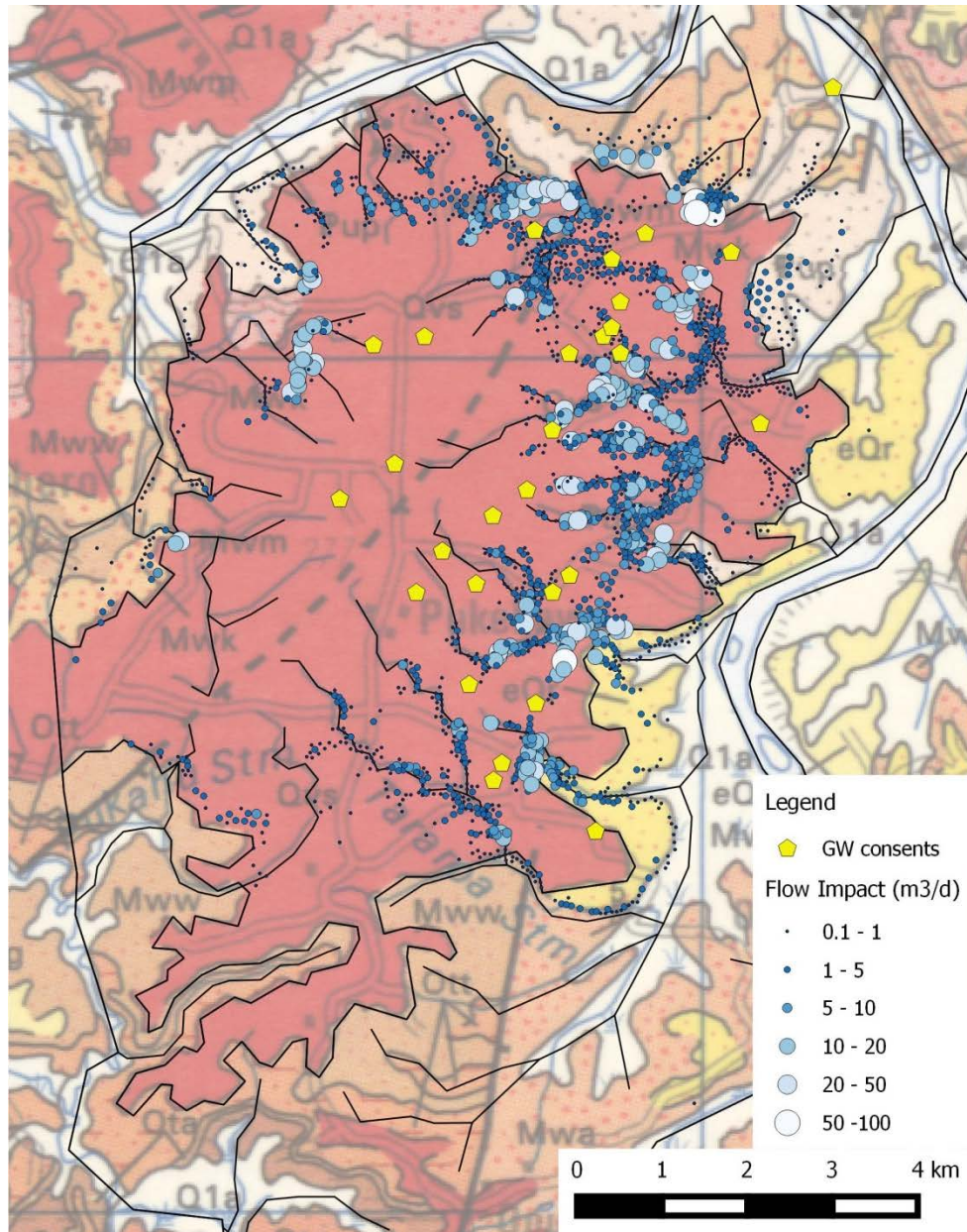
Figure 27: Distribution of modelled impacts on surface water discharge (consented abstraction scenario)

5.3.3   Timing of Impacts and Effects on Low Flows

The influence of seasonal abstraction variability on surface water flow reductions was examined by comparing simulated monthly surface water discharge volumes. The difference between surface water discharges for the base case (no abstraction) scenario and the scenario in question was evaluated on a monthly basis.

Figure 28 shows modelled impacts to surface water discharge for the current abstraction scenario for the final ten years of the simulation. The relationship between seasonally variable abstraction (dark red line), and the resulting impact on surface water discharges (light blue line) illustrates the likely temporal attenuation of pumping impacts. The degree of variability in surface water flow impacts is dependent on the variability of abstraction and the aquifer's capacity to buffer variable stresses via storage.

In the current abstraction scenario, the maximum monthly abstraction rate is 9,491 m^3/d in January. The average annual maximum surface flow impact for the scenario is 4,914 m^3/d. The overall average impact on surface water is equivalent to the average rate of abstraction (2,836 m^3/d). Hence, impacts to surface water were predicted to have a peak attenuation factor[2] of 69%.
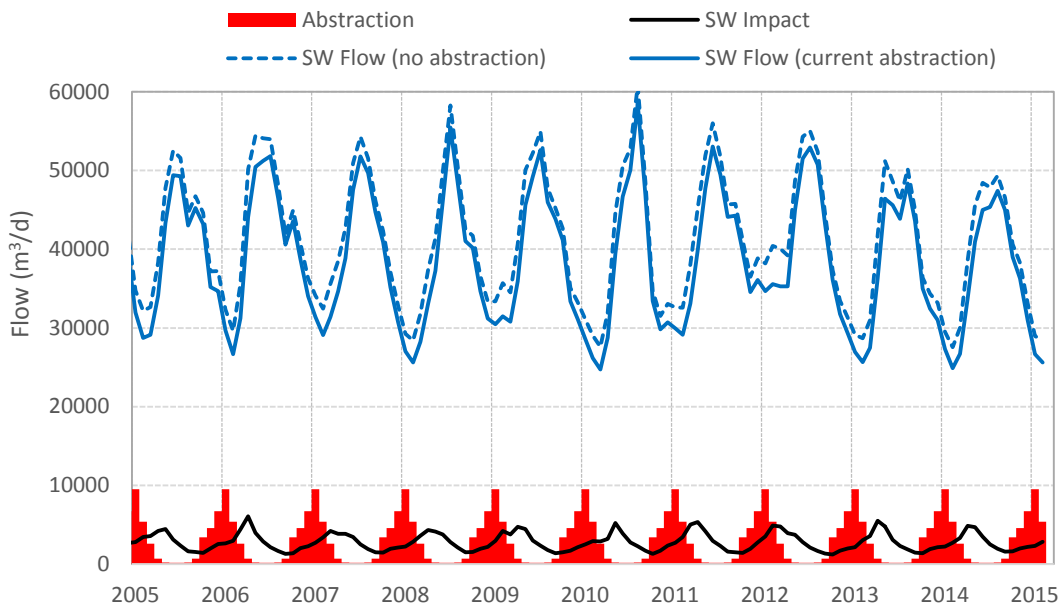
Figure 28: Time series of modelled impacts to surface water discharge (current abstraction scenario)

Figure 29 shows the time series surface water discharge impacts for the consented allocation scenario. This shows a similar response to the current allocation scenario, with increased effects in response to the increased abstraction. In this scenario, the maximum monthly abstraction rate is 19,881 m^3/d in January. The average annual maximum surface flow impact for the scenario is 10,886 m^3/d. The overall average impact on surface water is equivalent to the average rate of abstraction (6,687 m^3/d). Hence, flow impacts

---

[2] Peak attenuation factor = (peak GW abstraction – peak SW flow impact) / (peak GW abstraction – average GW abstraction) * 100. E.g. PAF = (9,491 – 4,914) / (9,491 – 2,836) * 100 = 69%

for this scenario have a peak attenuation factor of 68%, similar to the current abstraction scenario.
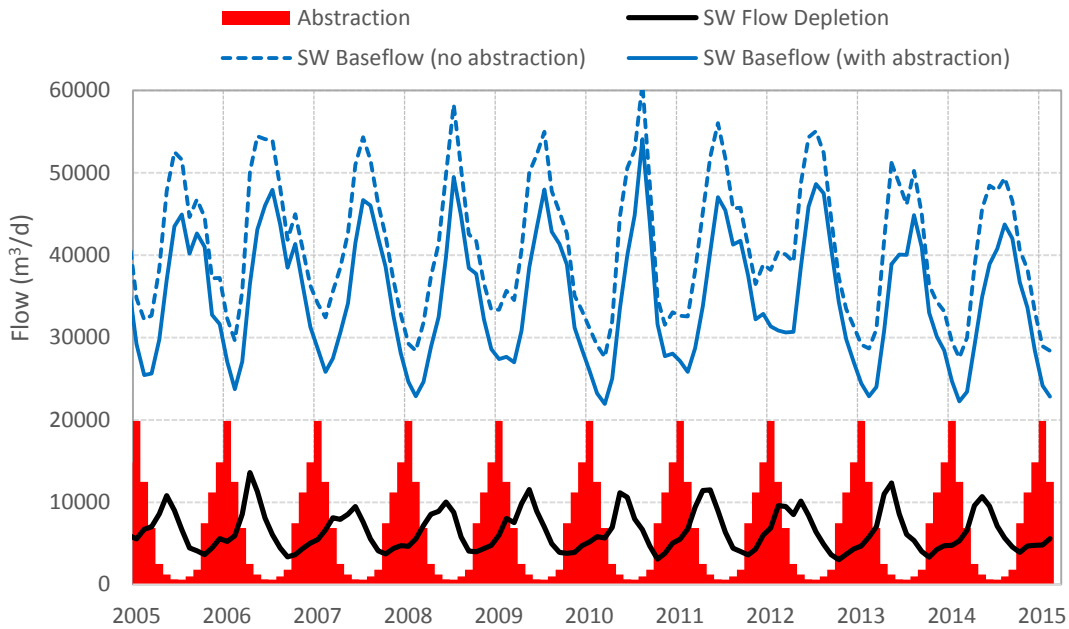
Figure 29: Time series of modelled impacts to surface water discharge (consented abstraction scenario)

Figure 30 shows the time series surface water discharge impacts for the increased allocation scenario with abstraction equal to 35% of recharge to the basalt aquifer. In this scenario, the maximum monthly abstraction rate is 34,858 m^3/d in January. The average annual maximum surface flow impact for the scenario is 18,764 m^3/d. The overall average impact on surface water is equivalent to the average rate of abstraction (11,725 m^3/d). Hence, the modelled peak attenuation factor for this scenario is 70%.
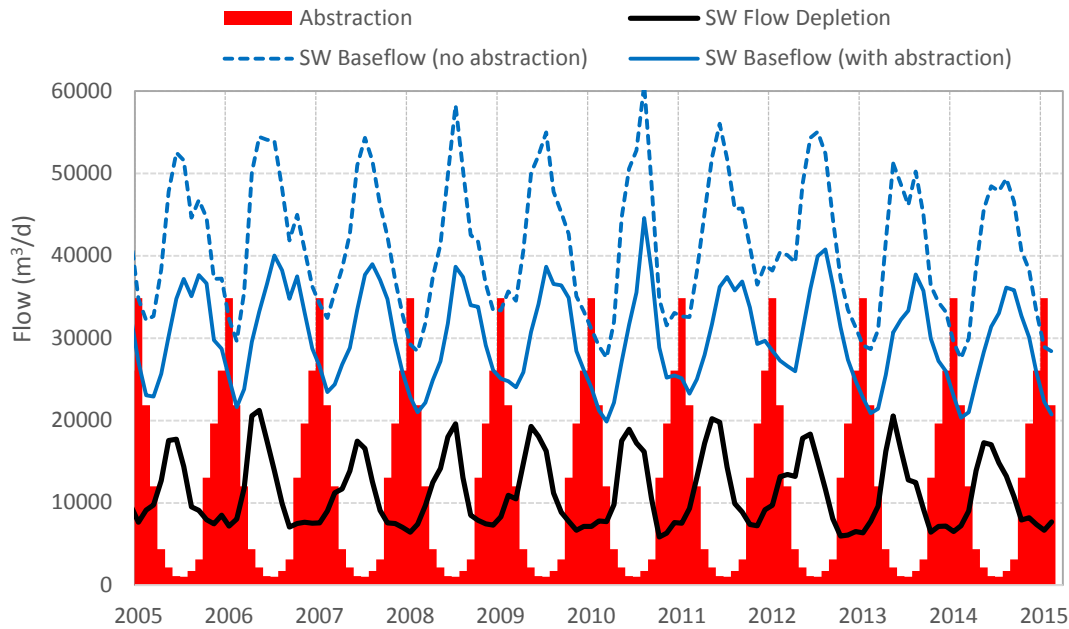
Figure 30: Time series of modelled impacts to surface water discharge (increased abstraction scenario; 35% basalt recharge)

5.3.4   Impacts on Q_5 flows

The impact on low flow statistics was also evaluated, in particular the 5 year low flow, or Q_5. The Q_5 was calculated for discharges to surface water over the whole model area for each of the scenarios. The modelled impact on the Q_5 flow, when compared to the no abstraction scenario was then evaluated. It is considered appropriate to ignore surface water runoff and consider only groundwater contributions to stream flows when assessing low flows, because these occur at times when surface waters are sustained only by baseflow.

Impacts on the overall Q_5 flow for each scenario are shown in Table 5. This indicates that with increasing allocation, the relative impact on the Q_5 slightly decreases. For instance, there is a 9% Q_5 impact simulated for the current abstraction scenario, which amounts to 8.2% of basalt recharge. Conversely, abstraction totalling 35% of basalt recharge results in a Q_5 reduction of 27%. This suggests that at increasing levels of allocation pressure, the lowest flows are supported by reserves in aquifer storage, and more of the impact is felt on groundwater discharge during average to wet months. This is observable in model results as a timing offset between the occurrence of annual flow minima and annual stream depletion maxima. Figure 31 shows the months in which surface flow minima typically occur, compared to the typical timing of peak stream depletion effects. This shows a three month offset (February to May) between typical flow minima and stream depletion maxima. While this analysis

is based purely on modelled results, it explains the differences noted between peak stream depletion effects and Q_5 impacts.
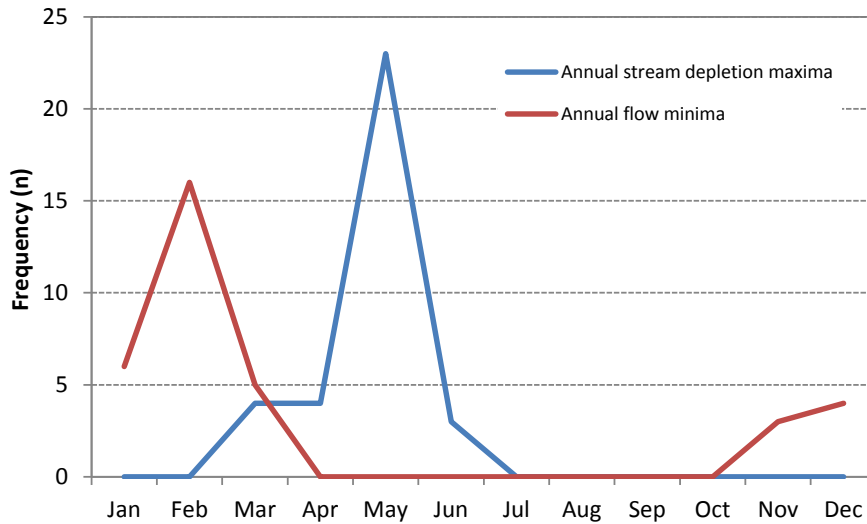
Figure 31: Seasonal distributions of annual stream depletion maxima and low flow minima (consented abstraction scenario)

The current surface water allocation regime operated in the Waikato region aims to preserve a minimum flow in surface water bodies of 70% of the Q_5 flow. Typically, up to 30% of the Q_5 is allowed to be allocated with varying levels of reliability applies such that some takes (with lower reliability) may be subject to restrictions during times of low flow, as necessary to preserve 70% of the Q_5.

Table 5: Modelled impacts on Q_5 flows				
Scenario	Abstraction (% of basalt recharge)	Q_5 flow (m³/d)	Q_5 impact (m³/d)	Q_5 impact (%)
No Abstraction	0%	31,156	-	-
Current Abstraction	8.2%	28,262	2,894	9%
Consented Abstraction	19.3%	25,143	6,012	19%
Increased Abstraction	35%	22,831	8,324	27%

The spatial distribution of the impacts on Q_5 flows was evaluated by subdividing the study area into 8 catchment zones, as set out in Figure 32.
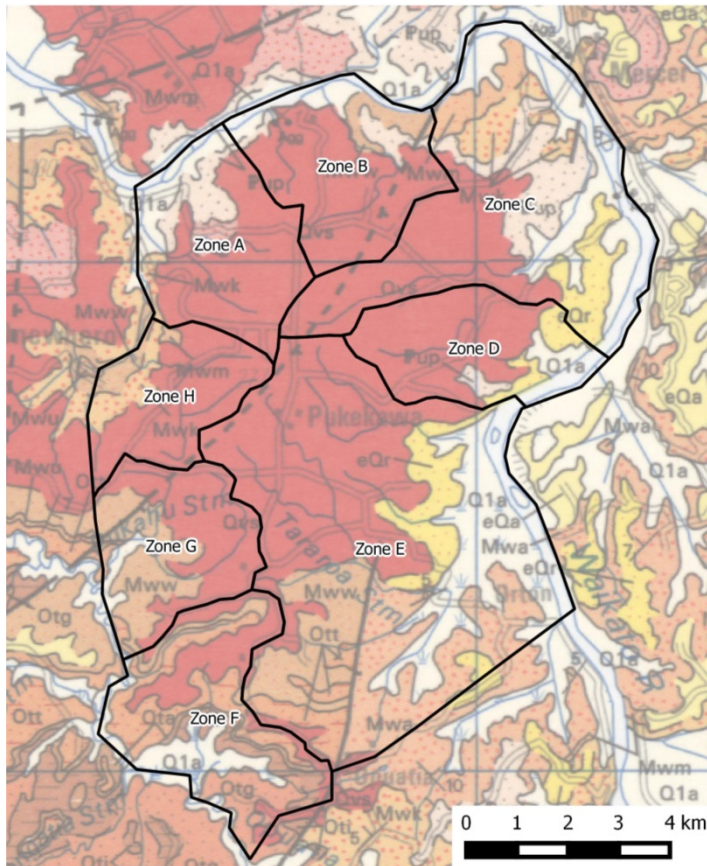
Figure 32: Flow analysis zones

Figure 33 shows the simulated Q_5 flows within each of the 8 analysis catchments. The greatest impact on Q_5, as indicated by the difference between the bars, is in Zone C, corresponding to the area with the most intensive abstraction demand. However, the impacts on low flows are relatively similar in magnitude, indicating distribution of low flow impacts across the broader study area.
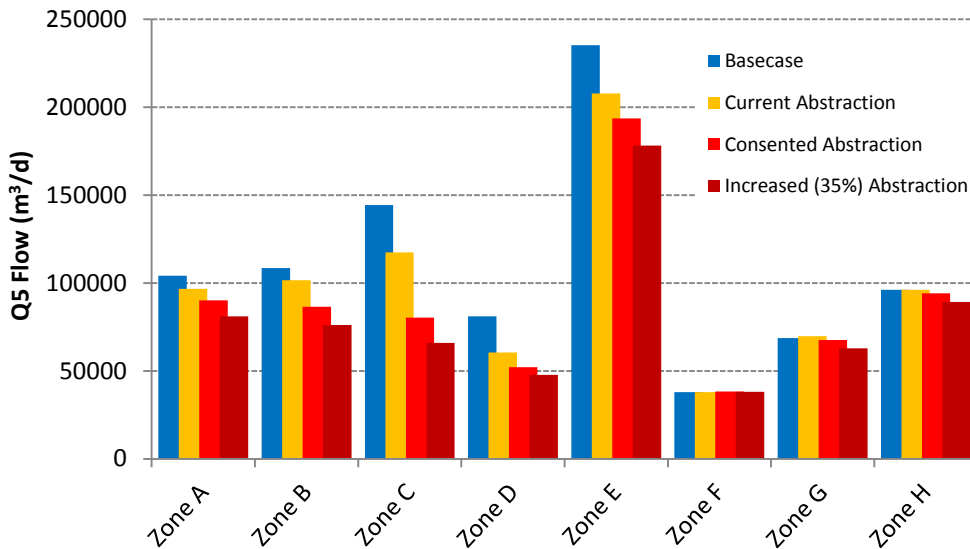
Figure 33: Simulated Q_5 flows by analysis zone for all scenarios

5.4   Predictive Uncertainty

The approach to assessing model prediction uncertainty was tailored to consider its influence on the key questions posed to the model. The key questions considered most important for decision making, for which the influence of uncertainty was assessed, were as follows:

1. To what degree are stream depletion effects temporally attenuated from seasonally variable groundwater pumping stresses?

2. To what extent are surface water low flows (i.e. the Q_5) affected by varying groundwater allocation levels?

Rather than carrying out an exhaustive sensitivity and uncertainty assessment, which would require a prohibitively large number of model runs, a focussed approach was adopted. This involved considering a limited number of "alternative calibrated models" with modified parameter values which still could be deemed acceptable in terms of calibration performance.

Parameters were selected for inclusion in the uncertainty assessment based on the conceptual hydrogeological understanding and insights gained during the model calibration process. Additionally, the parameters selected were those which required some iterative adjustment during model calibration and were expected to have a notable influence on prediction outcomes. On this basis, horizontal and vertical hydraulic conductivity, as well as specific storage were chosen to be varied during the predictive uncertainty assessment. Parameter values used for the alternative calibrated models were determined during calibration sensitivity assessment, which is described in Section 4.6.

5.4.1   Basalt Hydraulic Conductivity

Prediction uncertainty associated with horizontal and vertical hydraulic conductivity of the basalt was assessed using the "Consented Abstraction" scenario. It can be assumed that other scenarios would be subject to similar degrees of uncertainty relative to their results. K_h and K_v values in the basalt were varied by factors of 0.5 and 2 representing plausible alternative calibrated models, as derived during the calibration sensitivity assessment (Section 4.6). Each variation required two simulations to be run (i.e. with and without abstraction) to enable the calculation of relative effects. Hence, results are shown as a change or impact relative to a "no abstraction" scenario. It is worth noting that baseline results are different under each of the cases and the relative impact is shown.

Figure 34 shows simulated impacts to surface water low flows for the consented abstraction scenario, with additional plots (dashed lines) representing the results under the higher and lower K alternative models. This indicates the relative magnitude of prediction uncertainty regarding attenuation of stream depletion effects brought about by uncertainty in assumed basalt K values. A peak attenuation factor of 68% was derived from the "best estimate" model and this varied between 39% and 84% under the lower and higher uncertainty bounds on basalt K, respectively.
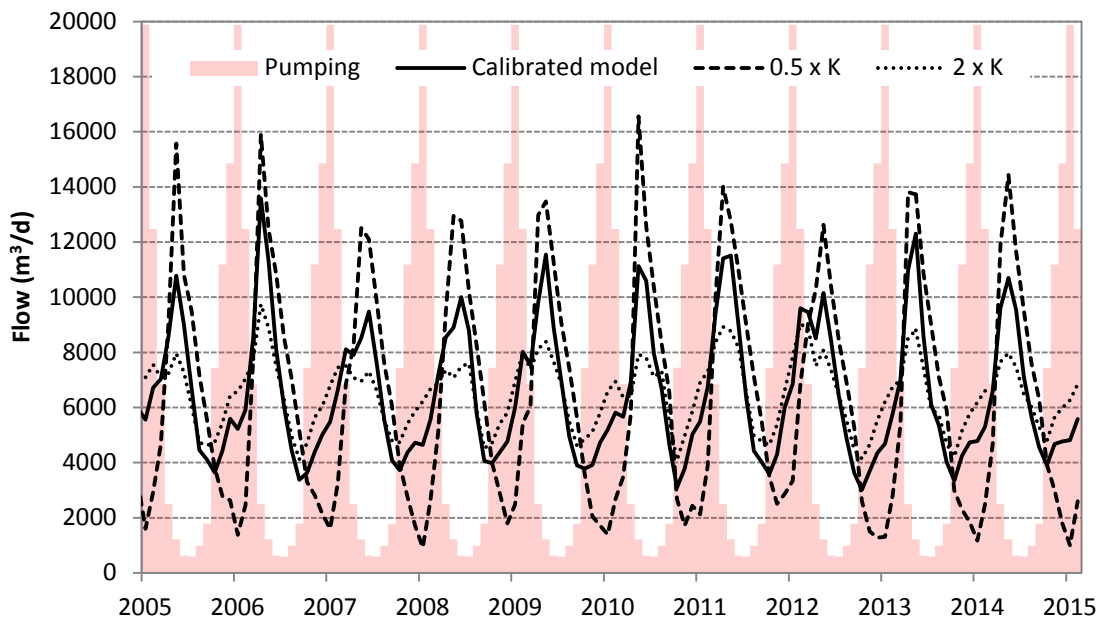
Figure 34: Time series of modelled impacts to surface water discharge (consented abstraction scenario) – predictive uncertainty assessment for basalt hydraulic conductivity (K)

Table 6 shows the predicted impacts to Q_5 low flows associated with the uncertainty bounds for basalt K. Compared to peak attenuation, Q_5 impacts are less sensitive to basalt K uncertainty, with a range of between 11.7% and 20.5% impact, around a central value of 19.3%. Additionally, the lower uncertainty bound on K produced a lower Q_5 impact. This result is owing to a lower baseline Q_5 flow, combined with the offset timing between low flow occurrence and stream depletion maxima (as discussed in Section 5.3.4).

Table 6: Predictive Uncertainty in Low Flow Impacts (Basalt K)				
Scenario	Q_5 (no abstraction) (m³/d)	Q_5 (consented abstraction) (m³/d)	Q_5 impact (m³/d)	Q_5 impact (%)
Basalt K × 0.5	23,215	20,498	2,717	11.7%
Calibrated model	31,156	25,143	6,012	19.3%
Basalt K × 2	34,882	27,724	7,158	20.5%

5.4.2   Specific Storage

Prediction uncertainty associated with aquifer storage properties was also assessed using the "Consented Abstraction" scenario. Specific storage (S_s) in model layer 1 (as a proxy for unconfined storage – refer to Section 3.5) was varied by multipliers of 0.2 and 2 following outcomes of the calibration sensitivity assessment.

Figure 35 shows simulated impacts to surface water low flows for the consented abstraction scenario, with additional plots (dashed lines) representing the results under the higher and lower S_s alternative models. This indicates the relative magnitude of prediction uncertainty regarding attenuation of stream depletion effects brought about by uncertainty in assumed storage parameters. A peak attenuation factor of 68% was derived from the "best estimate" model and this varied between 56% and 74% under the lower and higher uncertainty bounds on S_s, respectively.
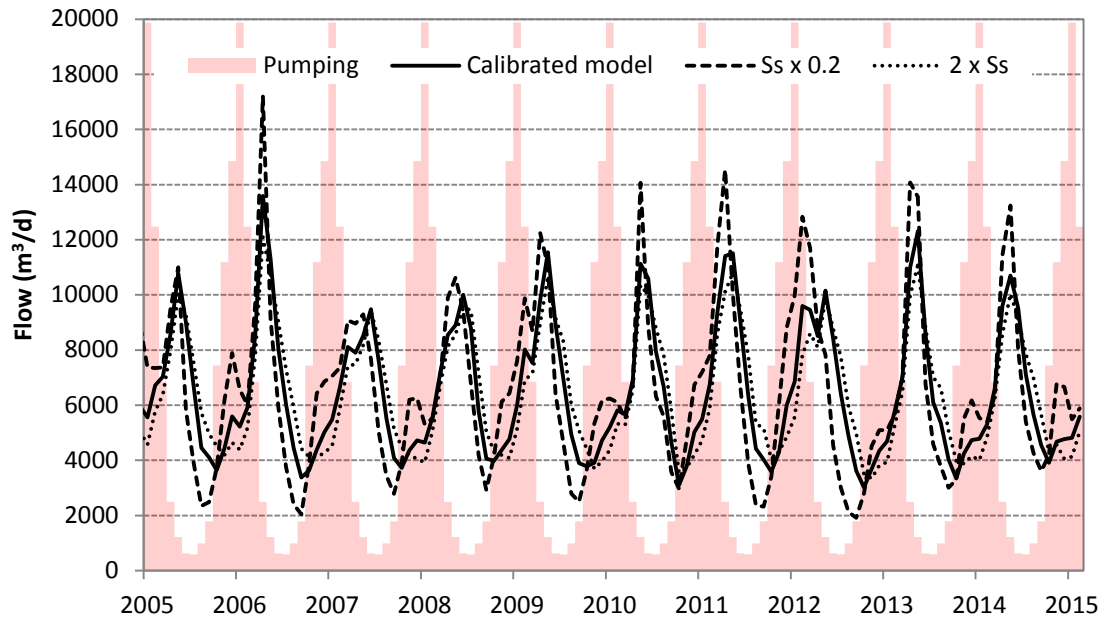
Figure 35: Time series of modelled impacts to surface water discharge (consented abstraction scenario) – predictive uncertainty assessment for specific storage (S_s)

Table 7 shows the predicted impacts to Q_5 low flows associated with the uncertainty bounds for S_s. Compared to peak attenuation, Q_5 impacts are also less sensitive to storage, with a range of between 16.7% and 23.4% impact, around a central value of 19.3%.

Table 7: Predictive Uncertainty in Low Flow Impacts (S_s)				
Scenario	**Q_5 (no abstraction) (m³/d)**	**Q_5 (consented abstraction) (m³/d)**	**Q_5 impact (m³/d)**	**Q_5 impact (%)**
$S_s \times 0.2$	26,508	20,308	6,200	23.4%
Calibrated model	31,156	25,143	6,012	19.3%
$S_s \times 2$	31,953	26,625	5,328	16.7%

6.0   Discussion

6.1   Allocation Limit Setting

In setting groundwater allocation limits for the Pukekawa aquifer, WRC seeks an understanding of the cumulative impacts expected with increasing levels of groundwater abstraction. Ultimately the allocation limit will reflect a level of impact deemed acceptable in terms of surface water flow depletion.

The modelling detailed in this report provided an assessment of impacts to Q_5 flows based on increasing levels of groundwater abstraction or groundwater allocation (Table 5). A key question asked of the model was the ability of the aquifer to buffer surface water flow depletion effects resulting from the seasonally variable abstraction. Modelling suggests that peak abstraction rates are likely to be attenuated by at least 68%. This is influential in the determination of predicted low flow impacts associated with each allocation scenario.

6.2   Management Zone Delineation

Results of the modelling have indicated that the surface water flow impacts arising due to abstraction from the basalt aquifer and the underlying sand aquifer are spatially broad, despite the concentration of demand in the north-east of the study area. As such, it is considered appropriate to manage total allocation for the basalt aquifer and underlying aquifers as a single management unit.

The depth and proximity of individual abstraction bores to streams will influence the level of short term surface water flow depletion. These impacts are best managed as part of the consenting process, via the assessments of environmental effects. However, from an allocation perspective, the cumulative impacts of abstraction within the management unit as a whole are of primary concern.

6.3   Groundwater Take Restrictions

Various approaches and methods are available for restricting groundwater takes during times of low stream flow, depending on their level of connection to surface water bodies. This is typically centred on the concept of hydraulic communication and the immediacy of stream depletion effects following groundwater pumping. Restrictions to groundwater takes are most effective where bores have a rapid stream depletion response and accordingly, a rapid stream flow recovery response.

In the case of groundwater abstraction from the Pukekawa basalt aquifer, the value in applying periodic water take restrictions to groundwater users is considered to be limited based on the results of the modelling. This is largely owing to the degree attenuation occurring between groundwater abstraction and

stream depletion effects. Furthermore, minimum stream flows typically occur between February and May, after peak abstraction demands which typically occur in January. Hence any stream flow recovery brought about by periodic groundwater take restrictions will be small when compared to the potential loss of supply to resource users.

6.4   Surface Water Flow Monitoring as Consent Conditions

WRC may consider placing conditions on new groundwater takes that require applicants to monitor surface water flows as a means to manage the potential surface water depletion effects. The usefulness of this approach is discussed below based on insights into system dynamics gained during the modelling.

Results of the modelling suggest that the surface water flow impacts resulting from groundwater abstraction are both spatially distributed across the basalt aquifer extent, and temporally attenuated due to seasonal aquifer storage. The implication for monitoring surface water flows are that:

- The response to abstraction in a stream flow record will likely be difficult to detect due to its gradual/delayed onset;

- It will be difficult to separate the effects of abstraction from the consent subject to the monitoring and other groundwater takes, due to the spatial distribution of impacts; and,

- It will be difficult to separate abstraction derived effects from natural variations in flow from climatic variations.

For the above stated reasons, it is not recommended that surface water flow gauging be adopted as a basis for setting resource consent conditions. Rather, setting appropriate allocation limits to manage the cumulative stream depletion effects is considered to be more pragmatic. If there are concerns that an individual application may have a more direct impact on surface flows, then would be evaluated in greater detail as part of the assessment of effects.

7.0   Conclusions

Key findings of the Pukekawa aquifer numerical groundwater modelling assessment include the following:

- Recharge to the basalt aquifer is considered to be in the order of 280 – 350 mm/year, amounting to approximately 12.6 million m^3/year over the basalt extent;

- Based on this model, approximately 58% of recharge to the basalt aquifer is likely to discharge directly to surface water;

- The remaining 42% is predicted to discharge to surface water bodies beyond the extent of the basalt. This can either be via horizontal

recharge to the adjacent sediments around the basalt margins, or from vertical recharge to sediments beneath the basalt (such as the Puketoka formation);

- While the split of water discharged to surface water inside or outside the basalt margin is subject to some modelling uncertainty, we know that at the broader scale of the study area, recharge is balanced by surface water discharge in equal volumes i.e. the groundwater catchment is closed within the study area;

- Over the long term all groundwater abstraction is balanced in equal volume by surface water flow depletion;

- Seasonally, depletion tends to increase gradually to a peak at the end of the irrigation season followed by a recession in impacts during the winter;

- Seasonally variable abstraction translates into a relatively constant surface water flow depletion, with over 68% attenuation of seasonal variability;

- The impact of varying levels of abstraction on Q_5 flows were assessed and results indicated that:

    - Ongoing abstraction at current rates would likely result in an average impact to Q_5 flows of 9%;

    - Full utilisation of current allocation limits would likely result in an average impact to Q_5 flows of 19%;

    - An increased allocation limit to 35% of recharge to the basalt aquifer would likely result in a 27% reduction to Q_5 flows;

- Examination of the spatial distribution of Q_5 impacts indicated that impacts are spread relatively evenly across the aquifer extent, with some locally elevated effects in areas of higher groundwater use; and,

- At the scale of analysed sub-catchments (as per Figure 32), the maximum Q_5 impact was 54% compared to the average impact of 27% for the 35% recharge allocation scenario. This indicates that the density and distribution of groundwater takes can have a localised impact on stream flows and the density of demand should be monitored.

8.0   References

Bell, A.R., Cochrane, P.R., Depledge, D., Maggs, G.R., 1991. Pukekawa-Onewhero Area Water Resources. Waikato Regional Council technical report 1991/29.

Golder Associates, 2013. Pukekawa Groundwater Assessment – Phase 1. Steady State Groundwater Model. Report prepared for Waikato Regional Council. February 2013.

Appendix A: Modelling Data Inputs

Climate Data

Daily rainfall and evapotranspiration data were obtained from NIWA's Virtual Climate Station Network (VCSN) (Agent No: 28640). The location of this virtual climate station is located 1.4 km NNE of the Pukekawa basalt cone at NZTM coordinates 1775006E 5867443N.

The VCSN contains continuous daily climate data for stations spaced on a 5 km grid across all of New Zealand. The data is generated by NIWA using actual climate data from physical stations but it contains no gaps, and has been spatially adjusted for elevation and other parameters affecting rainfall distribution.

Geospatial Data

General topographic data including 20 m elevation contours, hydrography, etc. was available from the NZMS 1:50:000 scale map series GIS data. Catchments were delineated based on the 20 m contour data.

Groundwater Levels

Refer to Section 2.3.1 of the main report, which details the groundwater level data used for model calibration.

Groundwater Abstraction Data

Current and historical groundwater take consent information was extracted from WRC's consents database (IRIS). For each consent, data were supplied describing the purpose of the take, the consent holder, Bore ID, consent dates and annual and seasonal water take limits.

Many of the consents also included metered abstraction data, which were extracted from WRC's WISKI database. Timeseries records of metered abstraction were available for 25 groundwater take consents in the model area and spanned from 2000 to the time of model development in 2015.

Surface Water Flows

Spot measurements of stream flow were available in WRC's WISKI database for eight (8) locations within the study area. The majority of records span from 1982 to approximately 1991. One record (946_1) also contains data between 2009 and 2013. A total of 204 flow measurements were available across the 8 sites. Figure A-1 shows the flow measurements at the 8 spot gauge sites.
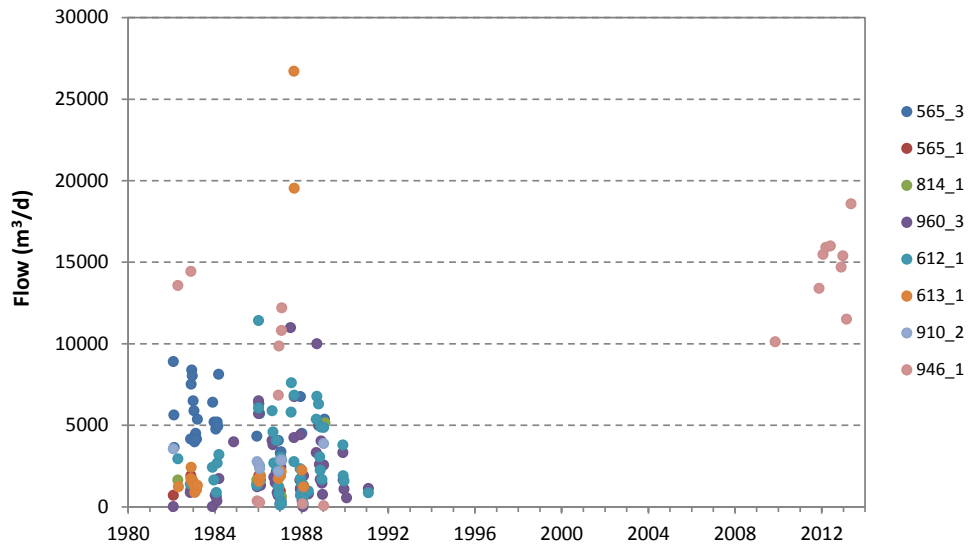
Figure A-1: Surface water flow spot gaugings in the study area.

The catchments of the two long term gauge sites are shown in Figure B-2 (in Appendix B).

Borehole Data

Bore data were derived from WRC's Located database which included a host of data such as:

- Bore ID
- Location coordinates
- Bore depth and construction
- Geological log entries
- Hydraulic testing and analysis records

Appendix B: Recharge Model Methodology

The spreadsheet water balance model method for recharge estimation is described below.
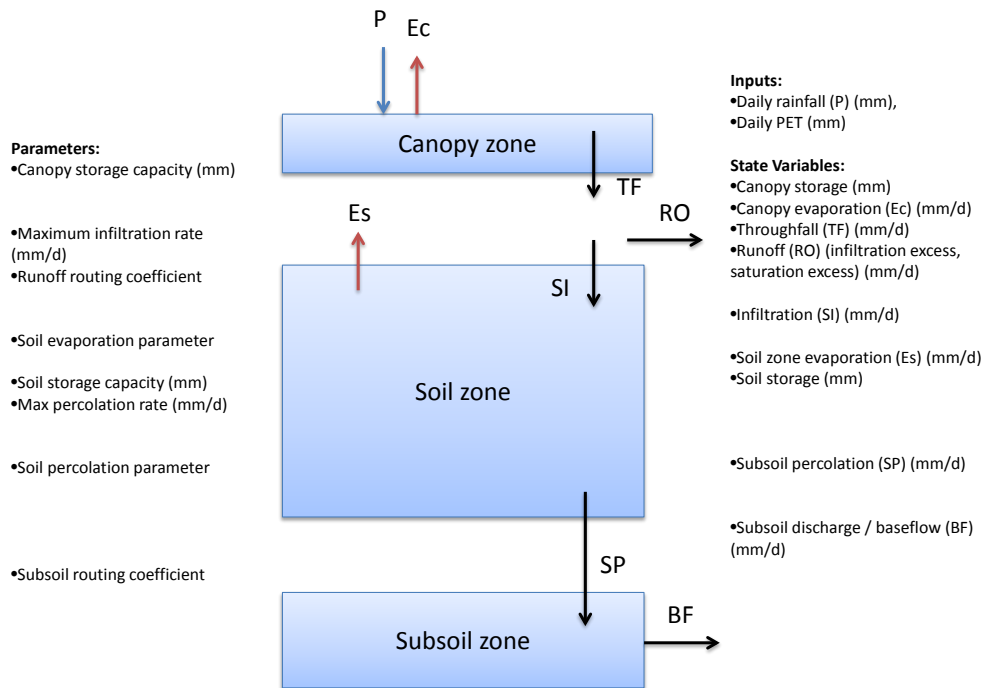
Figure B-1: Process diagram and parameters of the water balance spreadsheet model.

Water Balance Model Operation:

- Rainfall (P) is added to the canopy zone

- If rainfall is greater than canopy zone deficit, excess amount is converted to throughfall (TF)

- Evaporation (Ec) is removed from canopy store at maximum of potential rate and minimum of the depth of water available in the canopy store over one day

- Throughfall less than or equal to the maximum infiltration rate is added to the soil store as soil infiltration (SI)

- Any throughfall greater than the maximum infiltration rate is converted to runoff (RO)

- If throughfall (after any infiltration excess runoff) is greater than the soil zone deficit, the excess is converted to runoff (RO)

- Percolation to the subsoil (SP) (i.e. rainfall recharge to groundwater) is calculated as *(soil zone storage ÷ soil zone storage capacity)^percolation parameter × maximum percolation rate parameter*

- After percolation is removed from the soil zone, soil zone evaporation (Es) is calculated as *(soil storage ÷ soil zone capacity)^soil evaporation parameter × (daily PET rate - any canopy evaporation for that day)*.

- Runoff and baseflow are attenuated using a simple decay rate function using the runoff routing and subsoil routing coefficient.

Total catchment yield is calculated as *attenuated runoff + attenuated baseflow.*

Recharge Model Calibration

Two continuous stream flow gauging records were used for calibration of the water balance model. The positions of the two gauged catchments (83_1 and 960_1) are shown below. The catchment of gauge 83_1 (2.87 km²) is contained entirely within the surficial extent of basalt, while the catchment of 960_1 (10.17 km²) is only partly within the extent of basalt (7.72 km²).
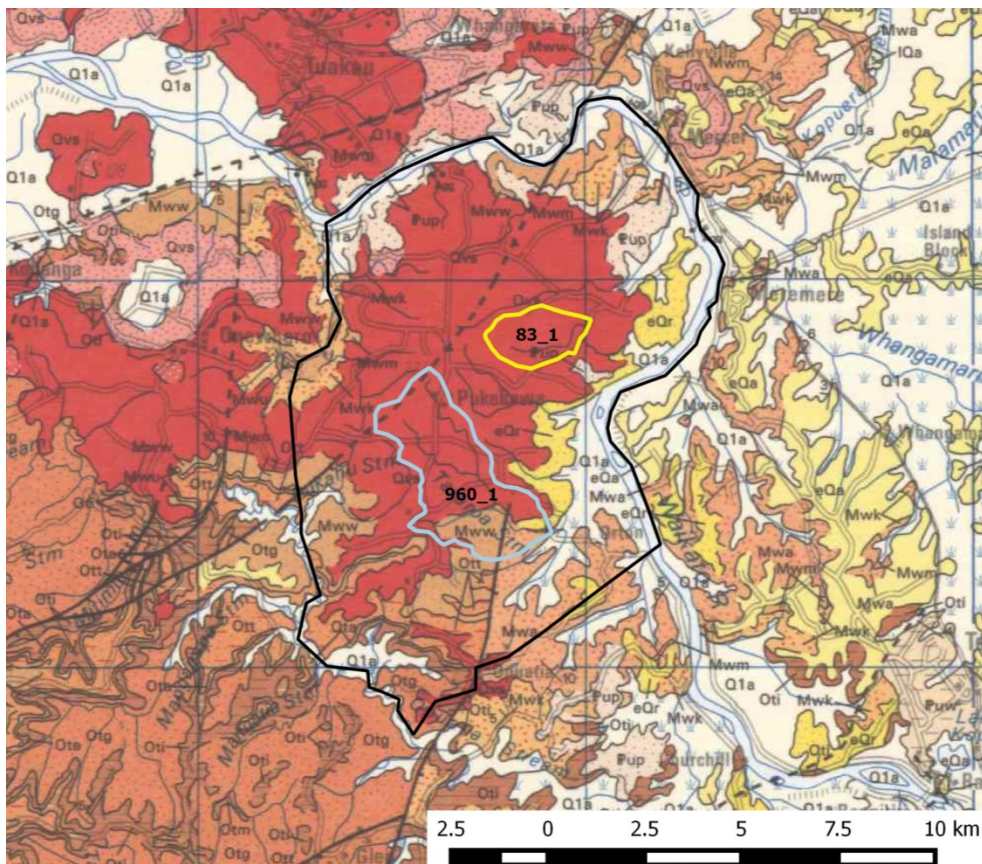
Figure B-2: Continuous gauged surface water catchments

Model parameters were initially selected based on the best fit of modelled and measured runoff. Parameters were adjusted further as part of an iterative process during groundwater flow model calibration.

Recharge timeseries generated by the model were aggregated to monthly totals for input to the groundwater flow model.
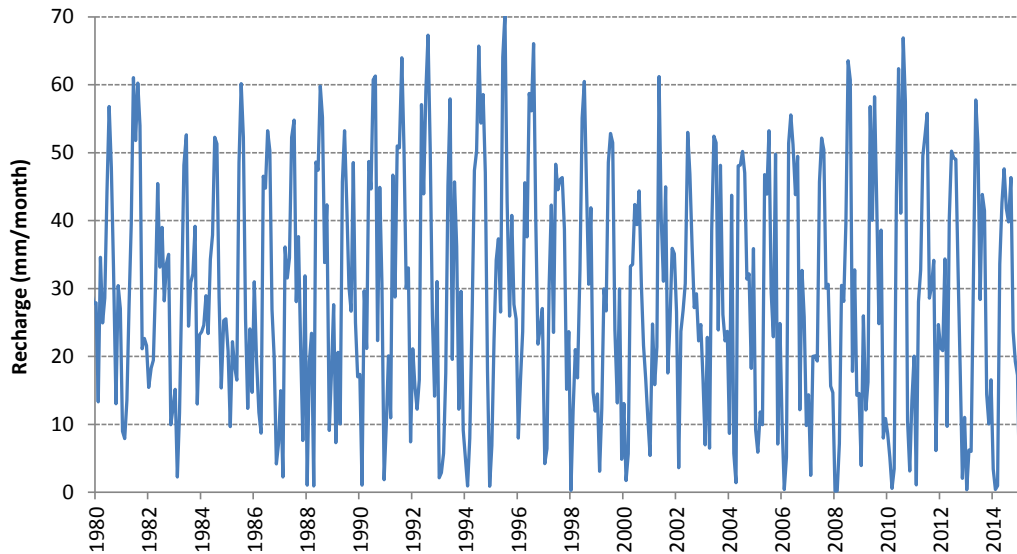
Figure B-3: Modelled monthly recharge rates (basalt zone 1)
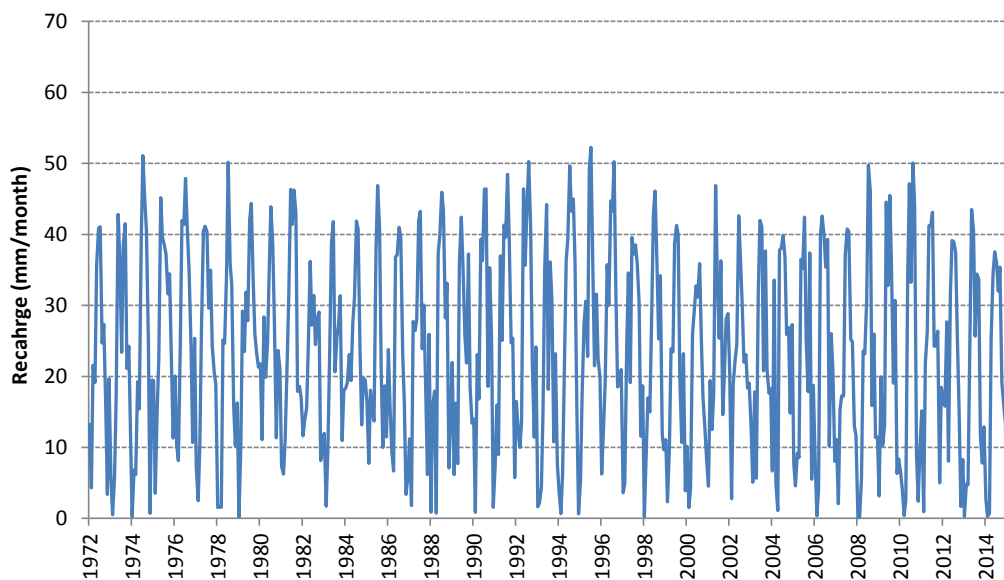
Figure B-4: Modelled monthly recharge rates (basalt zone 2)
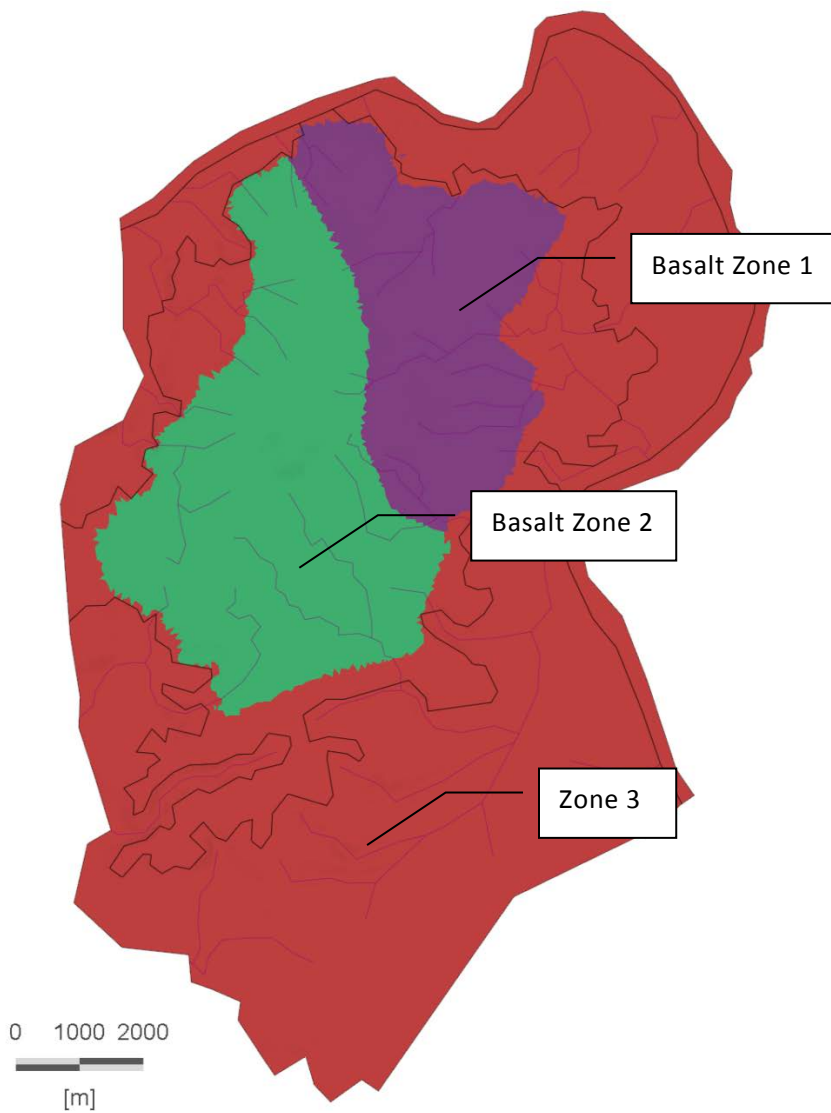
Figure B-5: Model recharge zones

Appendix C: Model Design and Construction

Domain and mesh definition

A model domain was delineated, primarily to include the area of interest (the Pukekawa Basalt Aquifer). Model boundaries were extended beyond the extent of Pukekawa Basalt such that significant flow boundaries or flow divides were encountered, and so that model boundaries would be unlikely to have a measureable influence on model calculations within the area of interest.

A finite element mesh was constructed within the model domain. Geometric features were manually digitised into a superelement mesh (the polygons, lines and points on which the mesh is constructed). Geological boundaries, stream lines and pumping bore locations were included in the superelement mesh. The finite element (triangular) mesh was then generated, with elements conforming to the geometry of features in the superelement mesh. Graduated mesh refinement was applied to point and line features within the superelement mesh. The area corresponding to the Pukekawa Basalt extent was provided a higher mesh density for more precise model calculations in the area of interest.
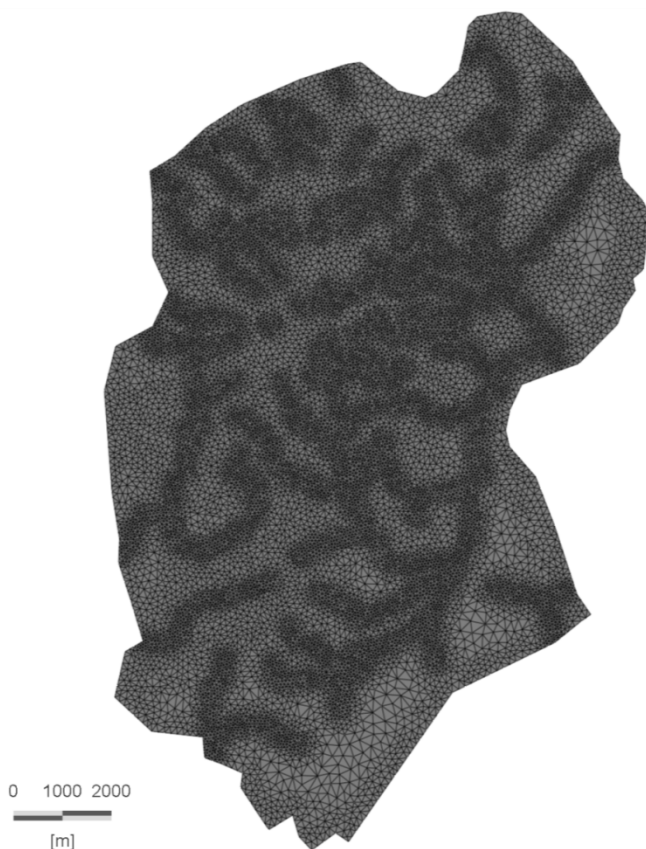
Figure C-1: Finite element model 2D mesh.

Layer Structure

Initially, five model layers (separated by six slices) were defined to represent the hydrostratigraphy of the study area. An adapted layer structure approach was selected, whereby model layers generally conform to geological layering with exceptions in some areas to improve model stability. To account for the imperfect relationship between model layers and geological layers, each model layer was allowed to contain elements of more than one geological unit. Zones of elements within each unit were mapped to enable fair representation of the geological model.

The main modifications to layer structure were required in areas where geological units pinch out at the surface. In a typical model layer structure, this leads to thin layers at the top of the model. This can create undesired numerical instability during simulations, particularly when the modelled water table is below the base of these thin model layers.

The approach that was used in this model was to set a minimum thickness in the top layer, based on its depth below the modelled water table. This required some ongoing adaptation during the model construction and calibration, due to the shifting position of the modelled water table.
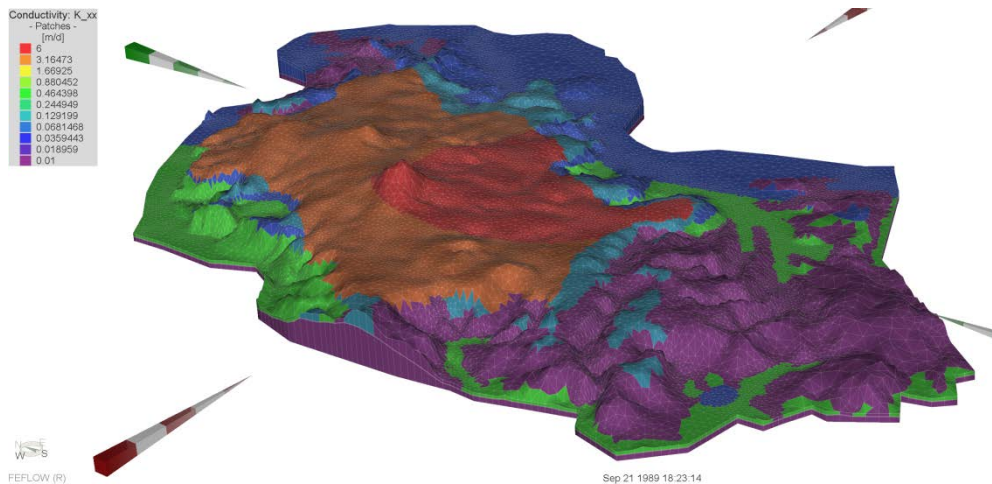
Figure C-2: Oblique view of 3D finite element model structure and K distribution.
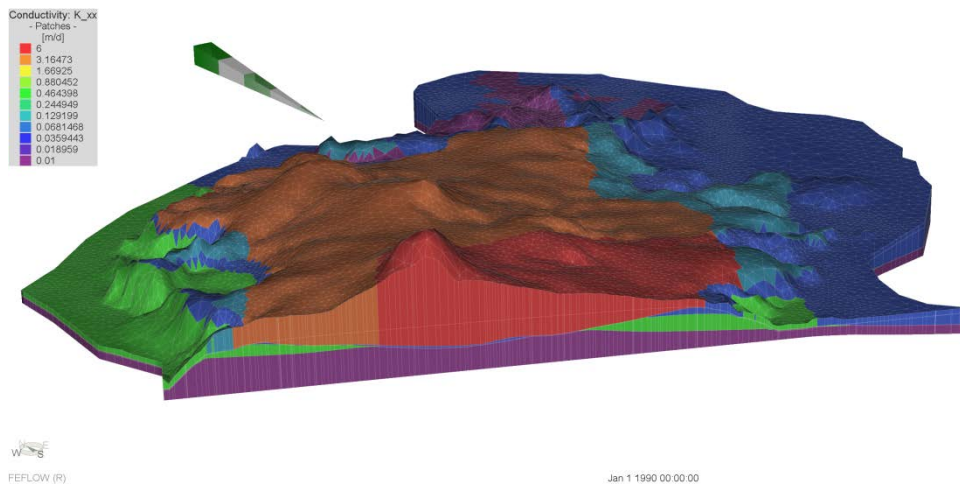
Figure C-3: Cut-away oblique view of 3D finite element model structure and K distribution.

Boundary conditions

The main boundary conditions in the Pukekawa model domain, neglecting no-flow boundaries, represented outflow to surface waters, and extraction from bores.

Discharges to surface water features were simulated using seepage face boundary conditions applied at ground level, as defined by the top surface of the model, which was set from a digital elevation model (DEM). These boundary conditions behave as constant head boundaries, but only allow discharge from the model and cannot produce recharge. These were applied to all nodes on the top slice of the model domain but discharge naturally occurs in topographic depressions and valleys associated with water courses. An advantage of this approach is that it ensures there are no areas of the model which simulate a phreatic surface in excess of ground level. Artesian pressures in deeper layers are still possible. The Waikato River was represented by constant head boundaries.

Pumping from bores was simulated using FEFLOW's Wells boundaries with transient abstraction data. These were applied to the model layer representing the geological formation targeted by the screen/uncased section of each bore. Groundwater abstraction was included in the model using actual abstraction records for individual consents (where available), aggregated to monthly totals.

Time stepping

FEFLOW allows timesteps to be calculated dynamically during model executions. This provides improved temporal resolution of model calculations when necessary, e.g. during sharp temporal variations in stress. As a minimum, time steps will conform to any time series data points used in any time-variable

boundary condition or recharge. A monthly time step was adopted for recharge and pumping data sets, so the maximum time step possible in the model is 31 days. During most simulations, there were typically two time steps calculated per one month interval.

A total simulation period for the calibration model was set from January 1980 to March 2015. The same time interval and corresponding recharge stresses were used for subsequent simulations.

Representation of confined / unconfined conditions

FEFLOW provides several options for representation of saturated and unsaturated aquifer conditions in three-dimensional flow models.

For this model, confined mode was found to be best suited to representing the hydrogeological conditions of this aquifer system, particularly the strong anisotropy in the basalt aquifer and resulting vertical head gradients. Confined mode also provided the most stable solution with fewer errors.

Appendix D: Model Calibration and Sensitivity Analysis

Groundwater Discharge Hydrographs
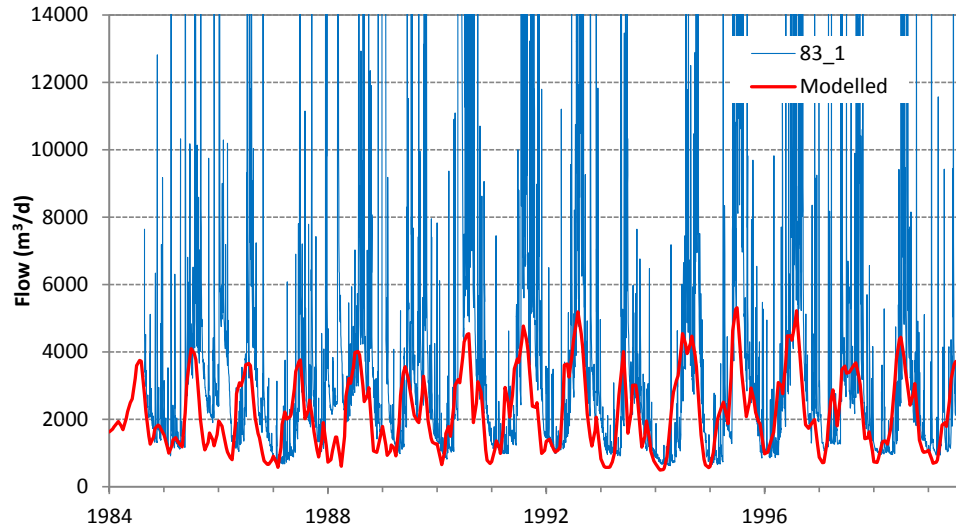
Figure D-1: Modelled baseflow and observed total stream flow at gauging site 83_1.
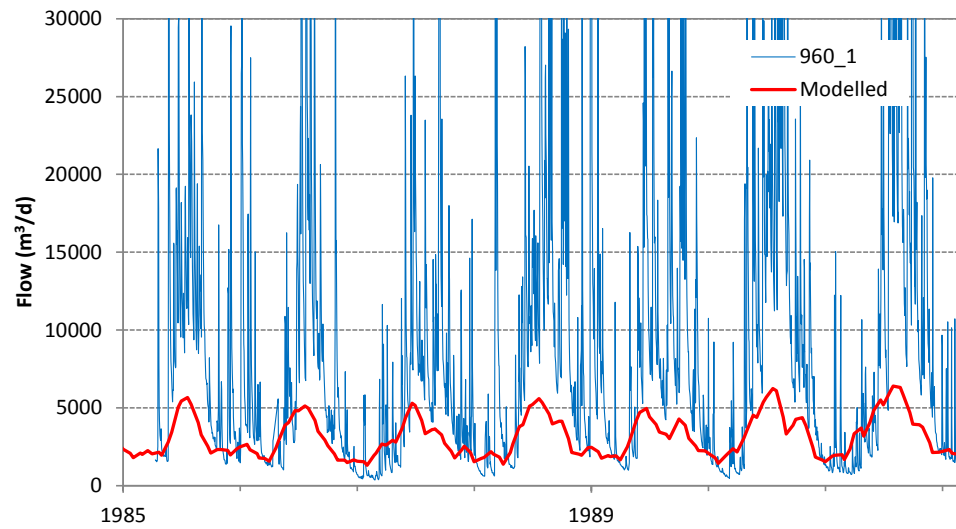
Figure D-2: Modelled baseflow and observed total stream flow at gauging site 960_1.
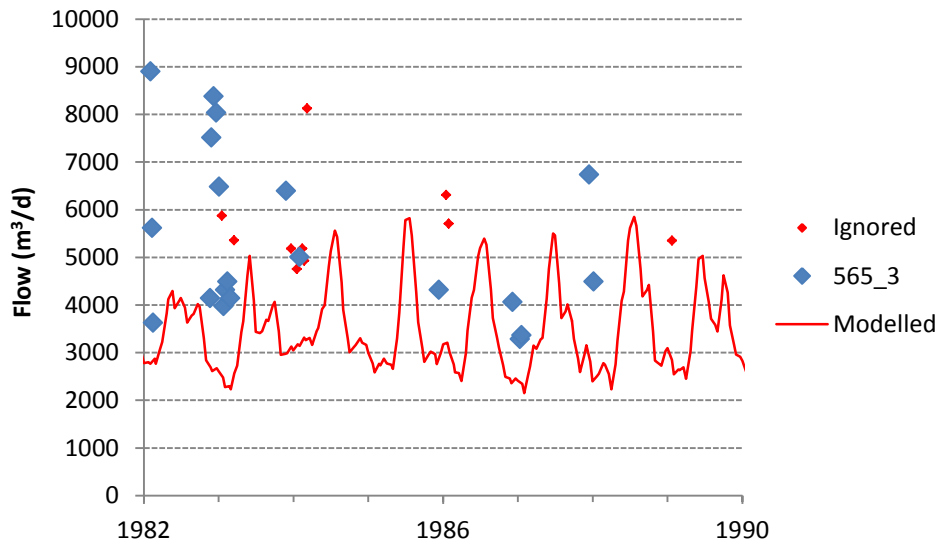
Figure D-3: Modelled baseflow and observed total stream flow at gauging site 565_3.
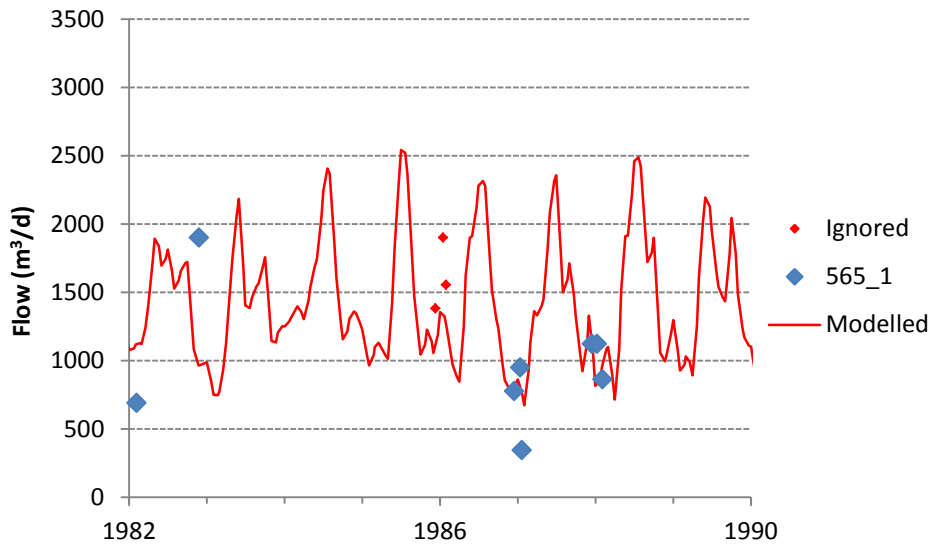
Figure D-4: Modelled baseflow and observed total stream flow at gauging site 565_1.
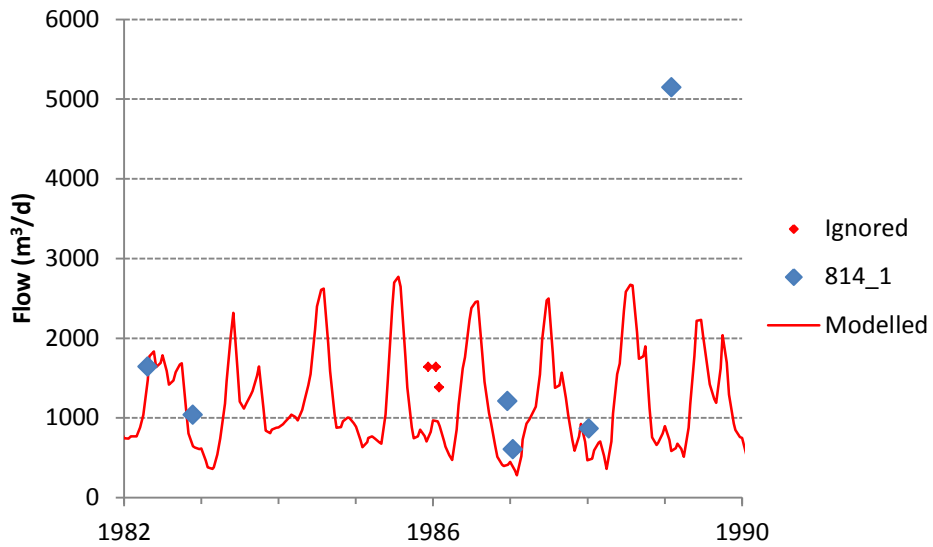
Figure D-5: Modelled baseflow and observed total stream flow at gauging site 814_1.
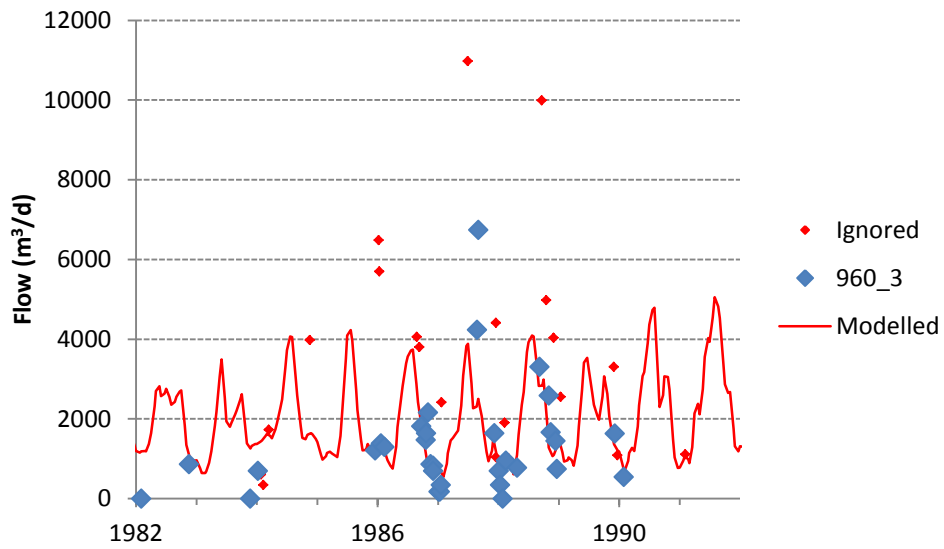
Figure D-6: Modelled baseflow and observed total stream flow at gauging site 960_3.
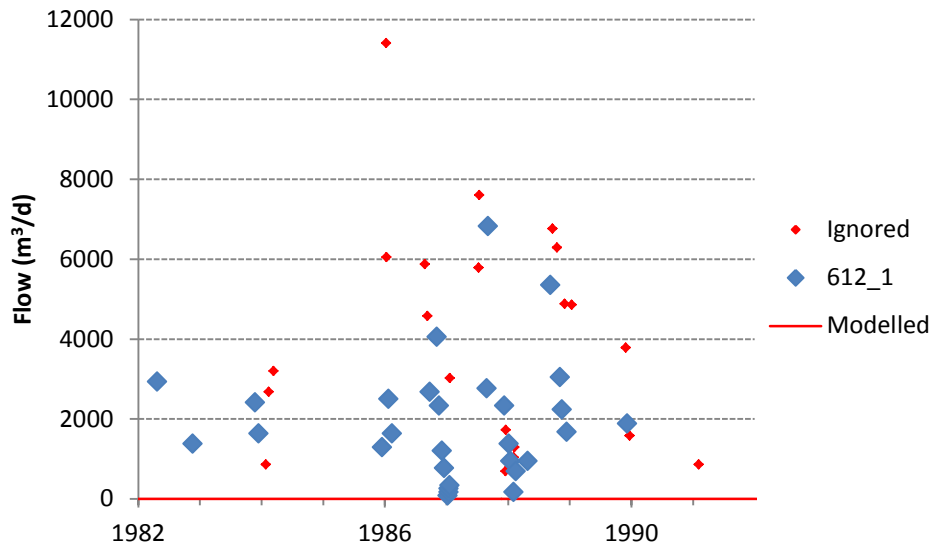
Figure D-7: Modelled baseflow and observed total stream flow at gauging site 612_1.
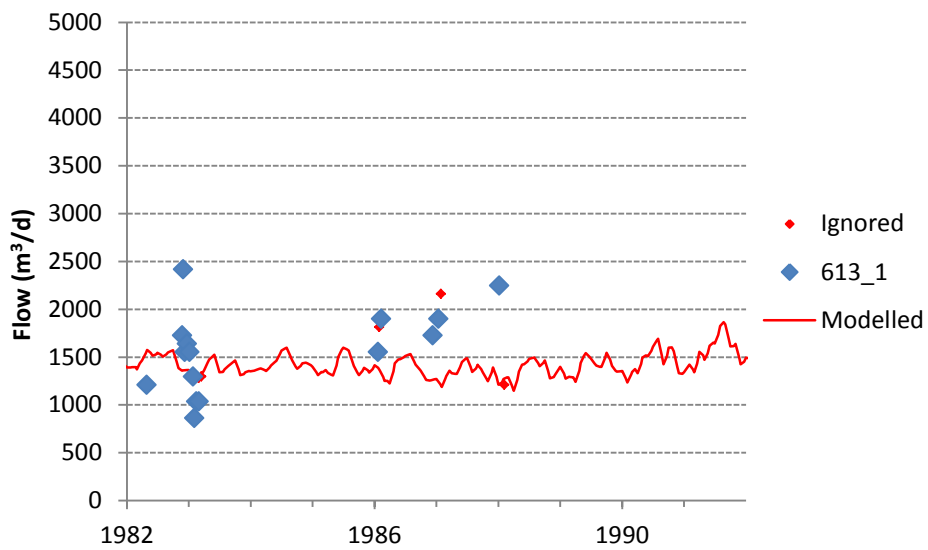
Figure D-7: Modelled baseflow and observed total stream flow at gauging site 613_1.
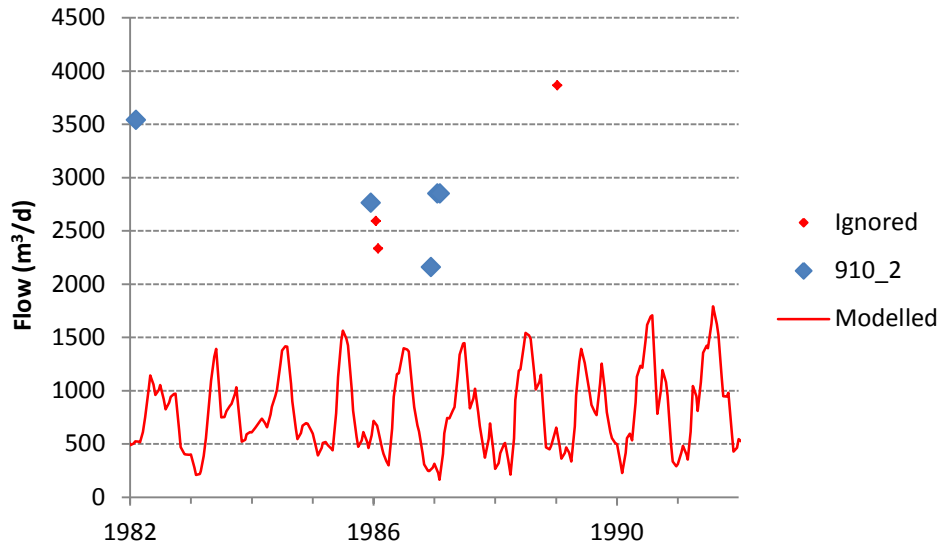
Figure D-8: Modelled baseflow and observed total stream flow at gauging site 910_2.
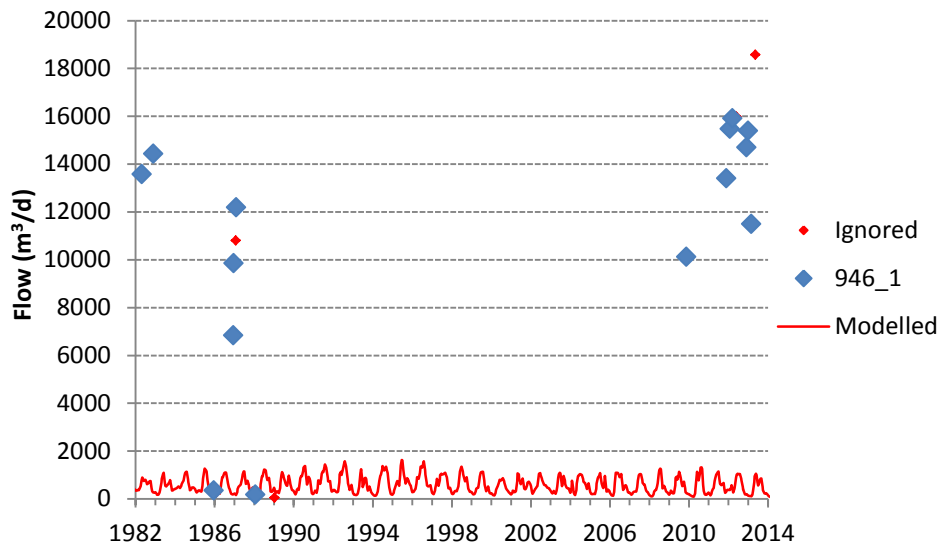
Figure D-9: Modelled baseflow and observed total stream flow at gauging site 946_1.
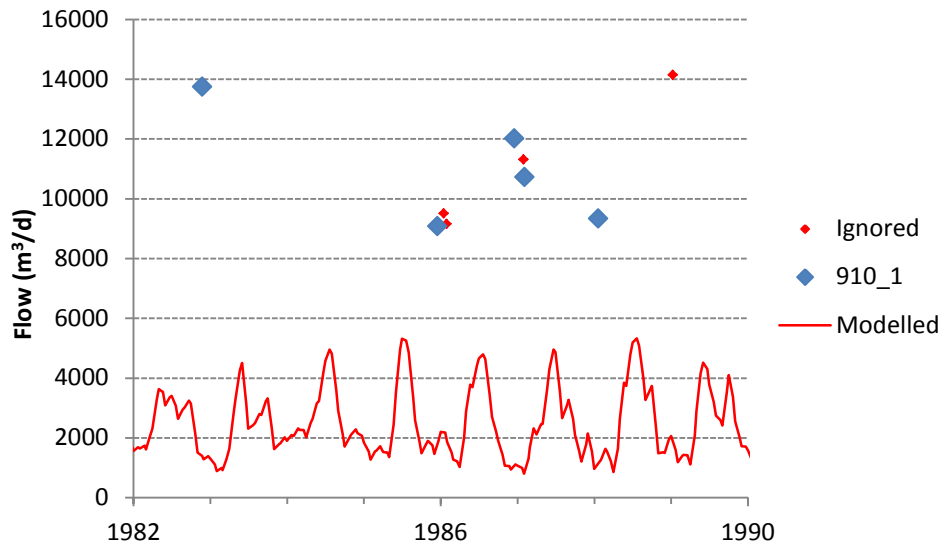
Figure D-10: Modelled baseflow and observed total stream flow at gauging site 910_1.

Groundwater Level Calibration Hydrographs
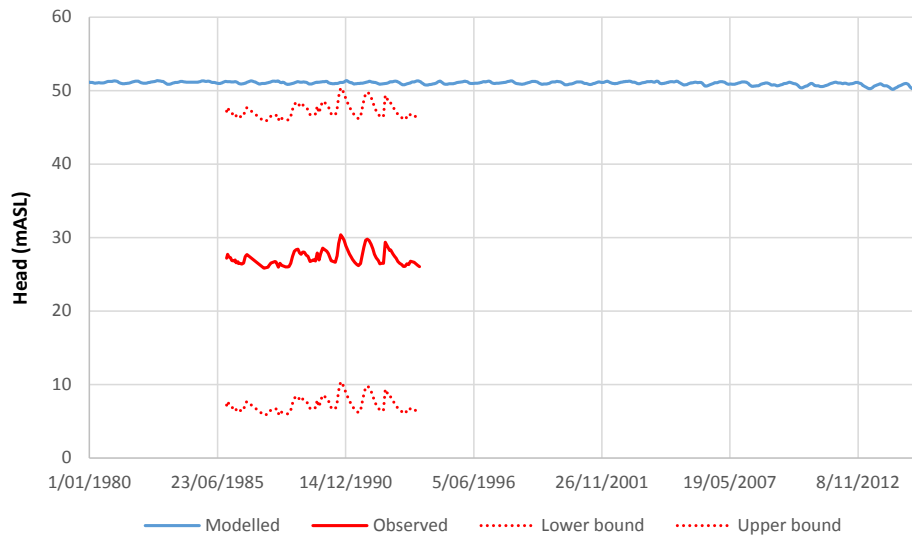
Figure D-11: Observed and modelled head at monitoring bore 61_60.
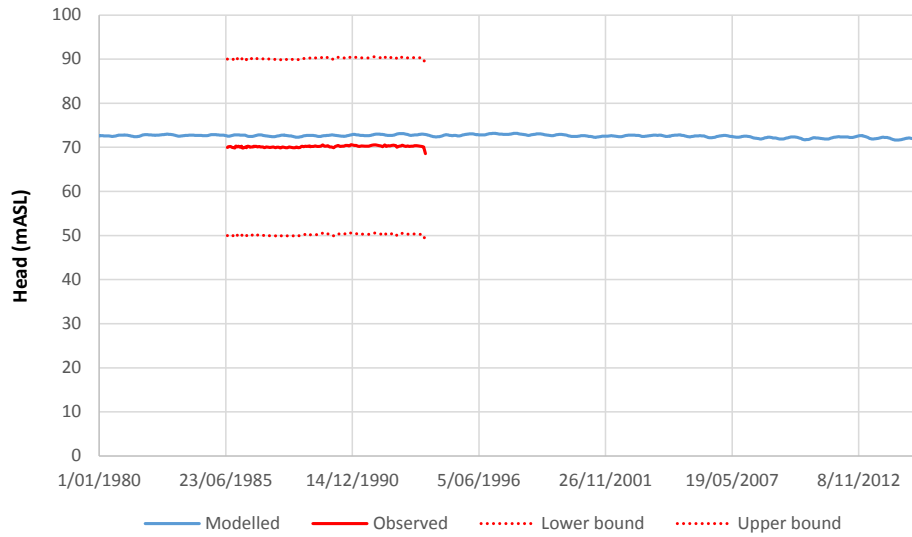
Figure D-12: Observed and modelled head at monitoring bore 61_68.
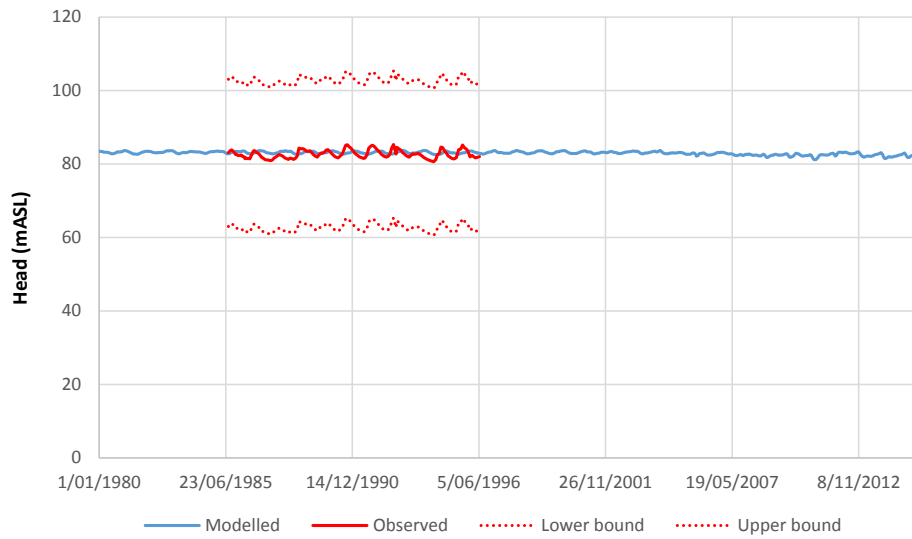
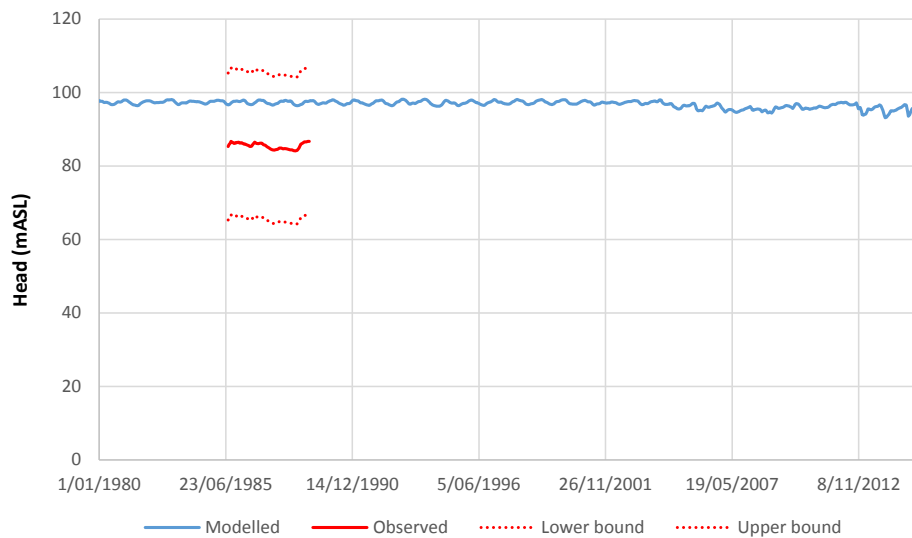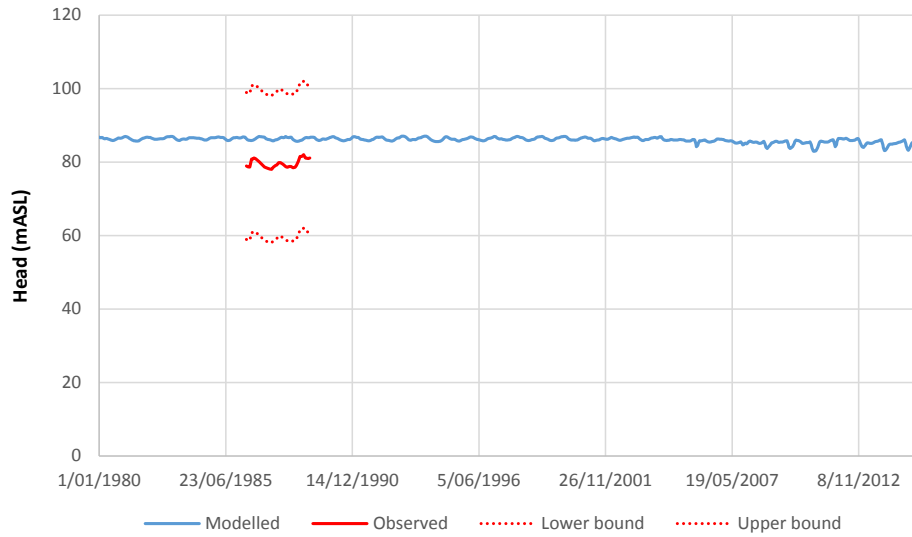**Figure D-13: Observed and modelled head at monitoring bore 61_239.**
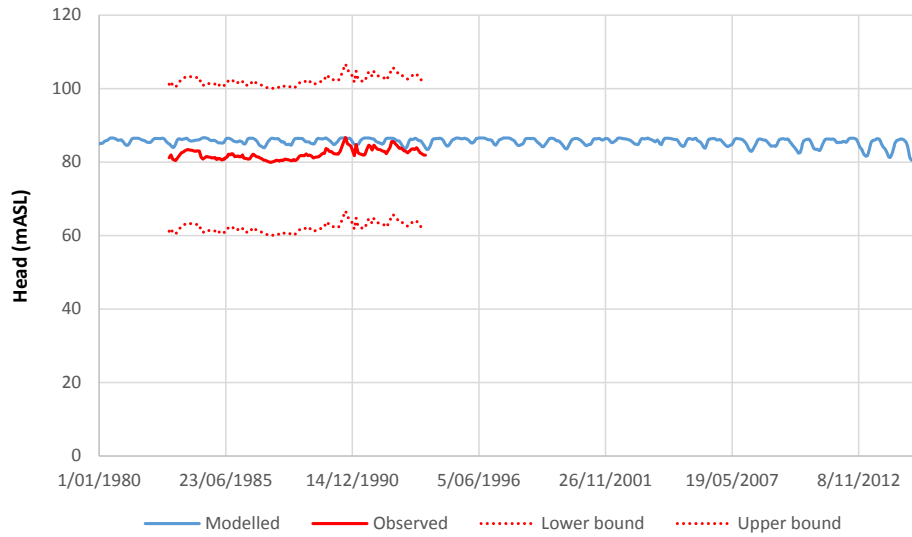
Figure D-14: Observed and modelled head at monitoring bore 61_8.
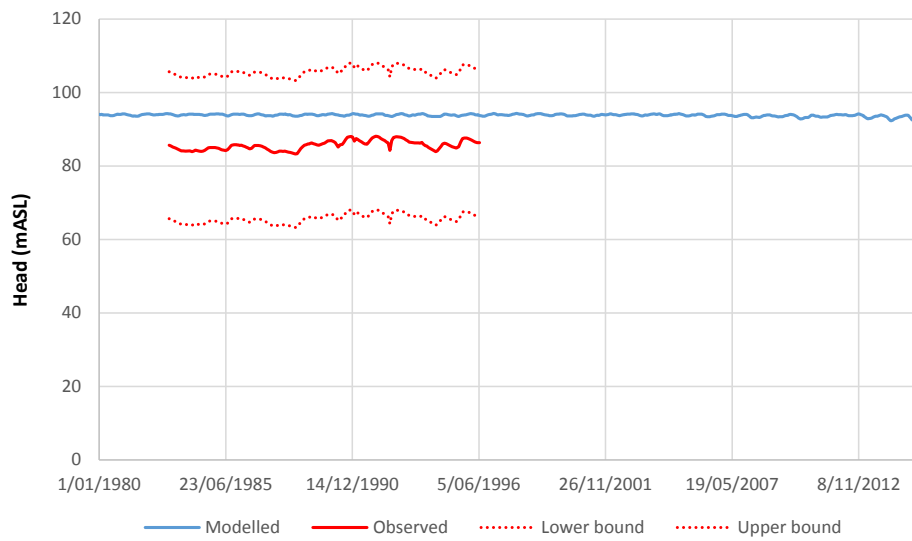
Figure D-15: Observed and modelled head at monitoring bore 61_154.
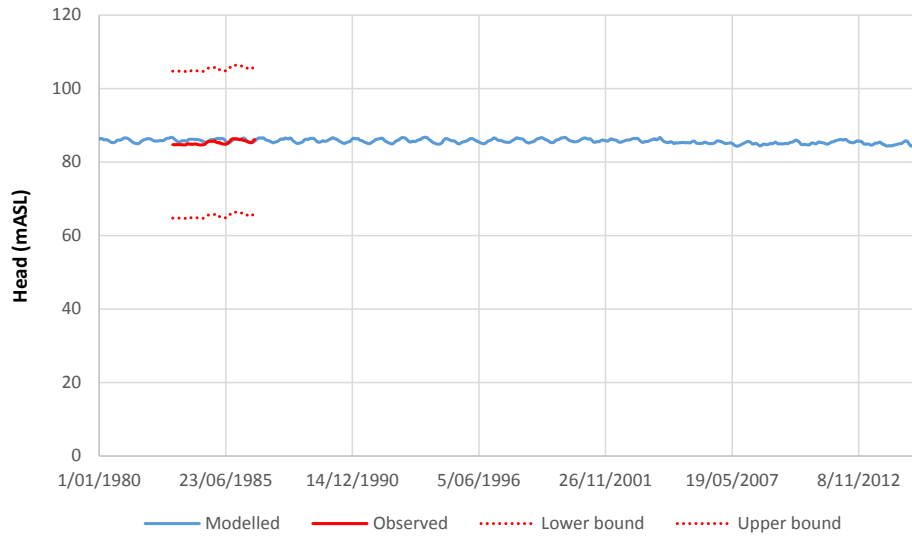
Figure D-16: Observed and modelled head at monitoring bore 61_32.
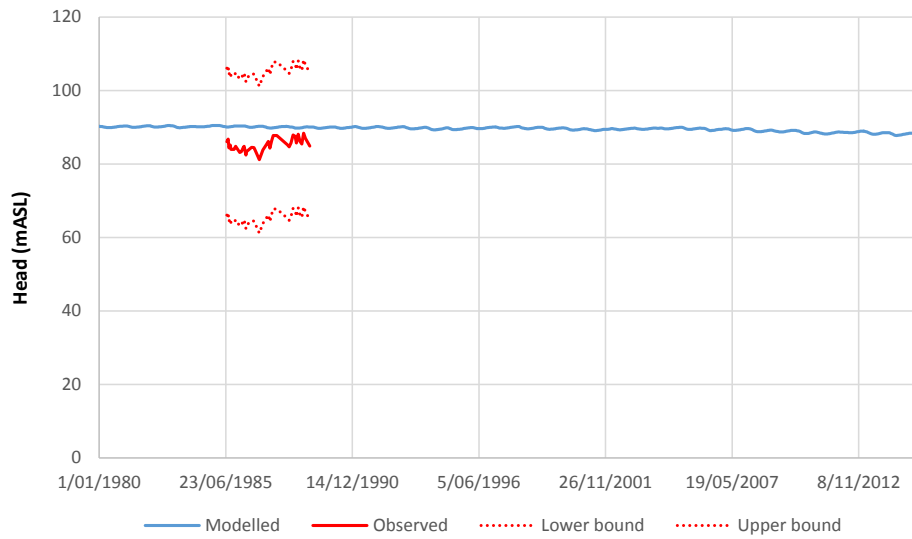
Figure D-17: Observed and modelled head at monitoring bore 61_33.
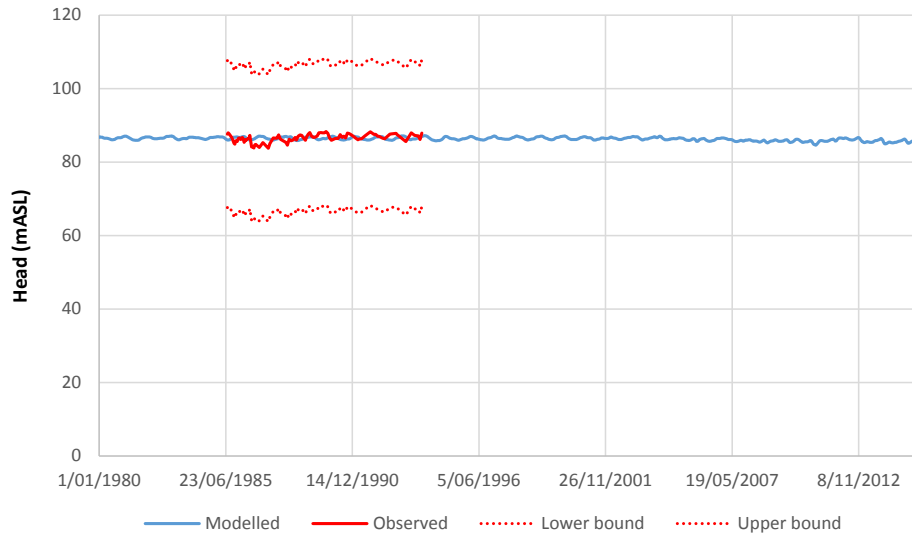
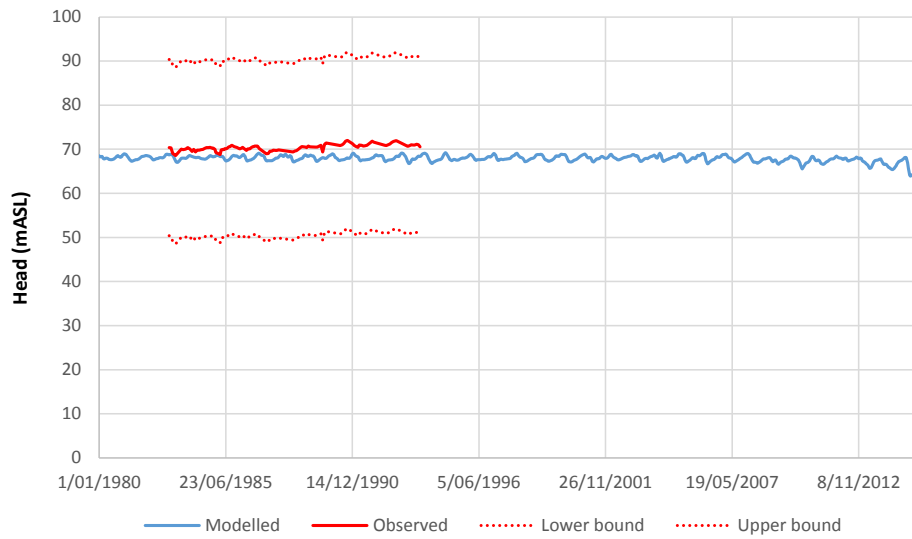**Figure D-18: Observed and modelled head at monitoring bore 61_35.**
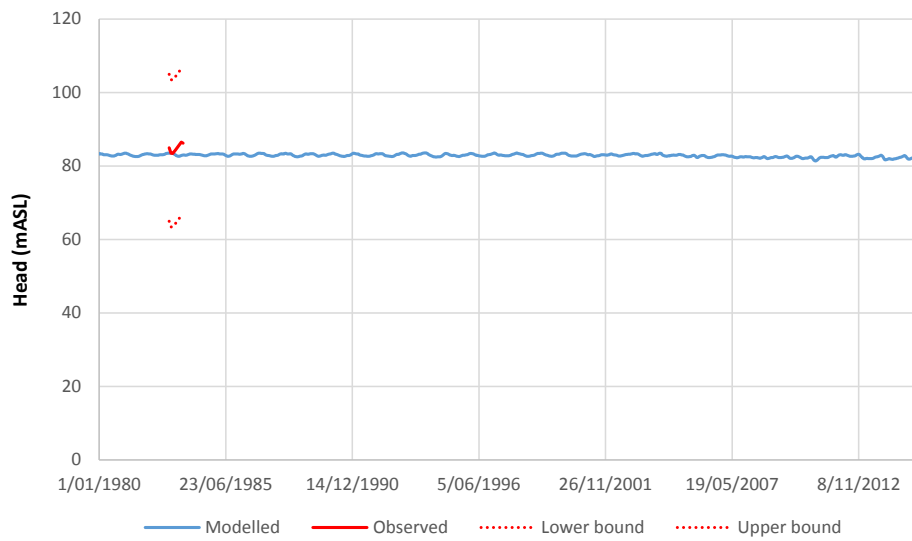
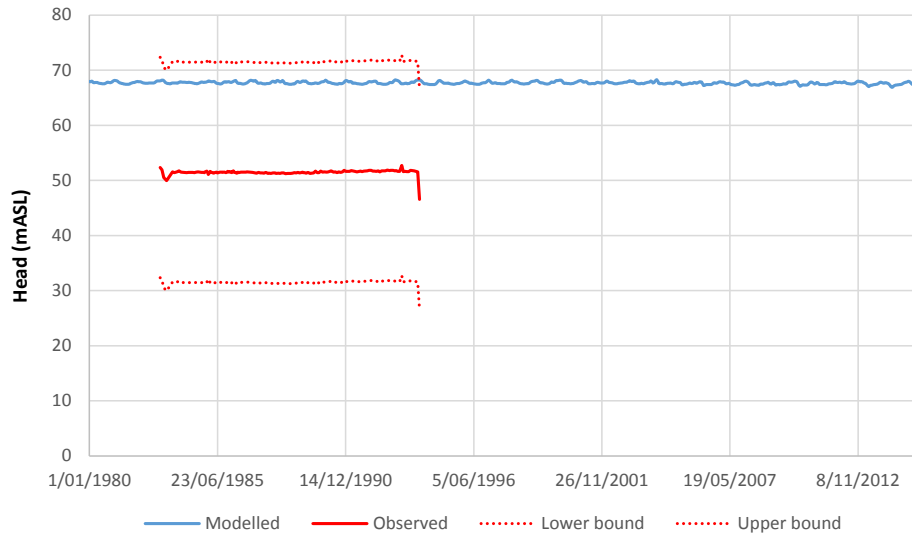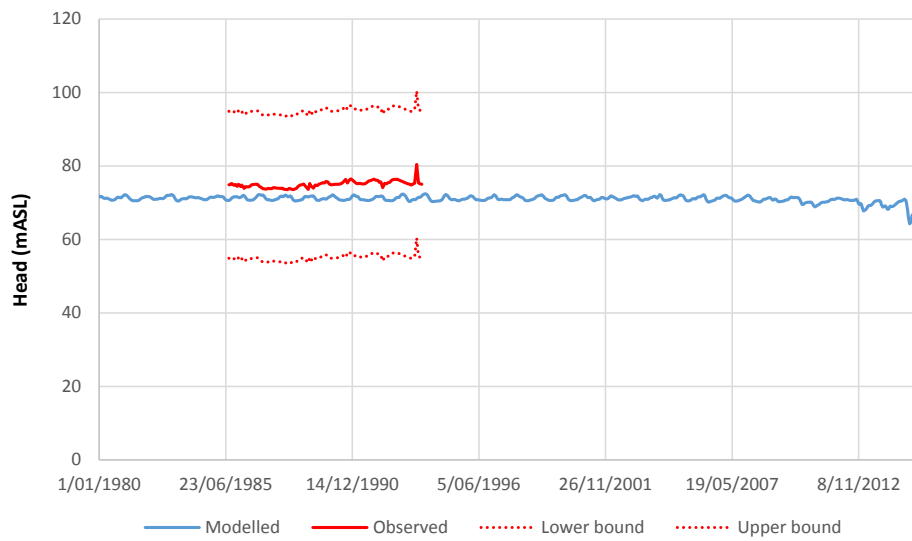**Figure D-19: Observed and modelled head at monitoring bore 61_125.**
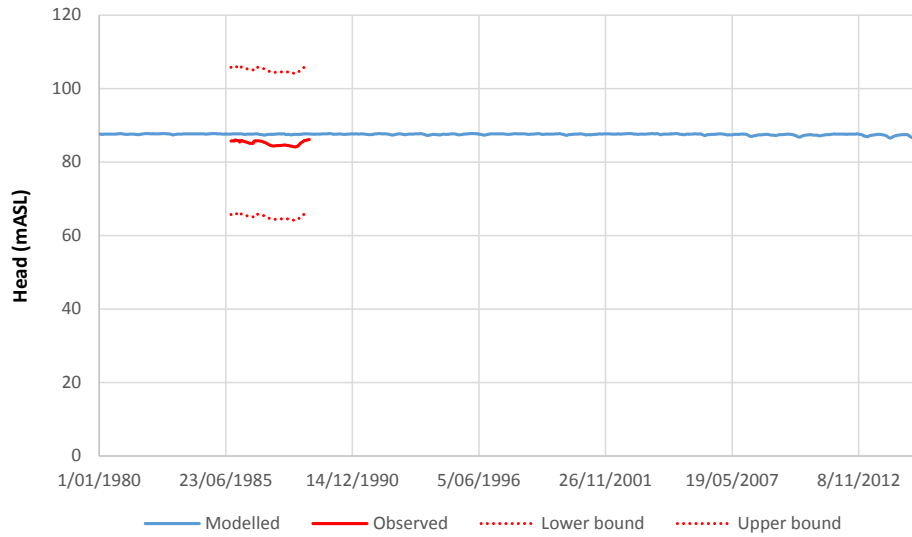
Figure D-20: Observed and modelled head at monitoring bore 61_41.
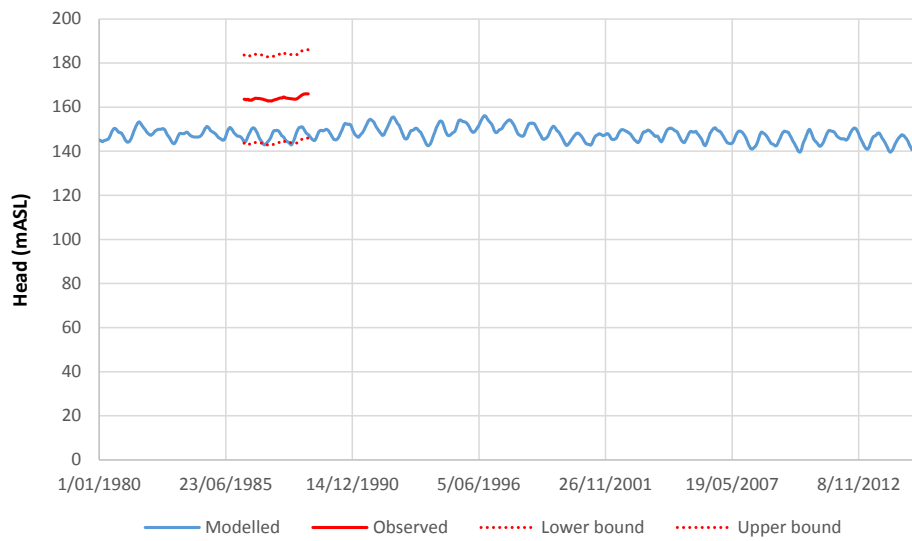
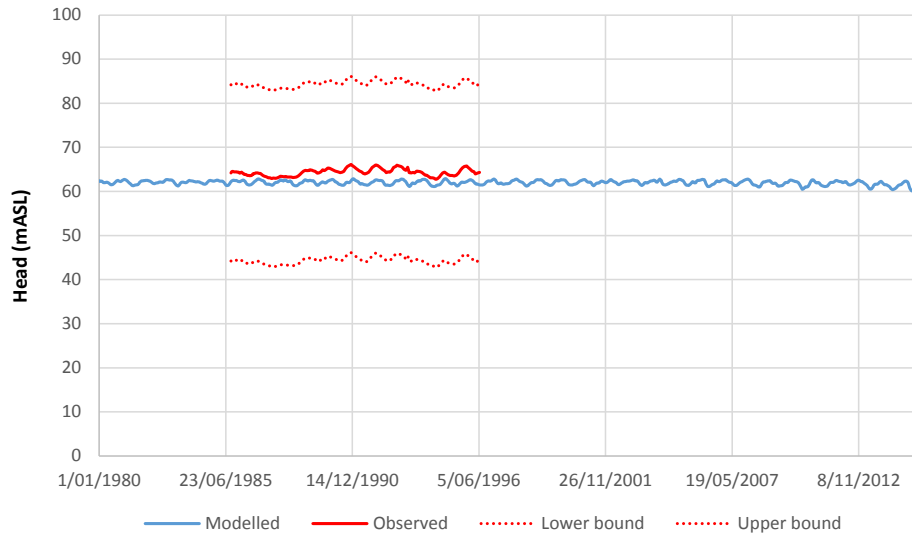**Figure D-21: Observed and modelled head at monitoring bore 61_40.**
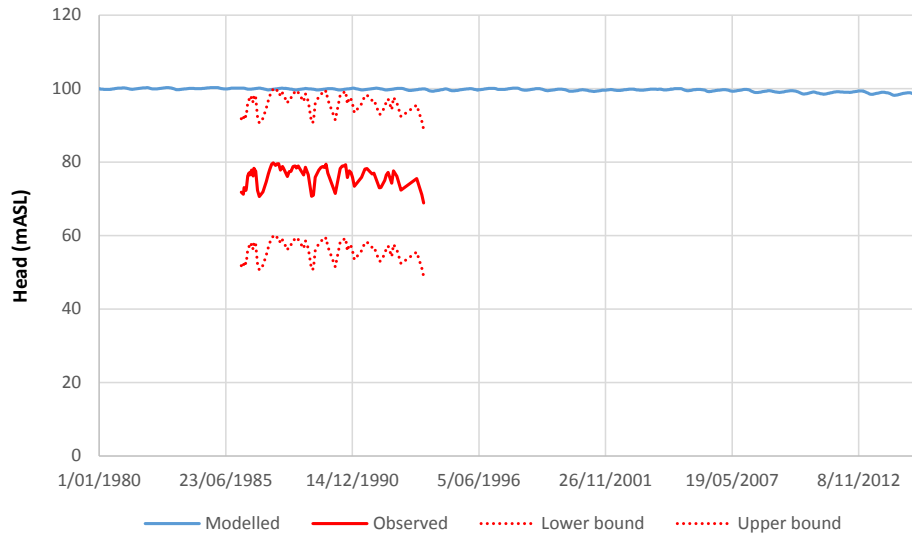
Figure D-22: Observed and modelled head at monitoring bore 61_42.
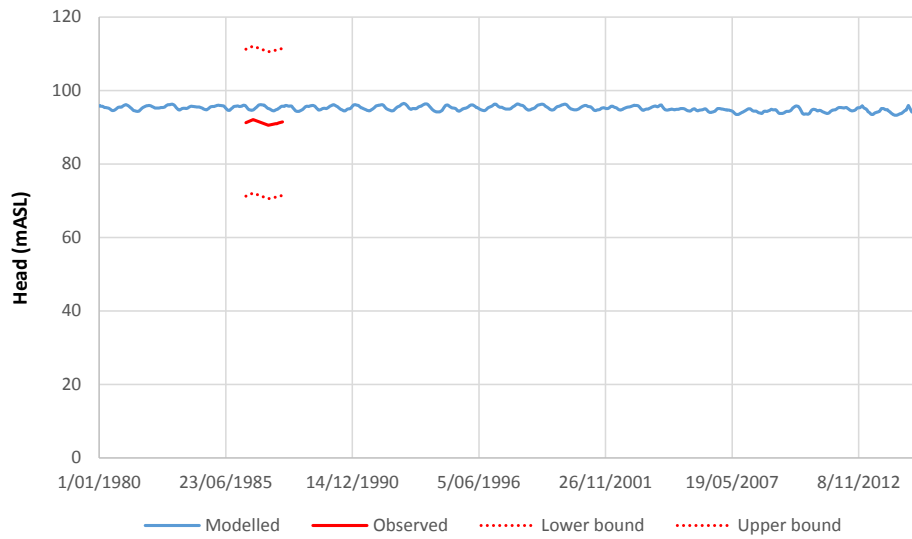
Figure D-23: Observed and modelled head at monitoring bore 61_52.
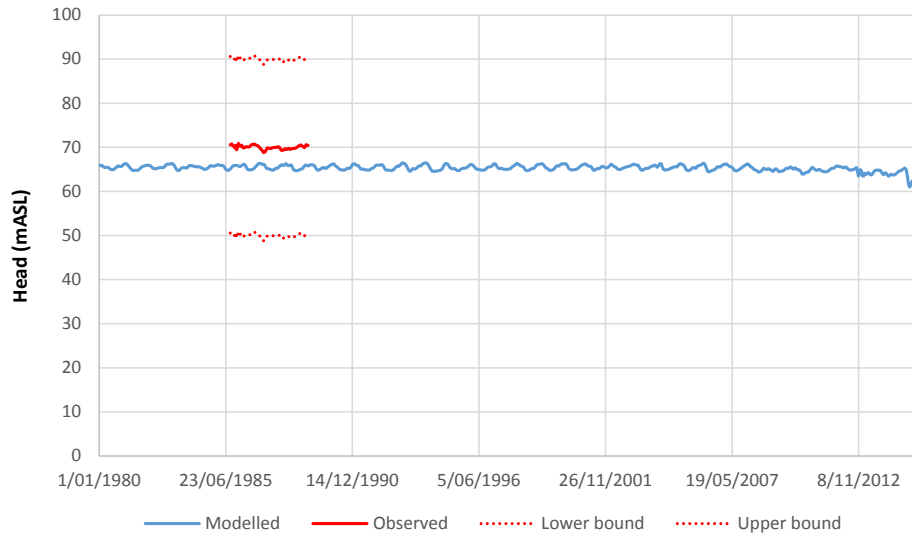
Figure D-24: Observed and modelled head at monitoring bore 61_170.
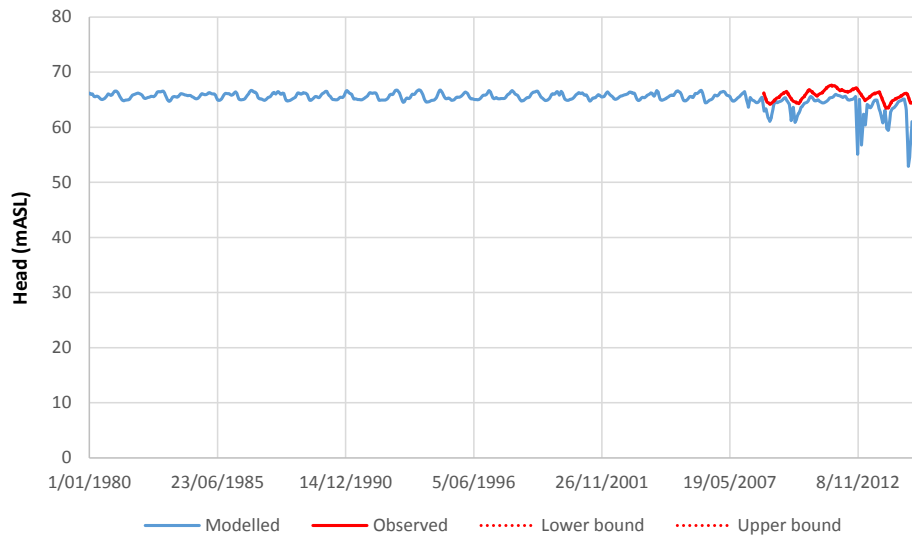
Figure D-25: Observed and modelled head at monitoring bore 61_461.
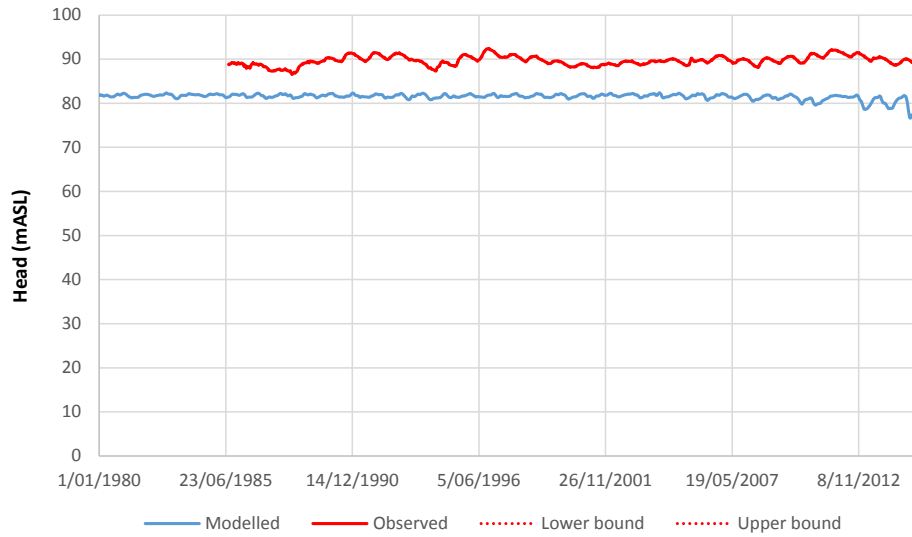
Figure D-26: Observed and modelled head at monitoring bore 61_138.
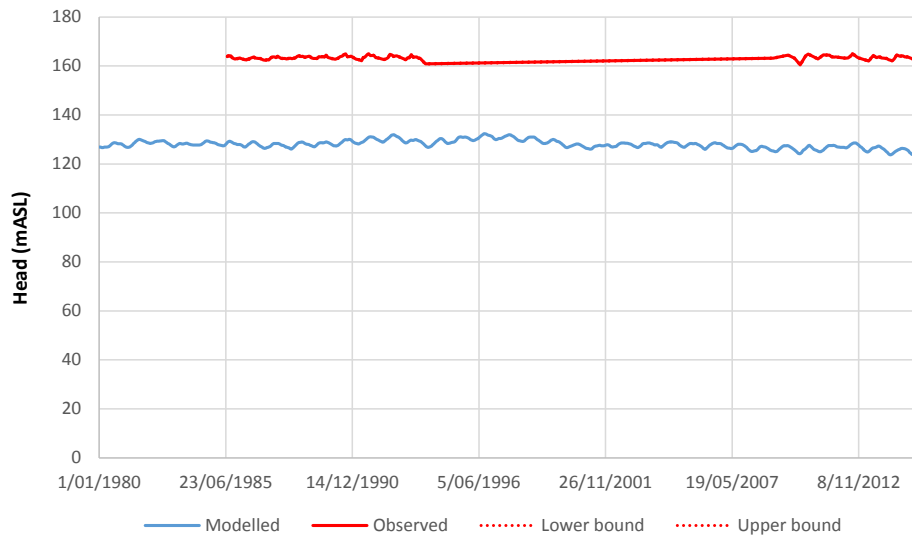
Figure D-27: Observed and modelled head at monitoring bore 61_143.
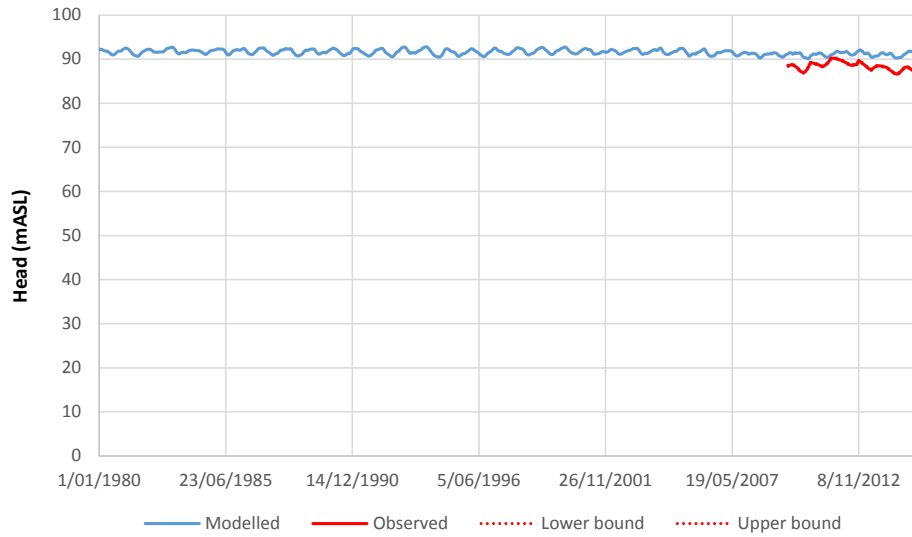
Figure D-28: Observed and modelled head at monitoring bore 61_1639.
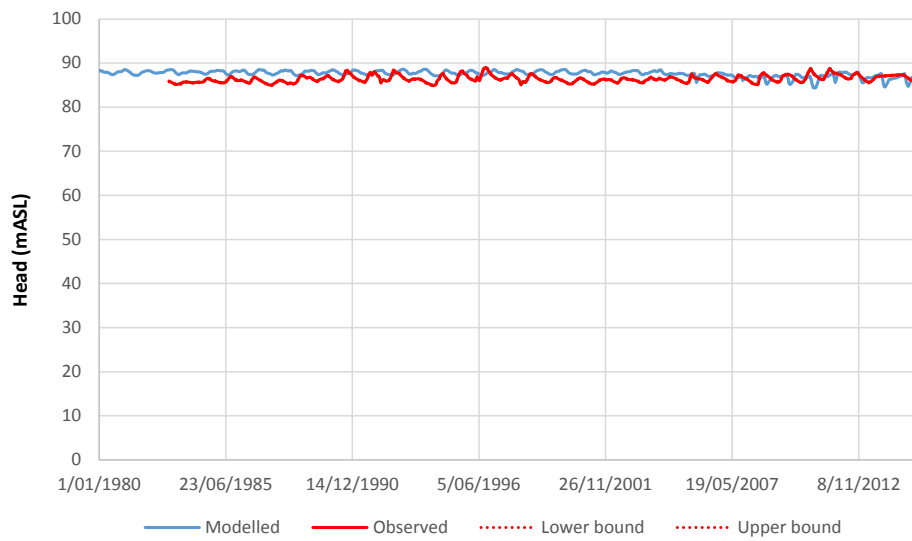
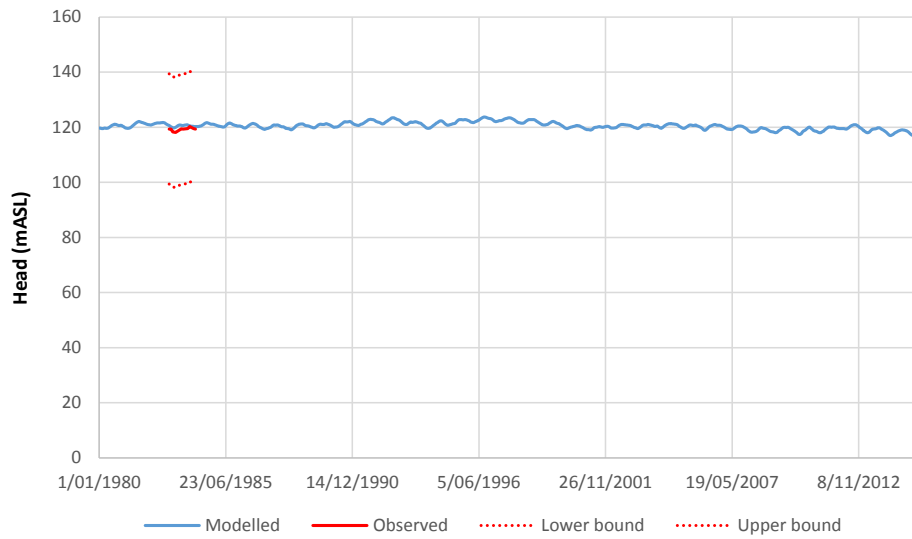**Figure D-29: Observed and modelled head at monitoring bore 61_284.**
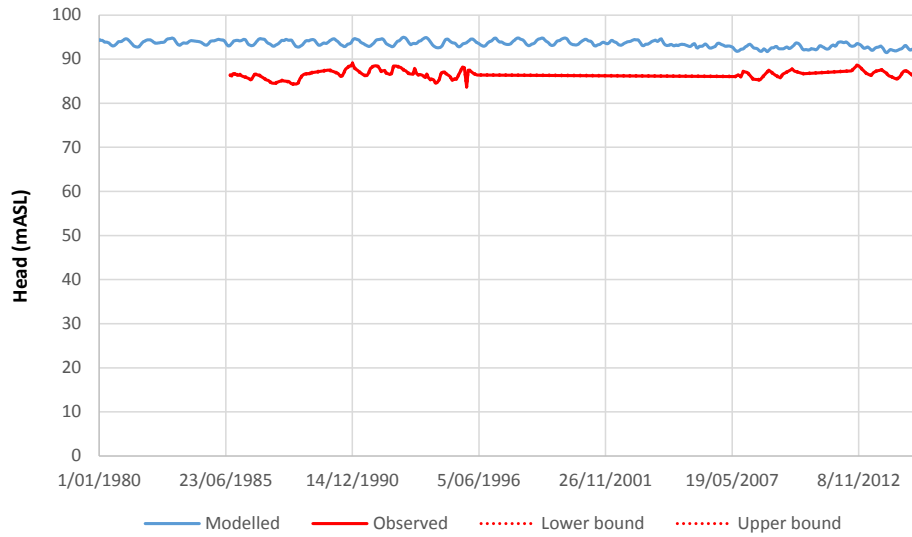
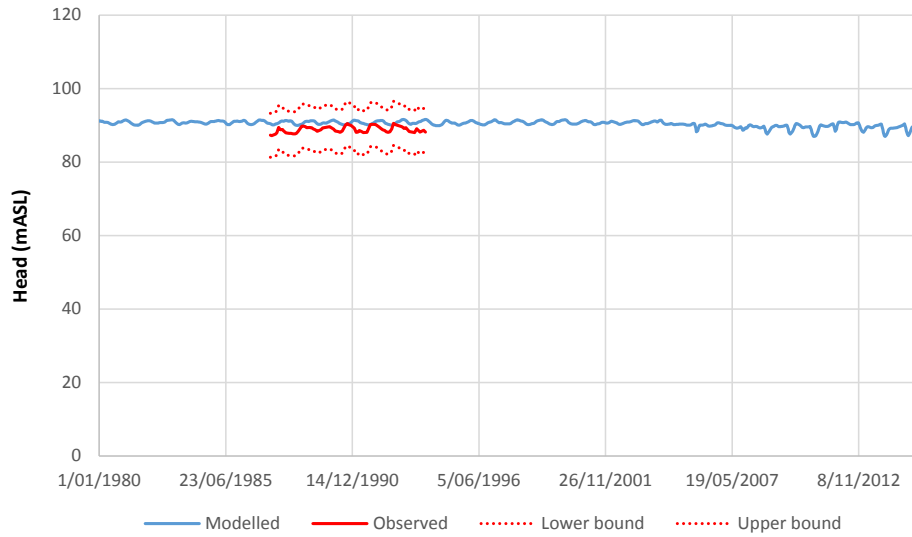**Figure D-30: Observed and modelled head at monitoring bore 61_229.**
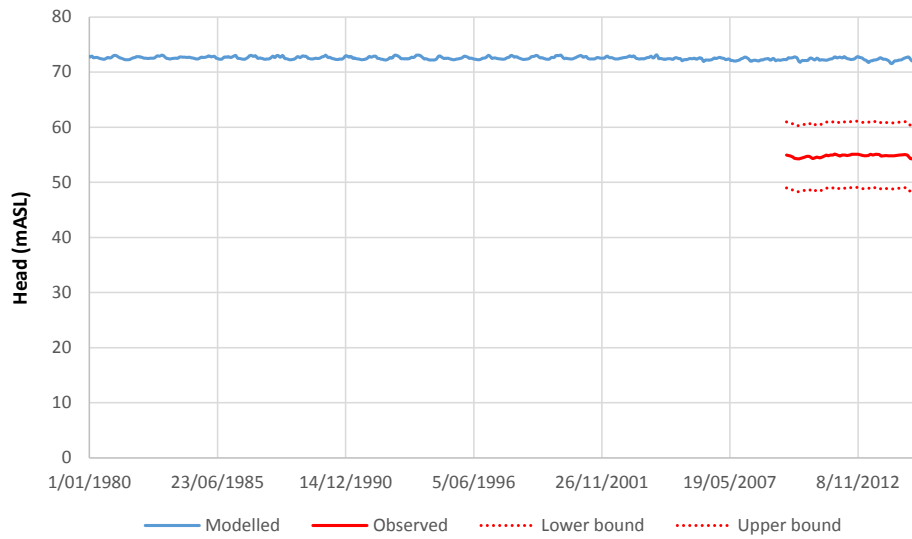
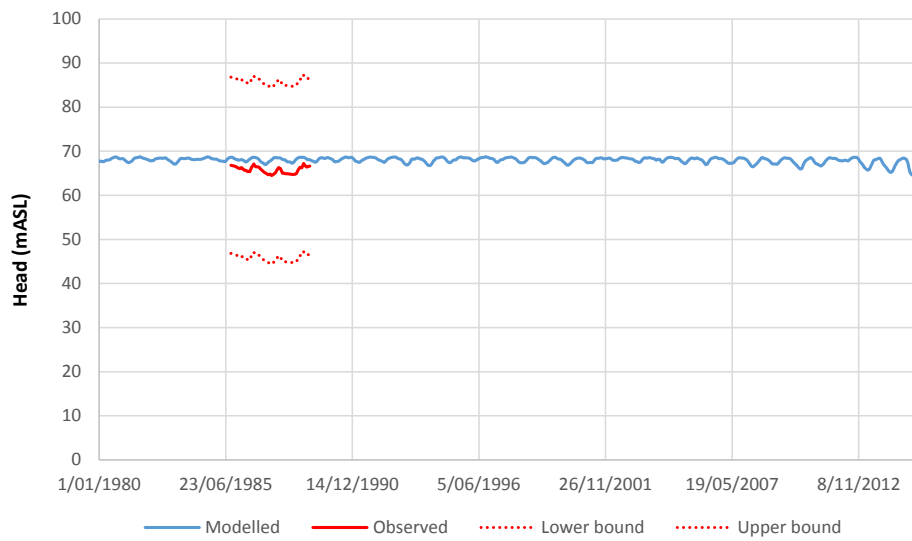**Figure D-31: Observed and modelled head at monitoring bore 72_1860.**
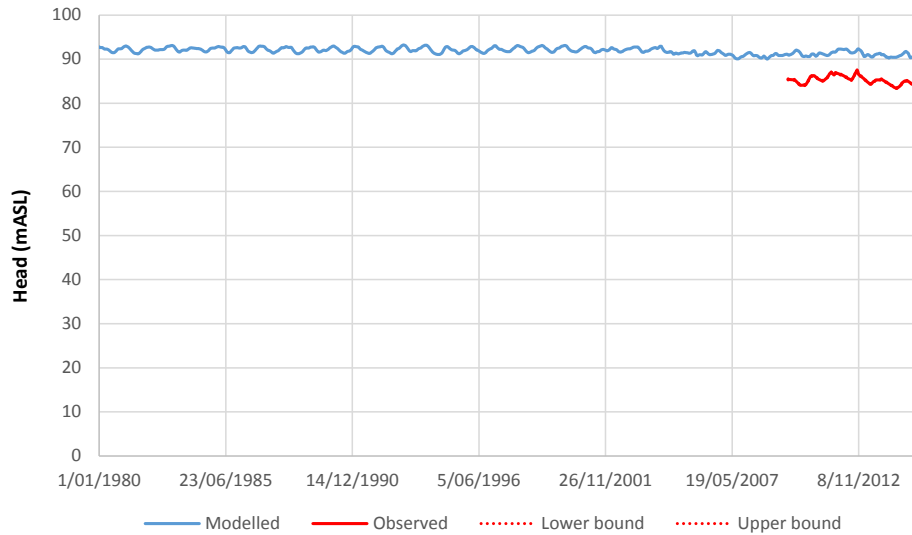
Figure D-32: Observed and modelled head at monitoring bore 72_4428.
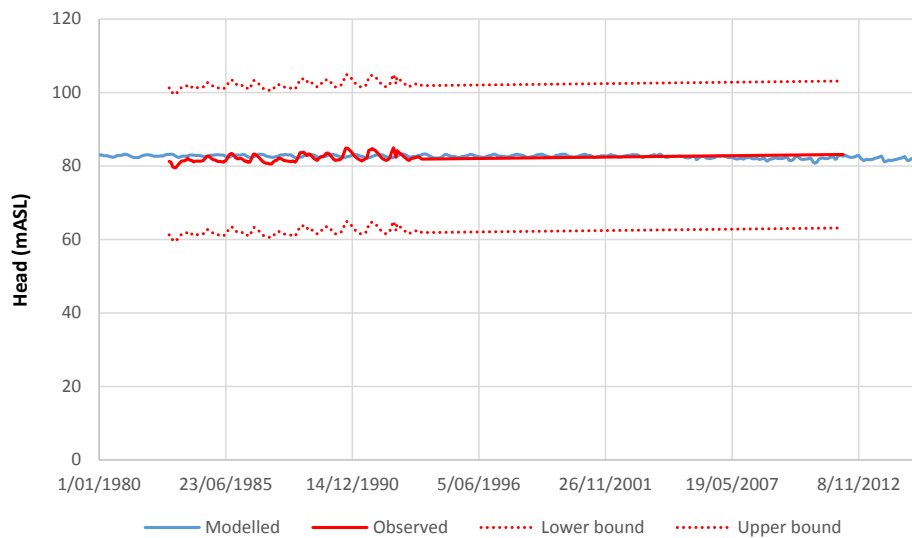
Figure D-33: Observed and modelled head at monitoring bore 61_221.
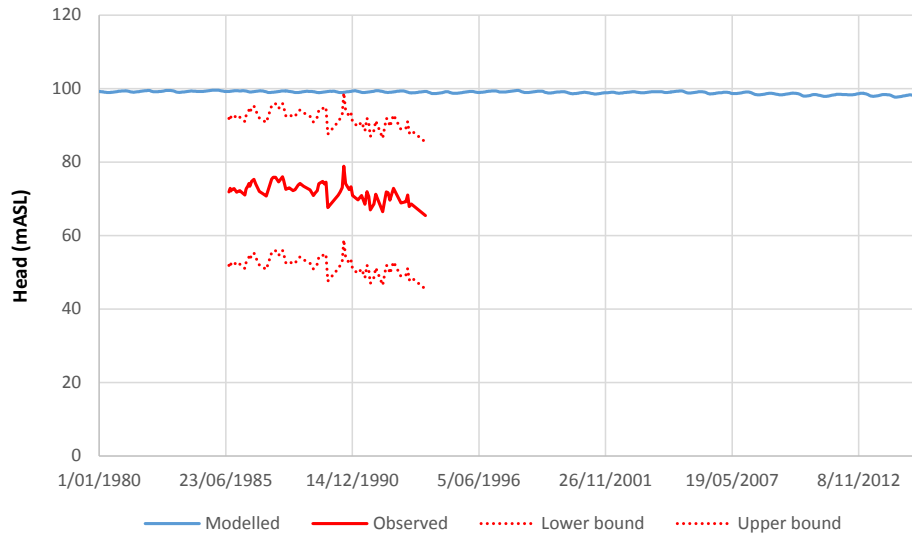
Figure D-34: Observed and modelled head at monitoring bore 61_134.
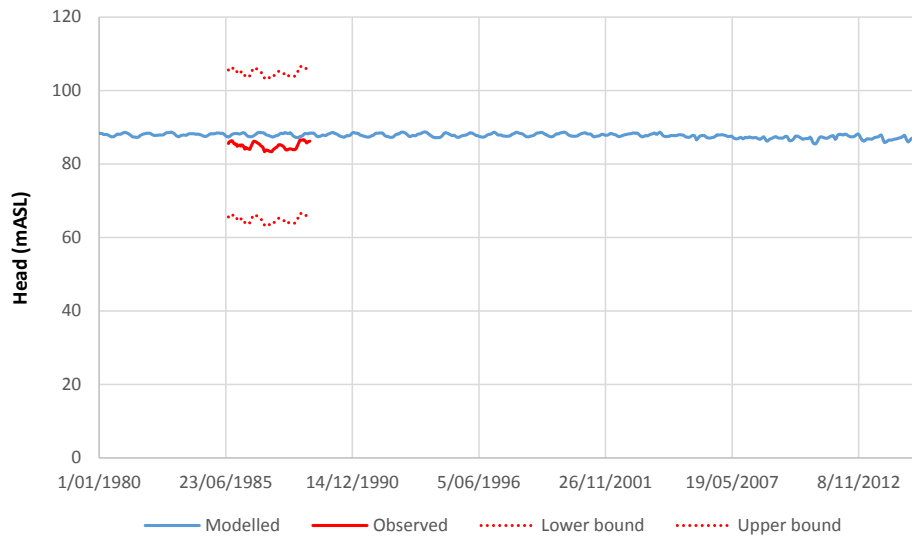
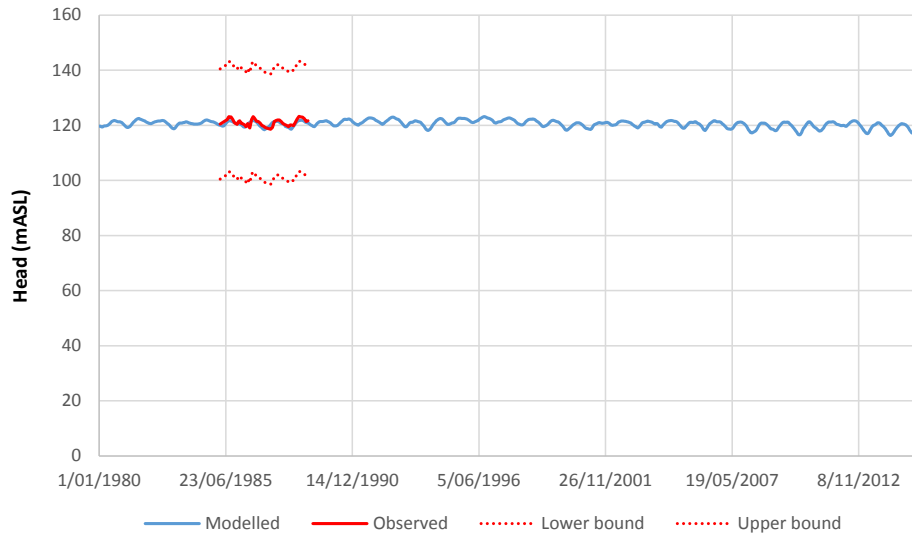**Figure D-35: Observed and modelled head at monitoring bore 61_82.**
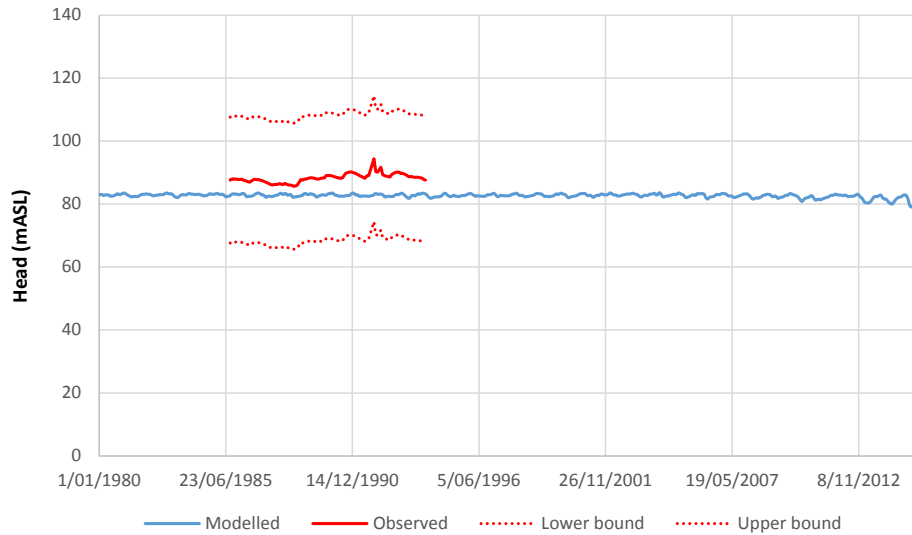
Figure D-36: Observed and modelled head at monitoring bore 61_116.

Figure D-37: Observed and modelled head at monitoring bore 61_141.
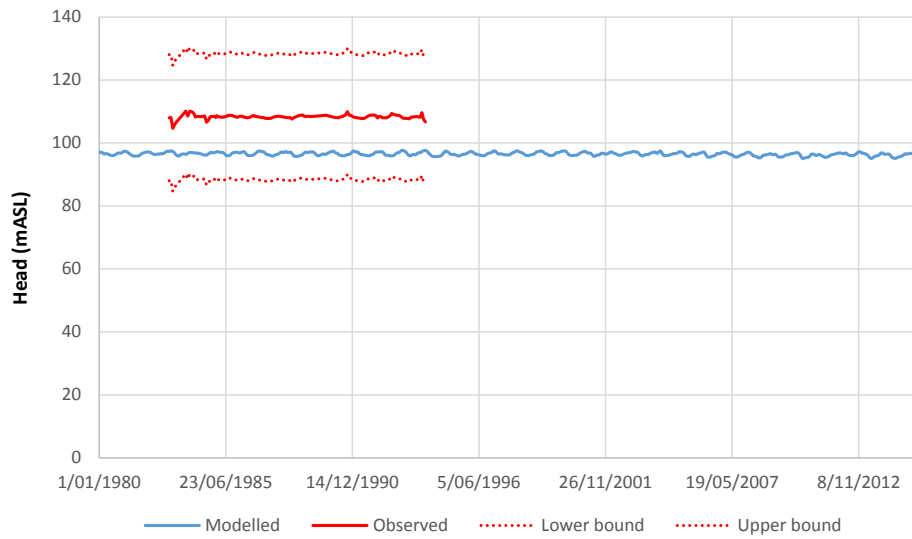
Figure D-38: Observed and modelled head at monitoring bore 61_160.

Figure D-39: Observed and modelled head at monitoring bore 61_163.

Figure D-40: Observed and modelled head at monitoring bore 61_164.

Figure D-41: Observed and modelled head at monitoring bore 61_167.

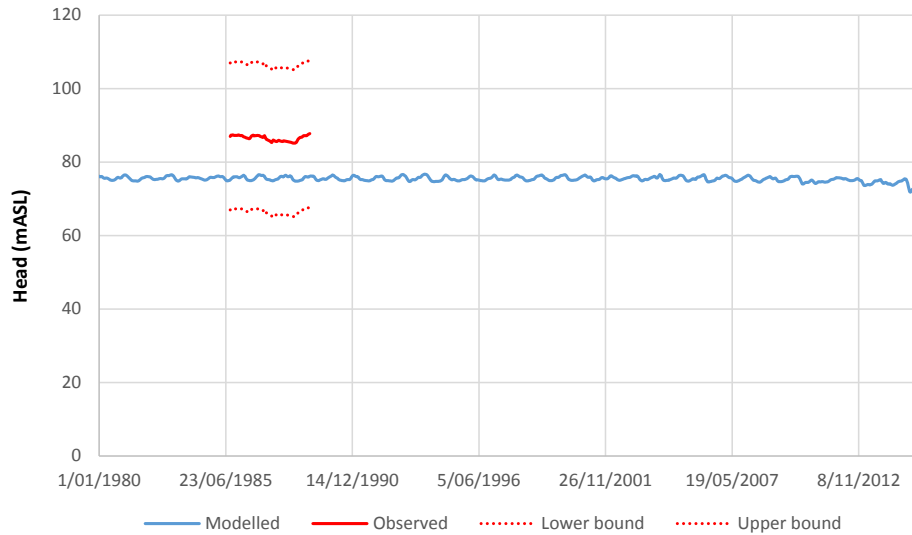**Figure D-42: Observed and modelled head at monitoring bore 61_87.**

Figure D-43: Observed and modelled head at monitoring bore 61_225.

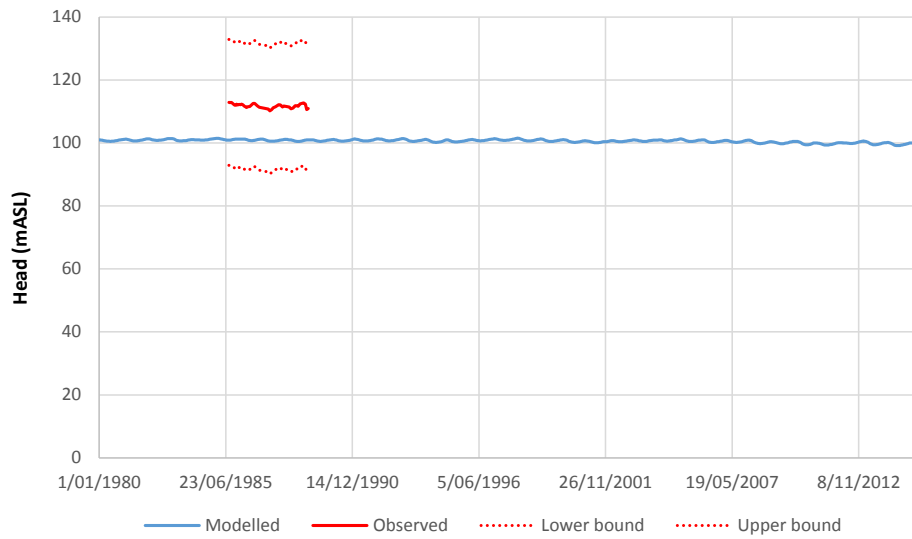**Figure D-44: Observed and modelled head at monitoring bore 61_118.**

Figure D-45: Observed and modelled head at monitoring bore 61_64.

Figure D-46: Observed and modelled head at monitoring bore 61_26.

Figure D-47: Observed and modelled head at monitoring bore 61_260.

Figure D-48: Observed and modelled head at monitoring bore 61_263.

Figure D-49: Observed and modelled head at monitoring bore 61_273.

Sensitivity Analysis

Figures D-50 and D-51 show observed and simulated surface water low flows for the calibrated model and alternative calibrated models with adjusted basalt K values.
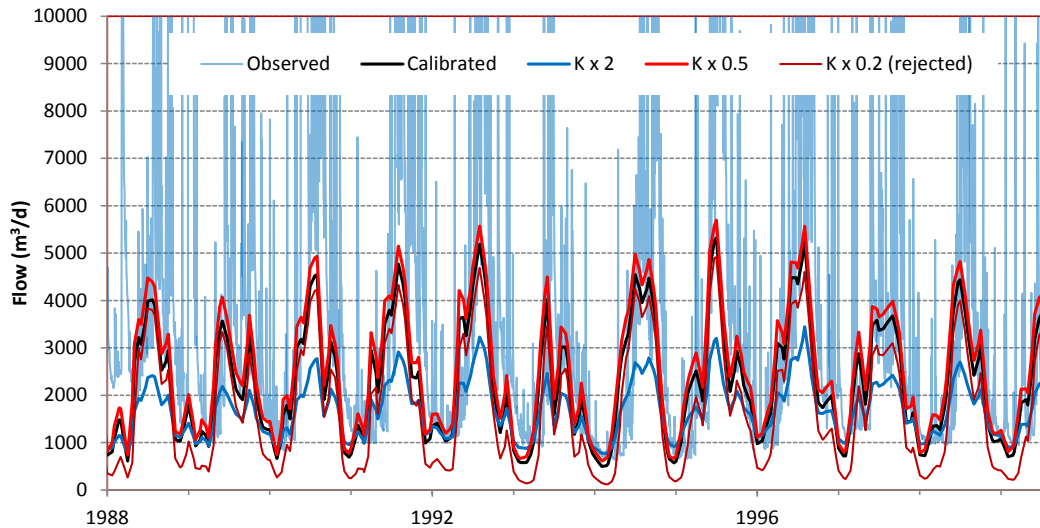

Figure D-50: Observed stream flow and modelled groundwater discharge at 83_1 – sensitivity to basalt K variation.
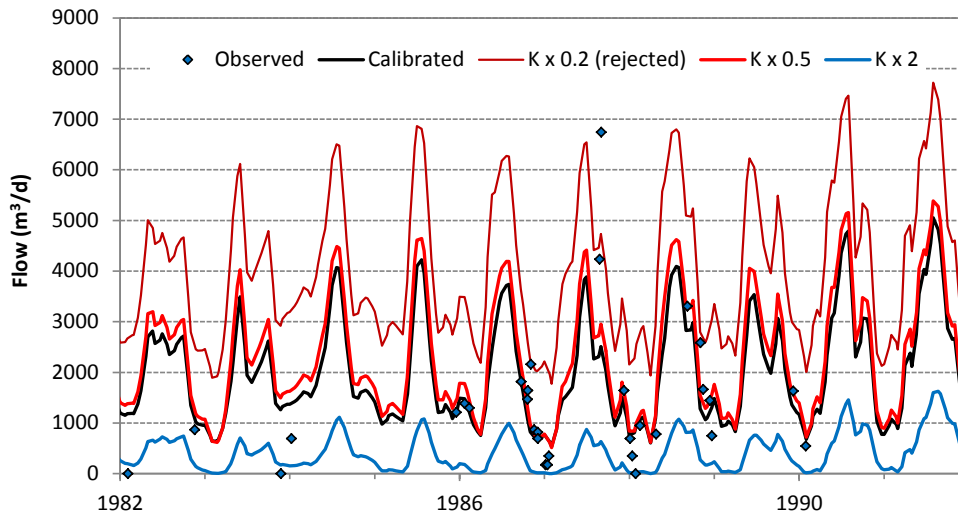

Figure D-51: Observed stream flow and modelled groundwater discharge at 960_3 – sensitivity to basalt K variation.

Figures D-52 and D-53 show observed and simulated surface water low flows for the calibrated model and alternative calibrated models with adjusted S_s values in model layer 1.
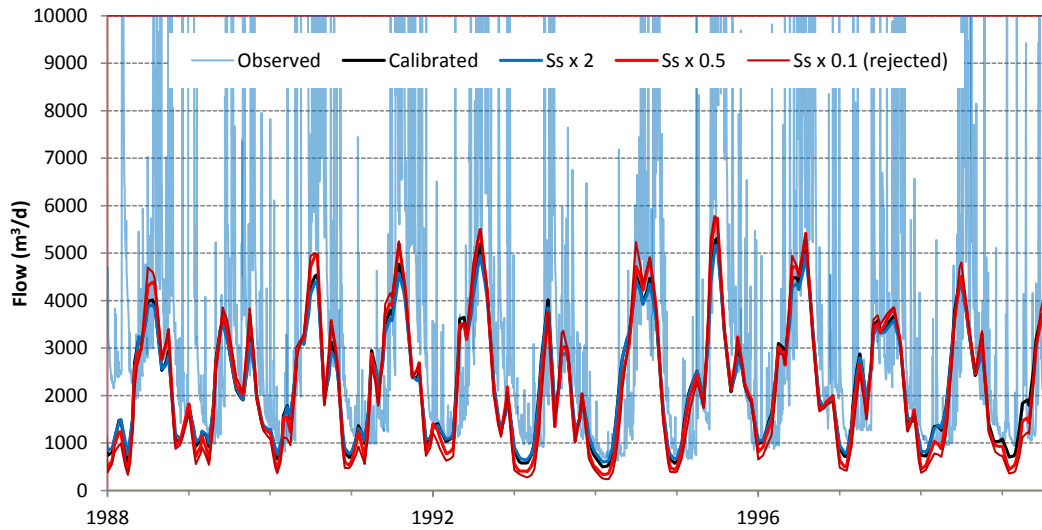
Figure D-52: Observed stream flow and modelled groundwater discharge at 83_1 – sensitivity to S_s variation.
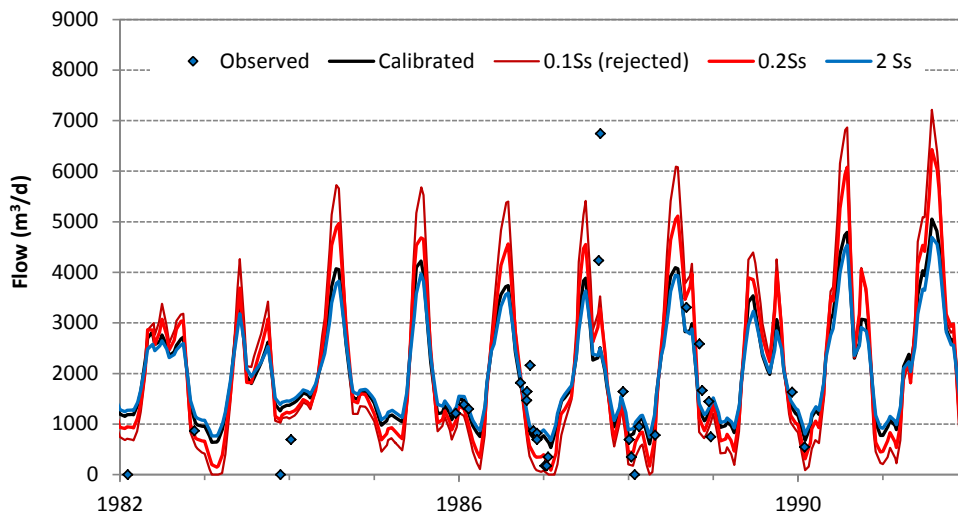

Figure D-53: Observed stream flow and modelled groundwater discharge at 960_3 – sensitivity to S_s variation.

While the sensitivity of the flow calibration was limited for variations in S_s, simulated groundwater levels were more sensitive and this formed the basis for selection of a plausible range in S_s values. An example of the sensitivity of groundwater level fluctuations to S_s is shown in Figure D-54.
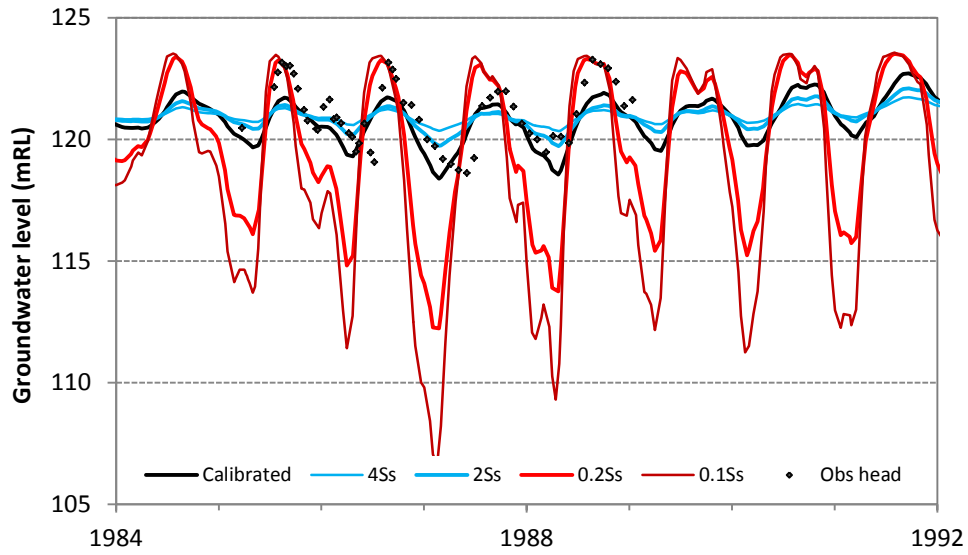
Figure D-54: Observed and modelled groundwater level at 61_26 – sensitivity to S_s variation.